論文 / 著書情報
Article / Book Information

題目(和文)	液晶モノマーの重合挙動と強誘電性を用いた画像定着
Title(English)	Polymerization behavior of liquid-crystalline monomers showing various phase structures and image storage using ferroelectric properties
著者(和文)	大桐小百合
Author(English)	
出典(和文)	学位:博士(工学), 学位授与機関:東京工業大学, 報告番号:甲第4126号, 授与年月日:1999年3月26日, 学位の種別:課程博士, 審査員:
Citation(English)	Degree:Doctor (Engineering), Conferring organization: Tokyo Institute of Technology, Report number:甲第4126号, Conferred date:1999/3/26, Degree Type:Course doctor, Examiner:
学位種別(和文)	博士論文
Type(English)	Doctoral Thesis

Polymerization Behavior of Liquid-Crystalline Monomers Showing Various Phase Structures and Image Storage Using Ferroelectric Properties

Sayuri Ogiri

Department of Environmental Chemistry and Engineering
Tokyo Institute of Technology

1998

Contents

Abbreviations

ac	alternating current
AIBN	2,2'-azobis(isobutyronitrile)
Ch	cholesteric
dc	direct current
DCC	dicyclohexylcarbodiimide
DEAD	diethyl azodicarboxylate
DMAP	4-dimethylaminopyridine
DMF	N,N'-dimethylformamide
DMSO	dimethyl sulfoxide
DSC	differential scanning calorimeter
FLC	ferroelectric liquid crystal
	ferroelecric liquid-crystalline
G	glassy
GPC	gel permeation chromatography
I	isotropic
ITO	indium-tin-oxide
K	crystal
k_p	propagation kinetic constant
k_t	termination kinetic constant
LC	liquid crystal
	liquid-crystalline
LCD	liquid crystal display
Mn	number-average molecular weight
Mw	weight-average molecular weight
Mw/Mn	molecular weight distribution
N	nematic
NMP	N-methyl-2-pyrrolidinone
PI	polyimide
PLC	polymer liquid crystal
Sm	smectic
SmA	smectic A
SmA*	chiral smectic A
SmB	smectic B
SmC	smectic C
SmC*	ferroelectric chiral smectic C
SmC_A*	antiferroelectric chiral smectic C
SmC_γ*	ferrielectric chiral smectic C
Tg	glass transition temperature
THF	tetrahydrofuran

Chapter 1

General Introduction

Polymer liquid crystals (PLCs) have been providing scientists and engineers with one of the most active and fascinating fields of scientific and industrial research. Since the PLCs possess the electric and optical anisotropy, and good film-forming properties, it is expected that PLCs can be applied to new display and recording materials. Kevlar (poly(*p*-phenyleneterephthalamide)) is well known as an example of PLCs. The fibers with good molecular alignment are formed by elongation in LC state and exhibit high strength and modulus of elasticity and thermal resistance. It is clear that control of orientation is one approach to obtain polymers with excellent properties. The properties of polymers are determined by higher-order structure as well as chemical properties of monomers and first-order structure. Therefore, if polymers are endowed with higher-order structure, they will show novel performance and function, and this may be feasible to prepare novel materials by new method.

The polymerization of LC monomers is a recent topics to obtain highly functionalized and high-performance PLCs.[1] LCs spontaneously form organized molecular systems and their alignment can be controlled by the application of an external field.[2] Then, it is expected that polymerization in a highly aligned state such as an LC phase can exhibit specific polymerization behavior, which may create polymers with special properties. Such control by molecular alignment in whole polymerization processes could be promising as a novel approach to control of the properties. Development in this approach will lead to improvement of liquid crystal display (LCD).

1-1. Radical Polymerization

Of all branches of polymerization free-radical processes are commercially most important and scientifically most thoroughly investigated. Among the reasons for this is the fact that useful high-molecular-weight polymers and copolymers can be prepared from a wide variety of monomers. Also, these processes are generally convenient to carry out and control. Thus, free-radical polymerization provides a convenient route to polymers with a wide range of properties.

In general, free-radical polymerizations are most amenable to scientific investigation, requiring less sophisticated techniques than their ionic counterparts, being free from the effects of counterions and not requiring traces of co-catalyst, essential to many ionic polymerizations. The concept of vinyl polymerization as a chain mechanism is not new, dating back to Staudinger's work in 1920. In 1937, Flory showed conclusively that radical polymerization proceeds by the steps of initiation, propagation, termination, and chain transfer reactions.[3]

The kinetics of a straightforward free-radical polymerization are those of a simple radical-chain polymerization in which the chain propagates by the addition of a monomer to the active chain carrier, regenerating the active radical intermediate. In the free-radical polymerization of vinyl monomers of the types CH_2=CHX and CH_2=CXY, propagation involves the addition of the radical to one end of the double bond of the monomer. Thus, at each step in the chain the free-radical intermediate increases in size by one monomer unit, and the average number of monomer molecules incorporated into each polymer molecule, or the degree of polymerization, is directly related to the length of the kinetic chain. As with most chain reactions, possible side-reactions exist. Over the years a number of complicating features have been identified and their influence on the rates of polymerization, and on the molecular weights of the final polymers are understood. Indeed, with some monomers the nature of the component reactions is sufficiently well understood to allow polymerization kinetics to be used as a means of determining rates of radical formation and hence, as a tool for investigating mechanisms

of radical formation in new initiating systems. However, polymerization behavior in specific system is not so well known.

1-1-1. Elementary Reaction of Radical Polymerization

When free radicals are generated in the presence of a vinyl monomer, the radical adds to the double bond with the regeneration of another radical. The radical formed by decomposition of the initiator I is designated by R· (Figure 1-1(A)). The regeneration of the radical is characteristic of the chain reactions. The chain radical formed in the initiation step is capable of adding successive monomers to propagate the chain (Figure 1-1(B)). Propagation would continue until the supply of monomer is exhausted. The termination step can take place in two ways: combination and disproportionation (Figure 1-1(C)). For example, polystyrene terminates predominantly by combination, whereas poly(methyl methacrylate) terminates by disproportionation as well as combination. The termination reaction is controlled by diffusion in many cases. It was recognized by Flory (1937) that the reactivity of a radical could be transferred to another species, which would usually be capable of continuing the chain reaction (Figure 1-1(D)).[3] The major effect of chain transfer to a saturated small molecule is the formation of additional polymer molecules for each radical chain initiated.

1-1-2. Initiators

In view of its importance in polymerization studies the author may state the thermal decomposition of azo-compounds.[4] The driving force in the thermal decomposition of these initiators is the scission of the weak C–N bonds in the azo-linkages with the elimination of a molecule of nitrogen. It is usually considered that 2,2'-azobis(isobutyronitrile) (AIBN) and its analogues decompose by the simultaneous cleavage of the two C–N bonds (Figure 1-2(A)). To be useful in initiating polymerization, a compound undergoing thermal decomposition to free radicals should have a first-order decomposition rate constant of 10^{-5} to 10^{-6} s^{-1} at the desired

(A) Initiation reaction

$$I \rightarrow 2R \cdot \qquad \text{(Eq. 1-1)}$$

$$R \cdot + M \rightarrow RM \cdot \ (\equiv M \cdot) \qquad \text{(Eq. 1-2)}$$

(B) Propagation reaction

$$M_n \cdot + M \rightarrow M_{n+1} \cdot \qquad \text{(Eq. 1-3)}$$

(C) Termination reaction

$$M_m \cdot + M_n \cdot \rightarrow P_{m+n} \qquad \text{(Eq. 1-4)}$$

$$M_m \cdot + M_n \cdot \rightarrow P_m + P_n \qquad \text{(Eq. 1-5)}$$

(D) Chain transfer reaction

$$M_n \cdot + A \rightarrow P_n + A \cdot \qquad \text{(Eq. 1-6)}$$

$$A \cdot + M \rightarrow AM \cdot \ (\equiv M \cdot) \qquad \text{(Eq. 1-7)}$$

Figure 1-1. Elementary reaction of radical polymerization. I, initiator; R ·, radical formed by decomposition of initiator; M, monomer; Pm (Pn), polymer with polymerization degree of m (n); A, chain transfer agent.

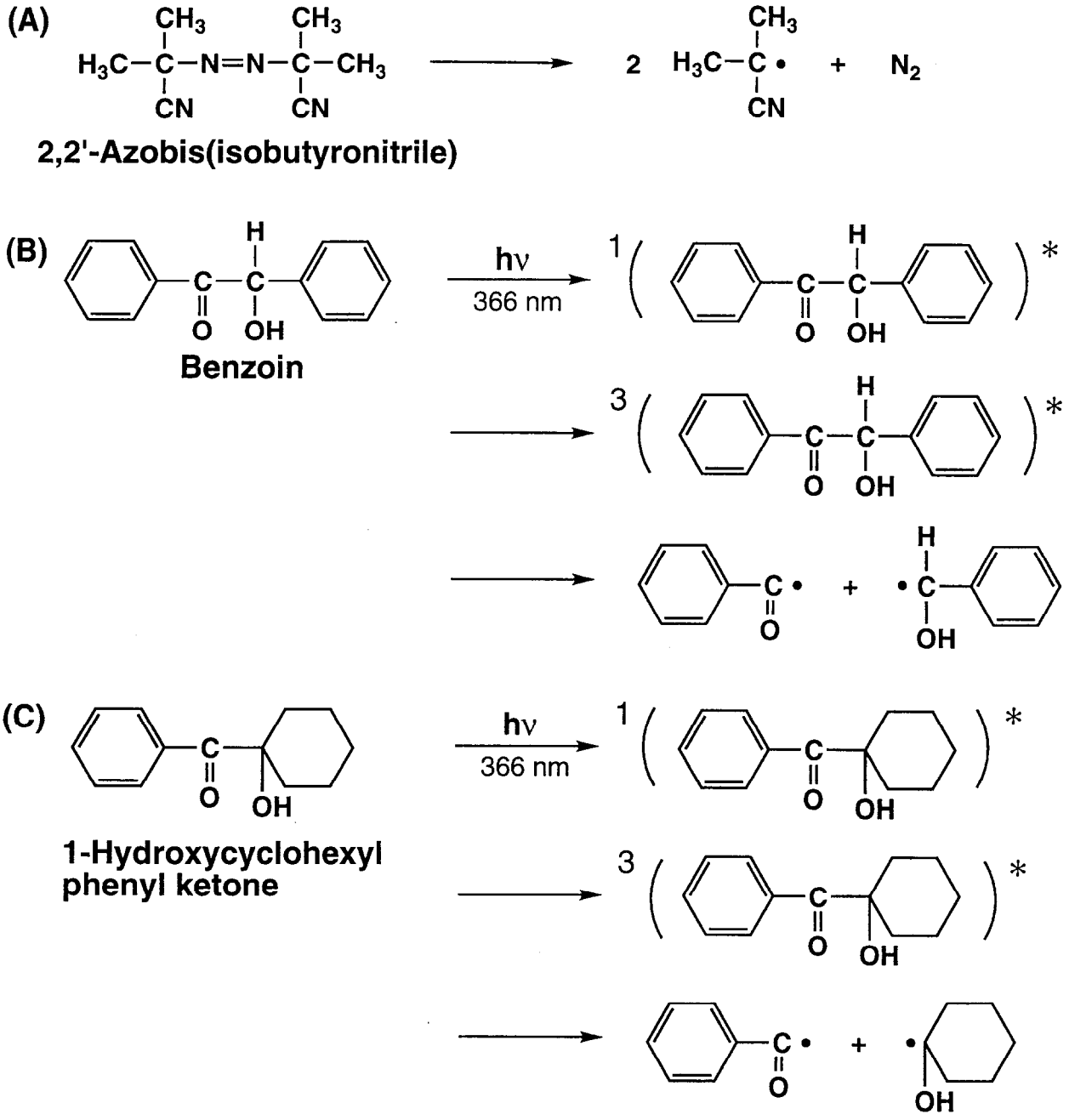

Figure 1-2. Decomposition of initiators.

polymerization temperature. Although thermal decomposition is a common means of generating radicals, it has a disadvantage in that the rate of generation of free radicals cannot be controlled rapidly because of the heat capacity of the system. Photoinitiated polymerization, on the other hand, can be controlled with high precision, since the generation of radicals can be made to vary instantaneously by controlling the intensity of the initiating light. The term of photopolymerization should be reserved for step polymerization processes in which each reaction step requires the absorption of at least one photon. Light of short enough wavelength, that is high enough energy per quantum, can initiate polymerization directly. It is customary, however, to use a photoinitiator such as benzoin derivatives, which is decomposed into free radicals by ultraviolet light in the 360-nm region, where direct initiation through decomposition of monomer does not occur. Photochemical α-cleavage from the triplet state by Norrish Type I mechanism is the main process for benzoin (Figure 1-2(B)), 1-hydroxycyclohexyl phenyl ketone (Figure 1-2(C)), et al.[5]

1-1-3. Homogeneous Reactivity of Monomers

The reactivity of monomers is determined by steric hindrance, and resonance and polarity effect of double bond. The reactivity of monomers is proportional, not to e-value, but to Q-value. Conjugated monomers possessing large Q-value have high reactivity with propagation radicals whereas non-conjugated monomers possessing small Q-value have small reactivity.[6] Resonance stabilization depresses the reactivity of radicals so that their order of reactivity is the reverse of that of their monomers. Since propagation, termination and chain transfer reaction are related to propagation radical, reactivity of radicals governs polymerization rate, structure and molecular weight of polymer produced. In general, the selectivity of reaction decreases as radicals are less stable, and non-conjugated monomers show high rate constant of each elementary reaction, which results in polymers with head-to-head structure and branched polymers.

Evans et al. have attempted to examine the interaction of radicals with monomers in terms of the potential energy for reaction.[7] Typical examples of such curves are shown in Figure 1-3. The curves represent, respectively, the repulsion energy between the radical and the atoms of the monomer which will form the new bond, and the potential energy of the new bond when formed. The point of intersection of the two curves, where the energies of the bonded and unbonded states are equal, corresponds to the transition state of the addition reaction and the energy difference between this point and the potential energy minimum of the bonded state is the activation energy for propagation.

Free-radical homopolymerizations of monomers that produce both linear and crosslinked polymer systems can show several distinctive features. Viscous and vitrification effects in bulk polymerizations produce autoacceleration, autodeceleration, and incomplete functional group conversion. Alternate termination mechanisms such as reaction-diffusion-controlled termination further complicate matters. During polymerization, the conversion of monomer to polymer generally results in an increase in viscosity. The increase of viscosity causes a decrease in both the translational diffusion of monomer and polymer and the segmental diffusion of the polymer. When the diffusional limitations become large enough to restrict the diffusion of growing polymer chains, the termination rate will decrease, causing a buildup in radical concentration and, hence, autoacceleration.

Once termination drops below a certain level, a different mechanism will become dominant: reaction-diffusion. Reaction-diffusion-controlled termination on the result of double-bond mobility in systems where growing chain-end radicals are relatively immobile. The termination kinetic constant (k_t) becomes proportional to the product of the propagation kinetic constant (k_p) and the double-bond concentration.

As conversion and viscosity continue to increase, the mobility in the system will reduce to a point at which the diffusion of the unreacted double bonds is limited. At

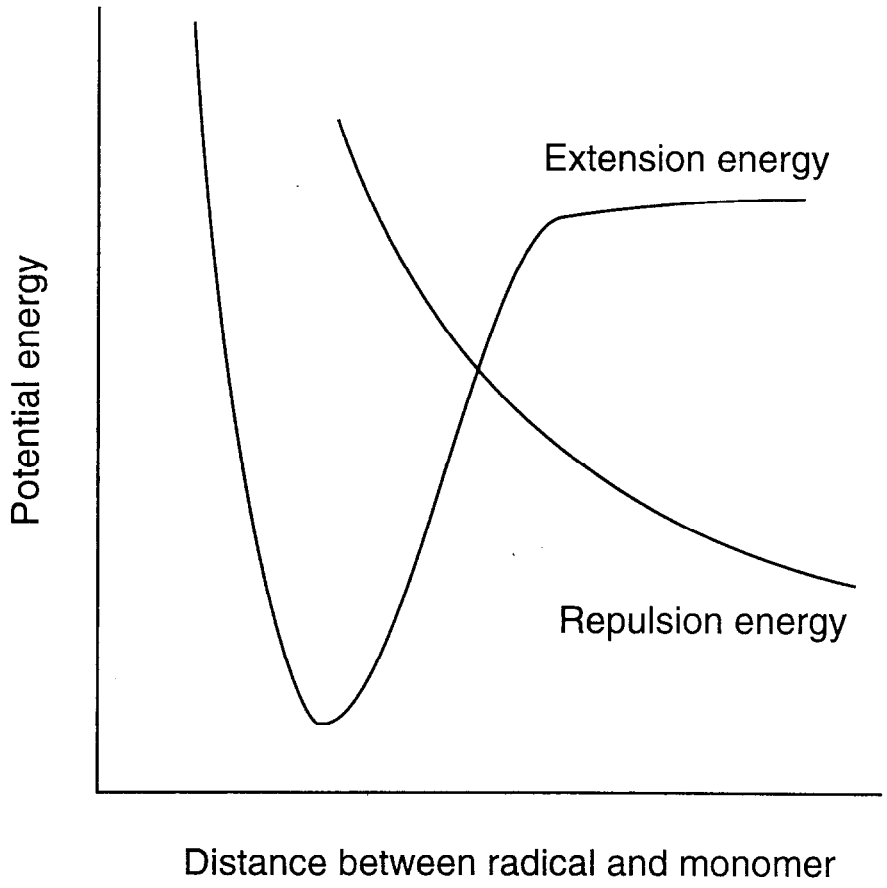

Figure 1-3. Potential energy diagram for addition of a radical to a monomer.

this point, k_p and the rate of polymerization drop. This effect is known as autodeceleration.

Consequently, polymerization can be broken up into four regions: (I) the normal polymerization region with no diffusional controls; (II) the autoacceleration region, in which termination is diffusion controlled but propagation is not; (III) the reaction-diffusion termination region, with constant k_p; and (IV) the autodeceleration region with termination still reaction-diffusion controlled.[8] These regions, along with the physical properties characterizing them, are summarized in Table 1-1.

Table 1-1. Physical description of the four regions examined by the analytical method

Region	Physical description	Free volume[a]	Reaction-diffusion ?
I	No diffusional limitations on either propagation or termination	$f >> f_{cp}, f_{ct}$	No
II	Autoacceleration	$f_{ct} > f >> f_{cp}$	No
III	Reaction-diffusion-controlled termination, propagation not diffusion limited	$f_{ct} > f >> f_{cp}$	Yes
IV	Autodeceleration with reaction-diffusion controlled termination	$f < f_{ct}, f_{cp}$	Yes

[a] f_{cp}, f_{ct}: Critical fractional free volumes at which propagation and termination, respectively, start to be diffusionally controlled.

1-2. Liquid Crystals

Liquid crystals (LCs) have been some derivatives of cholesterol in which Reinitzer and Lehmann detected the LC state in 1888.[9] Although LCs have been known for a century or more, it is only in the past 30 years that their unusual properties, especially the color changes, have found widespread application. LCs have become indispensable for the manufacture of many electrically controlled display devices. LCs are of great interest because of their uniqueness. The LC or mesomorphic state is intermediate between the crystalline and liquid state, and LCs exhibit certain aspects of both the crystal and liquid.[10] However, LCs also possess properties that are not found

in either liquids or solids. Their orientation, for instance, can be controlled by the temperature, magnetic field, electric field, light, *etc.* For some LCs, the optical activity is of an order of magnitude not met with in any solid, liquid or gas. Some LCs change color as a result of the sensitivity of their structure to temperature. There are the properties on which the practical applications of LCs are based.

LCs possess fluidity and optical anisotropy. In the LC phase for rod-shaped structure, molecules are assembled with their long axes aligned into a particular direction. For rod-shaped molecules, three types of the LC phases are designated as nematic (N), smectic (Sm), and cholesteric (Ch) phase, following a proposal by Friedel (Figure 1-4).[11]

It is generally known in solid state that some dielectrics exhibit a specific property of a non-zero and permanent value of electric polarization, called spontaneous polarization, even without an applied field or stress. When the direction of spontaneous polarization can be changed by an applied electric field, the term "ferroelectric" is used.

Ferroelectricity in solid crystals has been known since 1921, when Rochelle salt was discovered to exhibit dielectric hysteresis indicating a spontaneous electrical polarization.[12,13] Ferroelectricity in LCs was first demonstrated in 1975 by the physicist Meyer together with the chemists Strzeleski and Keller.[14] Chiral smectic C (SmC*) phase of ferroelectric liquid crystals (FLCs) exhibits spontaneous polarization (Ps) because of the presence of polar groups which give the molecules an electric dipole moment. In the SmC* phase, the FLC molecules are aligned parallel to each other to form a layer with a tilt between the direction of the long axis of the FLC molecule and the normal to the smectic layer.[13,15] The average direction of the molecular long axis is defined in each layer, and owing to the chiral group in the FLC molecules the director adopts a helicoidal structure with a characteristic pitch. When the FLC molecules are placed in a cell with a small gap, which is smaller than the helical pitch, the interaction of the FLC molecules and the cell surface is so strong that the helix structure becomes energetically unfavorable, and the molecular long axis in every layer is aligned in the

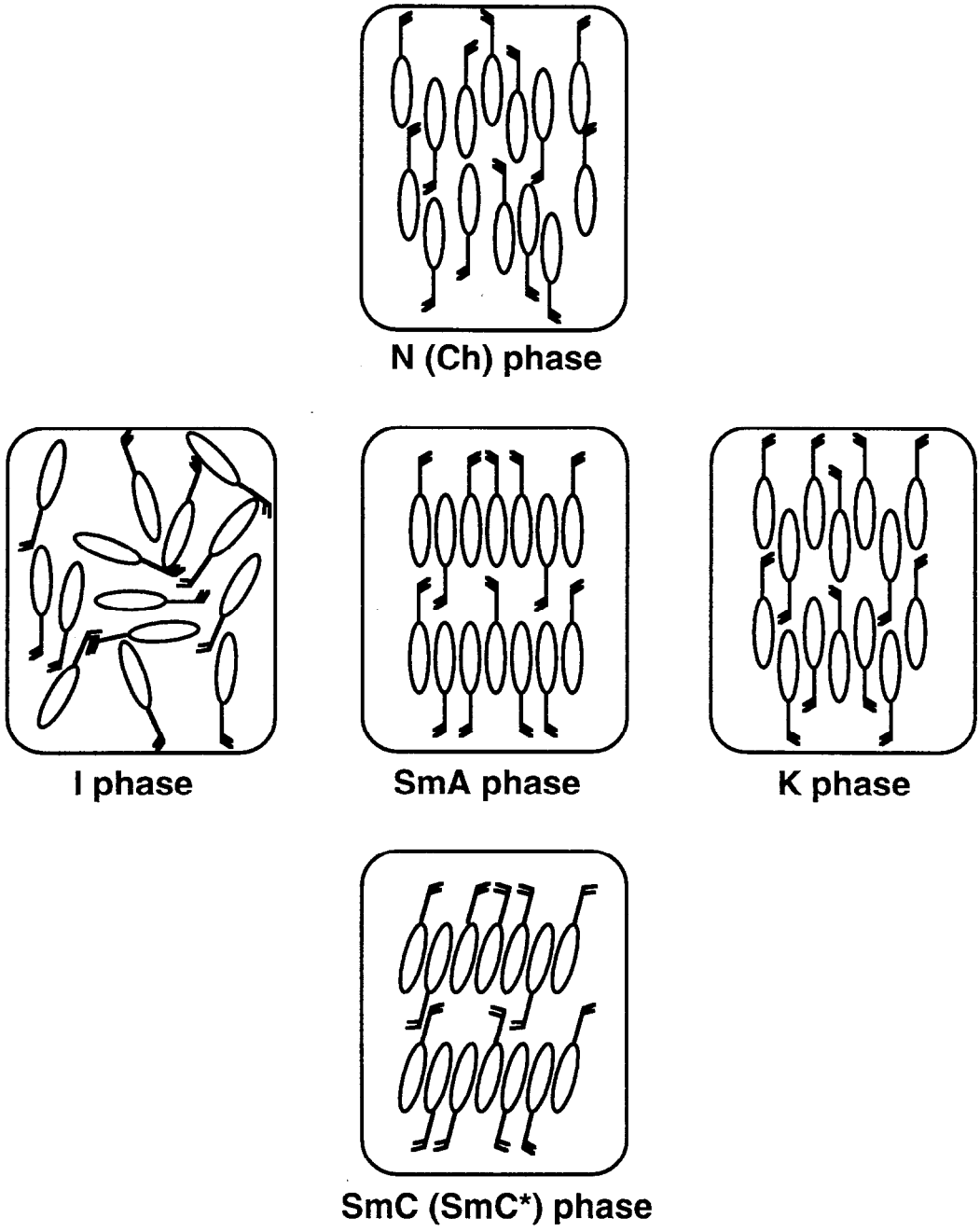

Figure 1-4. Phase structures of liquid-crystalline monomers.

same direction with the smectic layers oriented roughly perpendicular to the cell surface. As a result, the polarization of all layers is also aligned in one direction.[13] If an external electric field is applied across the cell, the polarization can be aligned upwards or downwards, depending on the polarity of the applied electric field. When the polarity of the electric field is reversed, the polarization flips. These two stable states are called surface-stabilized states and FLCs exhibit bistability.[15(a)]

Smectics which show ferro-, ferri-, or antiferroelectric properties have layer structures where the molecules are tilted with respect to the layer normal and where the tilt direction, in the unconstrained state, rotates from one layer to another, which results in helicoidal structure with the helix axis parallel to the smectic layer normal. In the SmC* phase, the tilt is rotating slightly from layer to layer. In the antiferroelectric SmC_A* phase the tilt in addition alters its direction by an angle π between adjacent layers.[16] As an example of the ferrielectric SmC_γ* phases every third layer tilts in the opposite direction.[16] Antiferro- and ferrielectricity show the field-induced transition to ferroelectric phase as well as the stability of the phase itself against an external electric field.[17]

1-3. Polymerization in Organized Systems

The effect of molecular alignment on the polymerization of monomers has been described. When polymers are formed in molecular alignment, the strains which take place at the same time are very small due to negligible energy of lattice in molecular alignment. The mobility of monomer units must stimulate the rapid relaxation of strain. It may affect polymerization rate and the molecular weight, and even the microtacticity of the polymer.

1-3-1. Polymerization Behavior of Liquid-Crystalline Monomers

Polymerization of LC monomers has been extensively conducted to obtain PLCs.[1] The LC monomers can be macroscopically oriented by external forces, such as

an electric or magnetic field, elongational flow and surface orientation. Monomer organization may affect the polymerization kinetics, the polymer structure, the microstructure of polymers, etc.[18] The effect of LC ordering on the rate of free-radical polymerization of mesomorphic vinyl monomers has been discussed extensively.[1]

Characteristic of phase structure and polymerizability of LC monomers are described below. Liquid, LC and crystal can be distinguished from the symmetry of each structure.[13] Isotropic (I) phase shows the highest symmetry, and then the position of center-of-gravity and the direction of long axis of mesogens are random. Therefore, the position of functional group is at random. Taking into account the orientation, it is expected that the polymerization proceeds slowly. Although fluidity of N phase is almost the same as that of I phase, the long axis of mesogens in N phase exhibits uniaxial orientation in the direction called orientation vector and then there exists anisotropy. However, the direction of polymerizable group is disordered and then it is expected that polymerizability is low. Sm phase forms layer and order parameter in Sm phase is higher than that in N phase. Therefore, it is thought that polymerizability increases because of high density of polymerizable groups. FLCs have the dipoles normal to molecular long axis and helicoidal structure. When the FLCs are injected in the cell with a small gap, which is smaller than the helical pitch, the dipoles of FLC molecules are in the same direction and polarization is formed macroscopically. Thus, it can be expected that polymerization behavior is affected by the orientation of LCs.

In the case where polymerization of vinyl oleate was conducted in I, Sm, and K phases, the rate of polymerization in Sm phase was largest.[19] The rate of initial polymerization in Sm phase was almost the same as that in N phase, although that in I phase was much smaller.[20] Because of phase transition from I to LC phase during polymerization, the viscosity increased steeply and no reorientation formed polydomain. In addition, the reactivity of diacrylate monomer in ordered state was higher than that in I state.[21] It was interpreted in terms of Trommsdorff effect, that is, in the system of high viscosity, decrease of propagation rate and further decrease of

termination rate increased an apparent polymerization rate. For LC methacrylate monomers containing a cholesteryl moiety, polymerization in the Ch phase was most rapid and the change from Ch to Sm phase occurred during polymerization.[22] The rate constant of termination in Sm phase decreased by about two orders of magnitude over in I phase, and then molecular weight of polymers produced in Sm phase increased. Polymerization kinetics such as molecular weight, polymerization rate etc. was accompanied by phase transition during polymerization.[23] In addition, polymerization in highly-ordered SmB phase was extremely efficient and molecular weight of polymer obtained was fairly high.[24] When polymerization was conducted in the I phase at only a few degrees above its clearing temperature, change to a low-order LC with Sm texture occurred during polymerization. The change was accompanied by an abrupt increase in the polymerization rate.[24] At higher temperature in the I phase no change in texture occurred during polymerization, and the quantum efficiency of polymerization was much lower than in the LC medium.

As mentioned previously, orientation of LCs can be controlled by external forces such as magnetic and electric field. Many studies of polymerization of LC monomers under an external force have been conducted. N phase with a magnetic field became homogeneous alignment and therefore polymerization rate increased.[25] X-ray diffraction pattern indicated no improvement of orientation in the I phase by an magnetic field. In addition, polymerization became fast and the film of homeotropic alignment was obtained by in-situ photopolymerization in the SmA phase under a dc electric field.[26] By applying the electric field, mesogens were completely homeotropic alignment. Therefore, the reactivity between monomers became high because of adjacent effect due to regular alignment of functional group.

In-situ photopolymerization behavior of monomers in the low-molecular-weight FLC solvent has been investigated.[27] They used monomer which showed only I phase and monomer which exhibited N phase. Small, flexible monomers were aligned parallel to the Sm layers and intercalated, whereas rod-shaped mesogen-like monomers

oriented normal to the Sm layers. Such specific segregation caused by Sm layer dramatically enhanced photopolymerization rates. The polymerization of these systems would result in networks with significantly different morphologies which affected the ultimate polymer characteristic such as structure, solubility, and elasticity of the gels.

Thus, polymerization behavior was strongly dependent on the orientation of LC molecules. However, it has been reported that the polymerizability was low as the order of molecules increased.[28-30] Polymerization of these systems was affected by kinetic factors such as molecular mobility rather than the orientation. The initial rate of polymerization of Schiff-base LC monomers increased with temperature despite phases of the monomer.[29] In addition, polymerization rate of a sterically hindered monomer in Sm phase was lower than that in I phase, although the polymer chain kinetic lifetime is markedly longer in the Sm phase.[31] This well contributed to the decrease in the propagation process due to steric hindrance at the radical-forming carbon site. Weight-average molecular weight has been controlled by irradiation dose and temperature. As mentioned above, polymerization behavior was affected by the structures of molecules and the kinetic factors such as mobility as well as phase structures and orientation. Polymerization of LC monomers might control termination reaction and number of polymer chains.

1-3-2. Control of Stereoregularity

PLCs have attracted growing interest due to their requirement as materials for recording and electrooptic devices. For these purposes, various side-chain PLCs with several types of main chains such as polyacrylate, polymethacrylate, polysiloxane, and poly(vinyl ether) have been synthesized. It is important to get information on the relation between the tacticity of the main chain and the liquid crystallinity in order to obtain high-performance and/or highly functionalized LC materials. Differences in thermal properties have been shown for iso- and syndiotactic polymers.[32] Furthermore, the LC phase was more unfavorable for isotactic side-chain mesogenic polymers than

for syndiotactic ones on the basis of their consideration of the conformational difference of stereoregular polymers.[33] These observations were interpreted by difference in conformation: zigzag and helical conformations of the main chain of syndio- and isotactic polymers, respectively. The characteristic performance and function are attributable to the conformation of polymer chain, and then the control of stereoregularity is essential for the development of the new materials.

On the other hand, it has been reported that structural characteristic, especially stereoregularity has been given by the orientation of the matrix. Polymerization has been conducted under various conditions in polymer matrix, LC, inclusion crystal, under external forces such as magnetic and electric field, etc. Radical polymerization of various alkyl methacrylates in LC solvent has been studied.[34] It was found that the polymerization behavior of methacrylates of butyl and longer alkyl chain was deviated from Bernoullian statistics and gave polymers more isotactic than those of methyl and ethyl methacrylates. Solid-state polymerization of a binary mixture of non-LC monomer and LC compound has been carried out using electron beam.[35] However, the tacticity of polymer produced in solid-state polymerization was almost the same as that of polymer obtained in solution.

In addition, it can be expected that polymerization using LC monomer as a monomer forms polymers reflecting the orientation of monomers. The stereoregular polymer has been obtained by means of polymerization of LC monomer in K and Sm phases under a magnetic field.[19] As mentioned in the previous section, FLCs became surface-stabilized state, and it is, therefore, expected that stereoregular polymers might be produced.

1-3-3. Orientation of Polymer Produced and Applications

Highly oriented PLCs exhibit anisotropy of optical, electrical and thermomechanical properties. It is expected that PLCs with highly oriented structure can be applied to new display and recording materials. To accomplish the macroscopic orientation many attempts such as surface treatments, application of shear stress, electric and/or magnetic fields have been made. However, the macroscopic orientation of PLCs proceeds relatively slow and incomplete in comparison with conventional low-molecular-weight LCs. On the other hand, it was found that a highly oriented side-chain PLCs was prepared by in-situ photopolymerization of macroscopically oriented LC monomers.[36] In addition, photopolymerization of difunctional monomers was mainly conducted to prevent the disorder due to heat.[37] The advantage of the oriented crosslinked polymers would be the thermal stability of the ordering, anisotropy of physical properties such as thermal expansion coefficient, modulus, and refractive index. Oriented polymer networks can also be produced by UV-irradiation of an oriented mixture of LC diacrylates and non-polymerizable LC molecules.[38] In this way anisotropic gels can be made containing LC molecules which can be switched by an external electric or magnetic field, although they align themselves with the mesogenic groups in the network when this external field is switched off. In this case light scattering can be induced upon application of an electric field. It has been shown that lightly crosslinked anisotropic networks can be obtained by in-situ photopolymerization of mixtures of mesogenic mono- and diacrylates.[39] The macroscopic orientation of the anisotropic networks was found to be highly reversible. The initial average orientation of the molecules could also be altered by application of an electric field. A highly transparent system was obtained when the polymerization was performed in a monodomain.[40] Such transparent systems can find applications as passive optical components. Polymerization of LC monomers by two coherent beams was also performed.[41]

Low-molecular-weight Ch LCs have different switching behavior with temperature, electric and magnetic field. These problems in low-molecular-weight Ch LCs were solved by Ch polymer networks. Ch polymer networks are excellent candidates for use in passive optical components such as reflective color filters, notch filters, and devices for polarization rotation.[40] By choosing the polymerization temperature, the bandwidth and the band position can be chosen and permanently stored.[38] Ch polymer films were produced by polymerization of LC diacrylates containing non-reactive LC molecules.[42] This technique causes the Ch polymer network to become partly dependent of temperature in a controllable way and switchable by an external electric or magnetic field by its interaction with the bound molecules. By introducing a gradient in the pitch of the Ch helix, Broer et al. could obtain reflection of one of the two circularly polarized components over the whole visible region.[43] Polarizers with such broad-band reflectivity would greatly improve the light yield and energy efficiency of LCD devices. The optical properties of the films could also be changed locally, making the materials suitable for recording purposes.

Furthermore, when FLC monomers were polymerized in the ferroelectric phase, crosslinked polymers with a stable dipolar orientation were obtained.[44-46] These polymers are of great interest as they show piezo- and pyroelectricity, and can also be used in the production of various nonlinear optical materials. The crosslinked pyroelectric polymer exhibited a high electrooptical coefficient.[47]

1-4. Scope of the Present Thesis

In the present thesis, various types of monomers which showed different phase structures were prepared, and then their polymerization behavior was explored intensively.

In Chapter 2, vinyl monomers having Schiff-base structure were synthesized and the polymerization behavior of the monomers was explored in different phases of the monomers. Polymerization behavior was discussed in terms of the phase structure by

using the monomers with the same structure except the end group but with a difference phase behavior. Furthermore, the author studied the molecular alignment of the polymer produced in each polymerization method.

In Chapter 3, emphasis was placed on the comparison of polymerization behavior between thermal polymerization and photopolymerization of monomers possessing biphenyl structure. The molecular alignment before and after photopolymerization was also investigated.

Polymerization behavior in molecular alignment was governed by molecular diffusion and their alignment. Photopolymerization offers an advantage in that the temperature can be chosen precisely. In Chapter 4, in order to explore the effect of phase structure on polymerization behavior, FLC acrylate monomer was prepared, and photopolymerization behavior was studied in various systems.

In Chapter 5, FLC methacrylate monomers were designed and phase transition temperature was studied. Two types of the FLC monomers (short and long methylene spacer) were used. The author explored the photopolymerization behavior without electric field and with dc electric field in terms of kinetics. In addition, the image storage was attempted by making use of bistable switching and immobilization.

The change in macroscopic structure by applying dc electric field was more effective in the polymerization of FLC monomer with a polymerizable group attached to the rigid core through a short methylene spacer. In Chapter 6, FLC monomer having short spacer was used as FLC monomer and the effect of frequency-controlled phase structures on photopolymerization behavior was discussed.

In Chapter 7, emphasis was placed on the comparison of properties of polymers produced between solution polymerization and photopolymerization in the SmC* phase with dc electric field.

In Chapter 8, the author summarized the results obtained in this study.

References

1 (a) Hoyle, C. E.; Chawla, C. P.; Griffin, A. C. *Polymer* **1989**, *60*, 1909. (b) Broer, D. J.; Mol, G. N. *Makromol. Chem.* **1991**, *192*, 59. (c) Hoyle, C. E.; Kang, D.; Chawla, C. P.; Griffin, A. C. *Polym. Eng. Sci.* **1992**, *32*, 1490. (d) Hoyle, C. E.; Watanabe, T.; Whitehead, J. B. *Macromolecules* **1994**, *27*, 6581. (e) Kurihara, S.; Iwamoto, K.; Nonaka, T. *J. Chem. Soc., Chem. Commun.* **1995**, 2195. (f) Hoyle, C. E.; Chawla, C. P. *Macromolecules* **1995**, *26*, 1946. (g) Kurihara, S.; Ohta, H.; Nonaka, T. *Polymer* **1995**, *36*, 849. (h) He, L.; Zhang, S.; Jin, S.; Qi, Z. *Polym. Inter.* **1995**, *38*, 211. (i) Favre-Nicolin, C. D.; Lub, J. *Macromolecules* **1996**, *29*, 6143. (j) Williamson, S. E.; Kang, D.; Hoyle, C. E. *Macromolecules* **1996**, *29*, 8656. (k) Stohr, A.; Strohriegl, P. *Mol. Cryst. Liq. Cryst.* **1997**, *299*, 211. (l) Baxter, B. C.; Gin, D. L. *Macromolecules* **1998**, *31*, 4419. (m) Kurihara, S.; Sakamoto, A.; Nonaka, T. *Macromolecules* **1998**, *31*, 4648. (n) Hikmet, R. A. M.; Kemperman, H. *Nature* **1998**, *392*, 476. (o) Schultz, J. W.; Chartoff, R. P. *Polymer* **1998**, *39*, 319.

2 Kelker, H.; Hatz, R. *Handbook of Liquid Crystals*; Verlag Chemie: Weinheim, 1980; Chapter 4.

3 Flory, P. J. *J. Am. Chem. Soc.* **1937**, *59*, 241.

4 Ayscough, P. B.; Pearson, J. M.; Evans, H. E. *J. Phys. Chem.* **1964**, *68*, 3889.

5 Gruber, H. F. *Prog. Polym. Sci.* **1992**, *17*, 953.

6 Flory, P. J. *Principles of Polymers Chemistry*; Cornell Univ. Press, Ithaca, New York, 1953; Chapter 5.

7 Evans, M. G.; Gergely, J.; Seamen, E. S. *J. Polym. Sci.* **1948**, *3*, 866.

8 Goodner, M. D.; Lee, H. R.; Bowman, C. N. *Ind. Eng. Chem. Res.* **1997**, *36*, 1247.

9 Demus, D. *Mol. Cryst. Liq. Cryst.* **1988**, *165*, 45.

10 Solladié, G.; Zimmermann, R. G. *Angew. Chem. Int. Ed. Engl.* **1984**, *23*, 348.

11 Friedel, G. *Ann. Phys. (Paris)* **1922**, *18*, 273.

12 (a), Goodby, J. W.; Leslie, T. M. *Mol. Cryst. Liq. Cryst.* **1984**, *110*, 175. (b), Skarp, K.; Handschy, M. A. *Mol. Cryst. Liq. Cryst.* **1988**, *165*, 439.

13 Fukuda, A.; Takezoe, H. *Structures and Properties of Ferroelectric Liquid Crystals*; Corona, Tokyo 1990.

14 Meyer, R. B.; Liebert, L.; Strzelecki, L.; Keller, J. *J. Phys. Lett.* **1975**, *36*, 69.

15 (a) Clark, N. A.; Lagerwall, S. T. *Appl. Phys. Lett.* **1980**, *36*, 899. (b) Decobert, G.; Dubois, J. C.; Esselin, S.; Noël, C. *Liq. Cryst.* **1986**, *1*, 307. (c) Ouchi, Y.; Takezoe, H.; Fukuda, A.; Kondo, K.; Kitamura, T.; Yokokura, H.; Mukoh, A. *Jpn. J. Appl. Phys.* **1988**, *27*, L733. (d) Skarp, K.; Handschy, M. A. *Mol. Cryst. Liq. Cryst.* **1988**, *165*, 439. (e) Ikeda, T.; Sasaki, T.; Ichimura, K. *Nature* **1993**, *361*, 428. (f) Sasaki, T.; Ikeda, T.; Ichimura, K. *J. Am. Chem. Soc.* **1994**, *116*, 625. (g) Sasaki, T.; Ikeda, T. *J. Phys. Chem.* **1995**, *99*, 13002. (h) Sasaki, T.; Ikeda, T. *J. Phys. Chem.* **1995**, *99*, 13008. (i) Sasaki, T.; Ikeda, T. *J. Phys. Chem.* **1995**, *99*, 13013. (j) Trollsås, M.; Sahlén, F.; Gedde, U. W.; Hult, A.; Hermann, D.; Rudquist P.; Komitov, L.; Lagerwall, S. T.; Stebler, B.; Lindström, J.; Rydlund, O. *Macromolecules* **1996**, *29*, 2590.

16 F. Gouda, A. Dahlgren, S. T. Lagerwall, B. Stebler, J. Bömelburg, G. Heppke *Ferroelectrics* **1996**, *178*, 187.

17 Fukuda, A.; Takanishi, Y.; Isozaki, T.; Ishikawa, K.; Takezoe, H. *J. Mater. Chem.* **1994**, *4*, 997.

18 Paleo, M. *Chem. Soc. Rev.*. **1985**, *14*, 45.

19 Amerik, Y. B.; Krentsel, B. A. *J. Polym. Sci., Part C* **1967**, *16*, 1383.

20 Broer, D. J.; Mol, G. C. *Makromol. Chem.* **1989**, *190*, 19.

21 Broer, D. J.; Boven, J.; Mol, G. N.; Challa, G. *Makromol. Chem.* **1989**, *190*, 2255.

22 Hoyle, C. E.; Chawla, C. P.; Griffin, A. C. *Mol. Cryst. Liq. Cryst.* **1988**, *157*, 639.

23 Hoyle, C. E.; Kang, D. *Macromolecules* **1993**, *26*, 844.

24 Hoyle, C. E.; Kang, D.; Jariwala, C.; Griffin, A. C. *Polymer* **1993**, *34*, 3070 .

25 Perplies, E.; Ringsdorf, H.; Wendorff, J. H. *J. Polym. Sci., Polym. Lett. Ed.* **1975**, *13*, 243.

26 He, L.; Zhang, S.; Jin, S.; Qi, Z. *Polym. Bull.* **1995**, *34*, 7.

27 Guymon, C. A.; Hoggan, E. N.; Clark, N. A.; Rieker, T. P.; Walba, D. M.; Bowman, C. N. *Science* **1997**, *275*, 57.

28 Paleos, C. M.; Labes, M. M. *Mol. Cryst. Liq. Cryst.* **1970**, *11*, 385.

29 Perplies, E.; Ringsdorf, H.; Wendorff, J. H. *Makromol. Chem.* **1974**, *175*, 553.

30 Hohn, W.; Tieke, B. *Macromol. Chem. Phys.* **1996**, *197*, 2753.

31 Hoyle, C. E.; Mathias, L. J.; Jariwala, C.; Sheng, D. *Macromolecules* **1996**, *29*, 3182.

32 Hahn, B.; Wendorff, J. H.; Portugall, M.; Ringsdorf, H. *Colloid Polym. Sci.* **1981**, *259*, 875.

33 Nakano, T.; Hasegawa, T.; Okamoto, Y. *Macromolecules* **1993**, *26*, 5494.

34 Tanaka, Y.; Yamaguchi, F.; Shiraki, M.; Okada, A. *J. Polym. Sci., Polym. Chem. Ed.* **1978**, *16*, 1027.

35 Shindo, T.; Uryu, T. *J. Polym. Sci., Part A* **1992**, *30*, 363.

36 Broer, D. J.; Finkelmann, H.; Kondo, K. *Makromol. Chem.* **1988**, *189*, 185.

37 Broer, D. J.; Hikmet, R. A. M.; Challa, G. *Makromol. Chem.* **1989**, *190*, 3201.

38 Broer, D. J.; Gossink, R. G.; Hikmet, R. A. M. *Angew. Makromol. Chem.* **1990**, *183*, 45.

39 (a) Hikmet, R. A. M.; Higgins, J. A. *Liq. Cryst.* **1992**, *12*, 831. (b) Andersson, H.; Trollsås, M.; Gedde, U. W.; Hult, A. *Macromol. Chem. Phys.* **1995**, *196*, 3667. (c) Hikmet, R. A. M.; Lub, J.; Higgins, J. A. *Polymer* **1993**, *34*, 1736.

40 Hikmet, R. A. M.; Lub, J.; Broer, D. J. *Adv. Mater.* **1991**, *3* , 392.

41 (a) Zhang, J.; Carlen, C. R.; Palmer, S.; Sponsler, M. B. *J. Am. Chem. Soc.* **1994**, *116*, 7055. (b) van Nostrum, C. F.; Nolte, R. J. M.; Broer, D. J.; Fuhrman, T.; Wendorff , J. H. *Chem. Mater.* **1998**, *10*, 135.

42 Heynderickx, I.; Broer, D. J. *Mol. Cryst. Liq. Cryst.* **1991**, *203*, 113.

43 Broer, D. J.; Lub, J.; Mol, G. N. *Nature* **1995**, *378*, 467.

44 Hikmet, R. A. M.; Lub, J. *J. Appl. Phys.* **1995**, *77*, 6234.

45 Hikmet, R. A. M. *Macromolecules* **1992**, *25*, 5759.

46 Semmler, K.; Finkelmann, H. *Macromol. Chem. Phys.* **1995**, *196*, 3197.

47 Trollsås, M.; Orrenius, C.; Sahlén, F.; Gedde, U. W.; Norin, T.; Hult, A.; Hermann, D.; Rudquist, P.; Komitov, L.; Lagerwall, S. T.; Lindström, J. *J. Am. Chem. Soc.* **1996**, *118*, 8542.

Chapter 2

Polymerization of Liquid-Crystalline Monomers Having Schiff-Base Structure

2-1. Introduction

Highly oriented polymers exhibit anisotropy in optical, electrical and thermomechanical properties.[1] Many works have recently been reported on polymer films with anisotropic molecular alignment obtained by bulk polymerization of LC monomers such as acrylate,[2] methacrylate,[3] vinyl ether,[4] epoxide[5] and styrene[6] derivatives. The LC monomers, especially NLC monomers which show lower viscosity than Sm LC monomers, can be macroscopically oriented by external forces such as an electric and a magnetic field, elongational flow and surface orientation (e.g. by a rubbed polyimide (PI) layer). Monomer organization may affect the polymerization kinetics, the polymer structure and the microstructure of macromolecules.[2e-2g,3a-3c,4] The effect of LC ordering on the polymerization behavior of mesomorphic vinyl monomers has been investigated extensively. However, there is little agreement concerning the influence of the two basic properties of LC materials on the polymerization behavior, orientation and mobility, and these two competing factors make it difficult to formulate a general statement on the effect of LC ordering on the polymerization behavior and hence explain the variance in results. Paleos et al. reported the synthesis and polymerization of acrylic and methacrylic Schiff-base molecules which formed LC phases.[7] The polymerization behavior was not affected by phase structures and external forces. On the other hand, Perplies et al. demonstrated that the polymerization behavior of Schiff-base molecules was affected by phase structure and external forces such as a magnetic field, then the rate increased suddenly

when the phase became I or an LC phase under an electric field.[8,9] Therefore, the polymerization of each mesomorphic monomer which has Schiff-base structure has to be studied in more detail. The aims of the present chapter are to elucidate the effect of the phase structure, N and I phases, on the polymerization behavior of monomers which have Schiff-base structure and to explore the orientation of polymers obtained by thermal polymerization and photopolymerization in detail. To eliminate the effect of molecular structure on the polymerization behavior, methacrylate monomers with the same structure except the end group but with a different phase behavior were examined: one with an ethyl end-group shows no LC phase while the other with an ethoxyl end-group exhibits an N phase.

2-2. Experimental

2-2-1. Materials

Three monomers, (4-methacryloyloxybenzylidene)-4-ethylaniline (**ME**), (4-methacryloyloxybenzylidene)-4-ethoxyaniline (**MBEA**), (4-acryloyloxybenzylidene)-4-butoxyaniline (**ABBA**), were synthesized and purified as reported previously (Scheme 2-1).[9-11]

General Method of Preparation. Unless otherwise noted, materials and solvents were purchased from commercial suppliers and were used without further purification. The structure and transition temperatures are shown in Figure 2-1. The compounds were characterized by means of ^{1}H NMR (Brucker AC200, 200 MHz), IR (Hitachi 260-10) and elemental analysis.

Synthesis of Schiff-Base Monomers

Potassium 4-formylphenoxide. 4-Hydroxybenzaldehyde (25 g, 0.20 mol) was dissolved in ethanol (300 mL) and potassium hydroxide (11 g, 0.20 mol) was added. The solution was stirred at room temperature for 24 h, then dried over anhydrous

Scheme 2-1. Synthetic route of monomers with Schiff-base structure

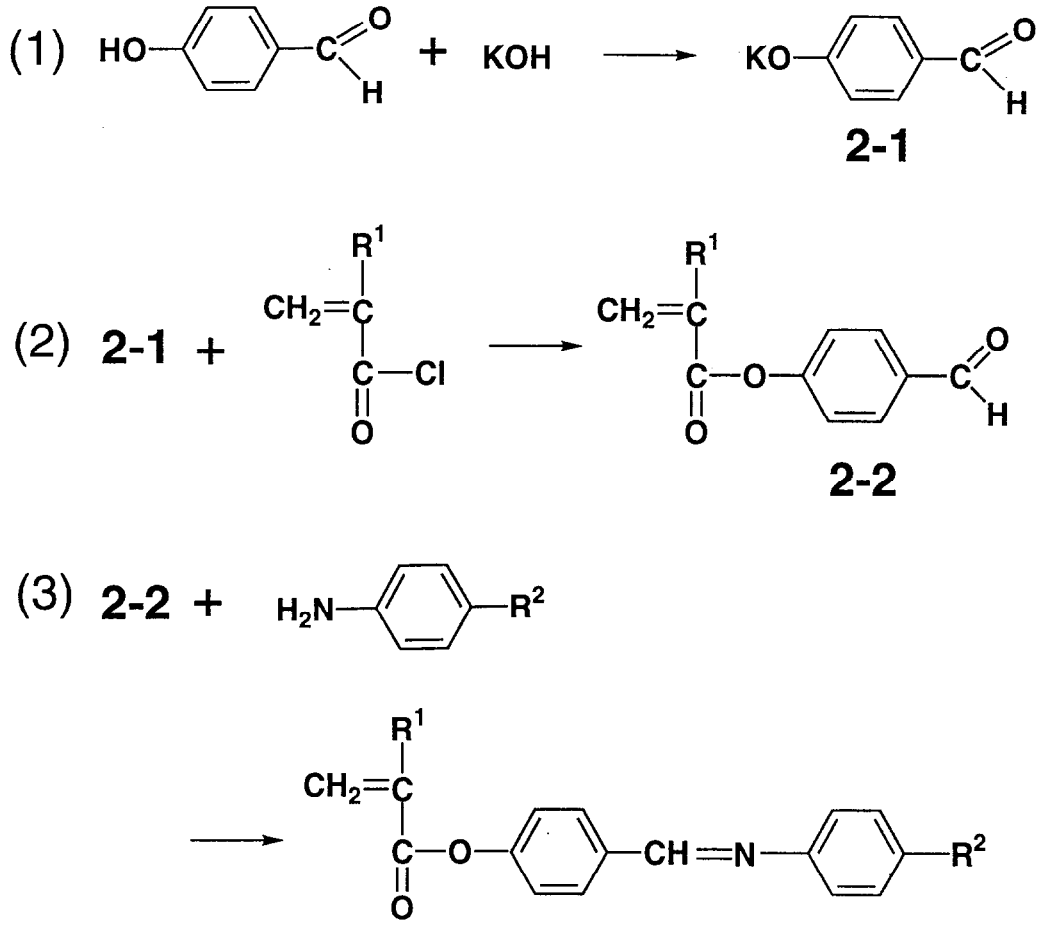

	R^1	R^2
ME	CH_3	C_2H_5
MBEA	CH_3	OC_2H_5
ABBA	H	OC_4H_9

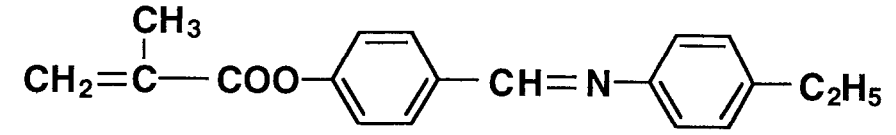

ME **K 62 I**

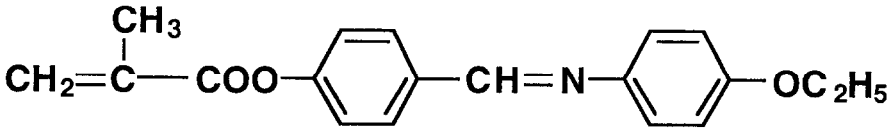

MBEA **K 96 N 110 I**

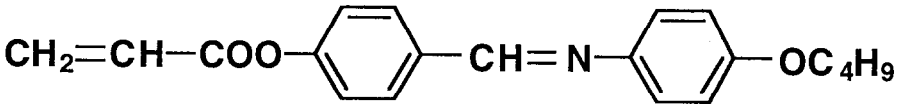

ABBA **K 80 N 123 I**

Figure 2-1. Structures and phase transition temperature of monomers used in this chapter.
Abbreviations: K, crystal; N, nematic; I, isotropic.

sodium sulphate. The solvent was removed by evaporation under reduced pressure. The grey crude was obtained.

Yield: 30 g (0.18 mol, 90 %)

4-Methacryloyloxybenzaldehyde. Potassium 4-formylphenoxide (30 g, 0.18 mol) and trace amount of hydroquinone were suspended in distilled dichloromethane (300 mL), and the resulting solution was cooled at 0 °C. With stirring, methacryloyl chloride (50 g, 0.48 mol) dissolved in distilled dichloromethane (50 mL) was added dropwise to the solution, and the reaction mixture was stirred at room temperature for 24 h. The reaction mixture was poured into saturated aqueous sodium hydrogen carbonate (100 mL x 3) and aqueous sodium chloride (100 mL x 2). The solution was dried over anhydrous sodium sulphate. After the solvent was removed, deep purple liquid obtained was purified by column chromatography on silica gel (dichloromethane) to yield a yellow oil.

Yield: 29 g (0.15 mol, 78 %)

^{1}H NMR (δ, $CDCl_3$): 10.01(s, 1H), 7.94(d, 2H), 7.32(d, 2H), 6.40(s, 1H), 5.82(s, 1H), 2.11(s, 3H)

IR (KBr, cm^{-1}): 2940, 2850, 1740, 1640, 1500, 1390, 950

(4-Methacryloyloxybenzylidene)-4-ethylaniline (ME). 4-Methacryloyloxybenzaldehyde (10 g, 0.053 mol) and trace amount of hydroquinone were dissolved in distilled diethyl ether (200 mL), and the resulting solution was cooled at 0 °C. With stirring, 4-ethylaniline (10 g, 0.080 mol) dissolved in distilled diethyl ether (40 mL) was added dropwise to the solution. After the reaction mixture was stirred at room temperature for 6 h, the precipitate was filtered off. The filtrate was evaporated to dryness. The crude product was purified by column chromatography on silica gel (dichloromethane/ethyl acetate = 30/1) and recrystallized from hexane to yield a cream crystal.

Yield: 5.5 g (0.019 mol, 36 %)

mp: 62 °C

^{1}H NMR (δ, $CDCl_3$): 8.46(s, 1H), 8.08-7.78(m, 2H), 7.43-7.00(m, 6H), 6.37(m, 1H), 5.78(m, 1H), 2.67(q, 2H), 2.07(m, 3H), 1.26(t, 3H)

IR (KBr, cm^{-1}): 2950, 1720, 1620, 1580, 1500, 970

Anal. Calcd for $C_{19}H_{19}NO_2$ (293): C, 77.79; H, 6.53; N, 4.77 %

Found. C, 77.71; H, 6.59; N, 4.75 %

UV: λmax (ethanol) = 270 nm, ε = 1.8 x 10^4

(4-Methacryloyloxybenzylidene)-4-ethoxyaniline (MBEA). 4-Methacryloyloxybenzaldehyde (15 g, 0.076 mol) and trace amount of hydroquinone were dissolved in distilled dichloromethane (200 mL), and the resulting solution was cooled at 0 °C. With stirring, *p*-phenetidine (16 g, 0.11 mol) dissolved in distilled dichloromethane (50 mL) was added dropwise to the solution. After the reaction mixture was stirred at room temperature for 24 h, the precipitate was filtered off. The filtrate was evaporated to dryness. The crude product was purified by column chromatography on silica gel (dichloromethane/ethyl acetate = 30/1) and recrystallized from hexane to yield a light yellow crystal.

Yield: 3.6 g (0.012 mol, 16 %)

mp: 96 °C

^{1}H NMR (δ, $CDCl_3$): 8.47(s, 1H), 7.98-7.86(m, 2H), 7.26-7.18(m, 4H), 6.98-6.88(m, 2H), 6.37 (m, 1H), 5.78(m, 1H), 4.06(q, 2H), 2.08(m, 3H), 1.43(t, 3H)

IR (KBr, cm^{-1}): 2950, 1730, 1620, 1580, 1510, 1480, 960

Anal. Calcd for $C_{19}H_{19}NO_3$ (309): C, 73.76; H, 6.19; N, 4.53 %

Found. C, 73.69; H, 5.94; N, 4.47 %

UV: λmax (ethanol) = 270 nm, ε = 1.2 x 10^4

4-Acryloyloxybenzaldehyde. Potassium 4-formylphenoxide (15 g, 0.091 mol) and trace amount of hydroquinone were suspended in distilled dichloromethane (300 mL), and the resulting solution was cooled at 0 °C. With stirring, acryloyl chloride (25 g,

0.28 mol) dissolved in distilled dichloromethane (50 mL) was added dropwise to the solution, and the reaction mixture was stirred at room temperature for 19 h. The reaction mixture was poured into saturated aqueous sodium hydrogen carbonate (100 mL x 3) and aqueous sodium chloride (100 mL x 2). The solution was dried over anhydrous sodium sulphate. After the solvent was removed, light brown oil was purified by column chromatography on silica gel (dichloromethane) to yield a yellow oil.

Yield: 15 g (0.084 mol, 92 %)

^{1}H NMR (δ, $CDCl_3$): 10.00(s, 1H), 7.94(d, 2H), 7.33(d, 2H), 6.67(dd, J = 2, 17 Hz, 1H), 6.33(dd, J = 10, 17 Hz, 1H), 6.07(dd, J = 2, 10 Hz, 1H)

IR (KBr, cm^{-1}): 2860, 1740, 1630, 1500, 1400, 980

(4-Acryloyloxybenzylidene)-4-butoxyaniline (ABBA). 4-Acryloyloxybenzaldehyde (15 g, 0.084 mol) and trace amount of hydroquinone were suspended in distilled dichloromethane (100 mL), and the resulting solution was cooled at 0 °C. With stirring, 4-n-butoxyaniline (16 g, 0.094 mol) dissolved in distilled dichloromethane (25 mL) was added dropwise to the solution, and the reaction mixture was stirred at room temperature for 22 h, then the precipitate was filtered off. The filtrate was evaporated, purified by column chromatography on silica gel (dichloromethane) and recrystallized from hexane to yield a light yellow crystal.

Yield: 7.7 g (0.024 mol, 28 %)

mp: 80 °C

^{1}H NMR (δ, $CDCl_3$): 8.46(s, 1H), 8.04-7.78(m, 2H), 7.39-7.07(m, 4H), 7.02-6.80(m, 2H), 6.65(dd, J = 2, 18 Hz, 1H), 6.31(dd, J = 10, 18 Hz, 1H), 6.03(dd, J = 2, 10 Hz, 1H), 3.98(t, 2H), 1.98-1.29(m, 4H), 0.98(t, 3H)

IR (KBr, cm^{-1}): 2950, 1740, 1620, 1600, 1500, 970

Anal. Calcd for $C_{20}H_{21}NO_3$ (323): C, 74.28; H, 6.55; N, 4.33 %

Found. C, 74.22; H, 6.58; N, 4.32 %

UV: λmax (ethanol) = 270 nm, ε = 1.4 x 10^4

2-2-2. Characterization of Schiff-Base Monomers

LC behavior and phase transition temperature were examined by differential scanning calorimetry (DSC; Seiko I&E SSC-5200 and DSC220C; heating and cooling rate, 5 °C/min) and optical polarizing microscopy (Olympus Model BH-2; Mettler FP82HT hot stage and Mettler FP90 central processor). The thermodynamic properties of the LCs are given in Figure 2-1.

2-2-3. Preparation of Reference Polymer by Solution Polymerization

Reference polymer of **ABBA** was prepared by solution polymerization by using AIBN as an initiator. **ABBA** (0.5 g) with 2 mol% of AIBN was dissolved in benzene (5 ml) and placed in a tube. The tube was evacuated under vacuum and sealed. Polymerization was conducted at 60 °C for 44 h. To purify the polymer, it was dissolved in chloroform and precipitated into methanol. The purification was repeated until no monomer was detected by GPC. The polymer was dried under vacuum at room temperature. Poly(**ABBA**) exhibited no LC phase and thermal decomposition occurred above 200 °C.

2-2-4. Polymerization Procedure

The author confirmed that spontaneous thermal polymerization occurred during injection of **ME** or **MBEA** into the glass cell. So **ME** and **MBEA** were thermally polymerized without an initiator. However, no thermal polymerization occurred spontaneously during injection of **ABBA** into the glass cell. Therefore, a mixture of **ABBA** and an initiator (2 mol%) was prepared by dissolving each component in dichloromethane and subsequent evaporation of the solvent under vacuum. Benzil was added as a photoinitiator and AIBN was used as a thermal initiator.

The thermal polymerization of the monomers was carried out isothermally at various temperatures within the range from 65 °C to 150 °C. Monomer samples (5-8 mg) containing AIBN (2 mol%) were placed in indented DSC pans and sealed, and they were kept in the I phase for 10 min in the calorimeter. For **ME** and **MBEA**, AIBN was

not added in the sample. Then, they were slowly cooled down to polymerization temperature. The conversion was determined by calculating the enthalpies from the area under the DSC curve.[12] Initial rate of polymerization was calculated from the initial slope of the time-conversion curve.

Photopolymerization was performed in a glass cell with a gap of 20 μm. Samples for photopolymerization were prepared by injecting **ABBA** containing benzil as a photoinitiator (2 mol%) into the glass cell in the I phase. After the samples were prepared, they were slowly cooled down to polymerization temperature. Photoirradiation was performed at > 430 nm (intensity at 436 nm, 90 mW/cm^2) isolated with glass filters from a 500 W high-pressure mercury lamp. The course of the polymerization was followed by gel permeation chromatography (GPC; Toyo Soda HLC-802; column, GMH6 x 2 + G4000H8; eluent, chloroform). The conversion was estimated from Equation 2-1.

$$\text{Conversion (\%)} = P / (P + M) \times 100 \qquad (2\text{-}1)$$

where P is the peak area in the GPC chart corresponding to the polymers produced and M is that corresponding to the unreacted monomers. The number-average molecular weight (Mn) of the polymers was determined by GPC calibrated with standard polystyrenes.

Gel was extracted with chloroform in the Soxhlet extractor for 15 h. The extract was concentrated and soluble polymer was recovered by precipitation of the solution into a large excess of methanol. The gel fraction was estimated by Equation 2-2.

$$\text{Gel fraction (\%)} = G / (S + G) \times 100 \qquad (2\text{-}2)$$

where S is the yield of the soluble polymer and G is that of the insoluble part.

2-3. Results and Discussion

2-3-1. Polymerization Behavior

Polymerization was performed in three distinct temperature regions: (a) in crystalline (K) phase, (b) in N phase, and (c) in I phase. The results are shown in Figures 2-2, 2-3 and 2-4 where final conversions are plotted as a function of the polymerization temperature. No polymerization occurred in K phase of the monomers used in this study. The final conversion decreased as temperature increased in the I phase in every monomer (Figures 2-2, 2-3 and 2-4). However, the conversion increased with temperature in the N phase. These results are in fair agreement with those of Perplies et al.[8,9] They suggested that orientation of monomers affects the polymerization behavior. Furthermore, viscosity decreases as temperature increases, then addition of monomers to the propagating polymer radicals becomes favored due to enhanced diffusion of each species, which may result in higher conversion with temperature in the N phase. For **ME** and **MBEA**, glass transition temperature (Tg) of polymers were 216 °C and 210 °C, respectively. Maximum conversions were below 75 % for three monomers in this study. It is assumed that maximum conversions are affected by both equilibrium polymerization and diffusion-controlled termination. Since Mn decreased with temperature in **MBEA** at higher temperature (> 120 °C), it is expected that equilibrium polymerization mainly affects kinetics. For **ABBA**, it is expected that the half life of initiator decreases because of high polymerization temperature. It can therefore be presumed that dead-end polymerization occurs in this system.

Figure 2-5 shows initial rates of thermal polymerization of **ABBA** with AIBN (2 mol%) at various temperatures. The initial rate of polymerization increased monotonously with temperature. Similar results were obtained for the other monomers used in this chapter. The rate of thermal polymerization (R_p) is expressed by Equation 2-3,[13]

$$R_p = (k_p/k_t^{1/2}) \times k_i^{1/2} \times [M]^2 \qquad (2\text{-}3)$$

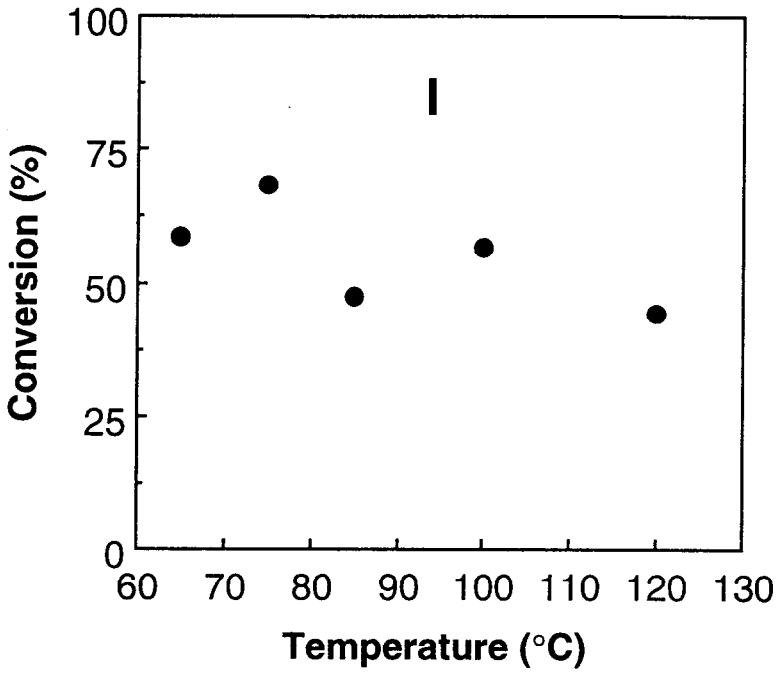

Figure 2-2. Final conversion in thermal polymerization of **ME** at various temperatures. Initiator was not used in the polymerization.

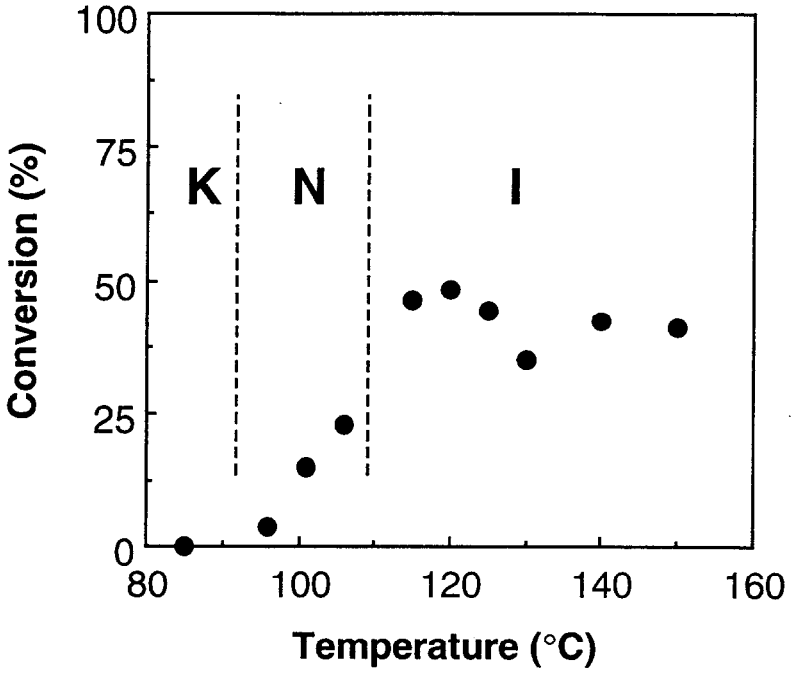

Figure 2-3. Final conversion in thermal polymerization of **MBEA** at various temperatures. Initiator was not used in the polymerization.

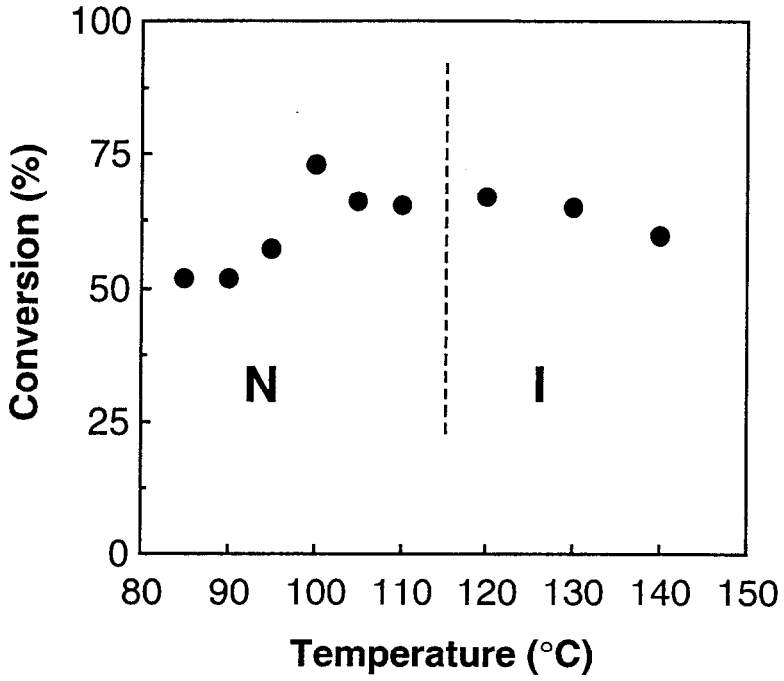

Figure 2-4. Final conversion in thermal polymerization of **ABBA** with AIBN (2 mol%) at various temperatures.

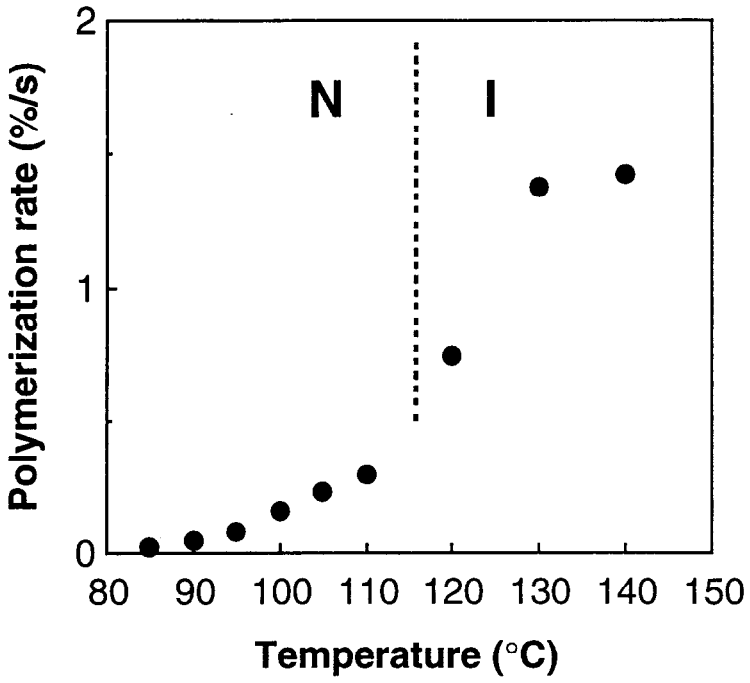

Figure 2-5. Initial rates of thermal polymerization of **ABBA** with AIBN (2 mol%) at various temperatures.

where k_p, k_t and k_i are the rate constants of propagation, termination and initiation, respectively, and [M] is the concentration of monomer. It may be expected that the increase of k_p with temperature is larger than that of k_t in the present Schiff-base monomers. Then, the terms of $(k_p/k_t^{1/2})$ and $k_i^{1/2}$ increase with temperature and R_p increases with temperature.

Figure 2-6 shows Arrhenius plots for the initial rates of thermal and photopolymerization of **ABBA**. It was observed that in the thermal polymerization the activation energy was larger in the N phase than in the I phase. The thermal polymerization in the N phase occurs simultaneously with alignment of monomers, so polymerization competes with the alignment process. It is expected that the alignment process of monomers interferes with propagation process in the polymerization. It is reasonable, therefore, that activation energy of the thermal polymerization in the N phase is larger than that in the I phase. On the other hand, the activation energy of photopolymerization was constant regardless of the phase structure of monomer. This is presumably because photopolymerization can be carried out after the state of the monomer is completely in equilibrium with its intrinsic phase structure.

Figure 2-7 shows the relation between Mn of the polymer obtained and the polymerization temperature. It must be mentioned here that Mn of the polymer produced by thermal polymerization of **ME** which showed only I phase was constant regardless of polymerization temperature as shown in Figure 2-7(A). On the other hand, Mn of the polymer produced by thermal polymerization of **MBEA** depended on the temperature: as is shown in Figure 2-7(B), Mn of the polymer obtained in the N phase was higher than that in the I phase, and Mn increased discontinuously at slightly higher temperature than the N-I phase transition temperature. At the N-I phase transition temperature, the orientation of monomer is absent macroscopically, but it remains microscopically, then this microscopic orientation of monomers might be advantageous for the reaction between propagating radicals and monomers. At lower temperature in the I phase of monomers, phase transition occurs from I to glassy (G) phase during polymerization of **ME**, although phase transition occurs from I to G phase

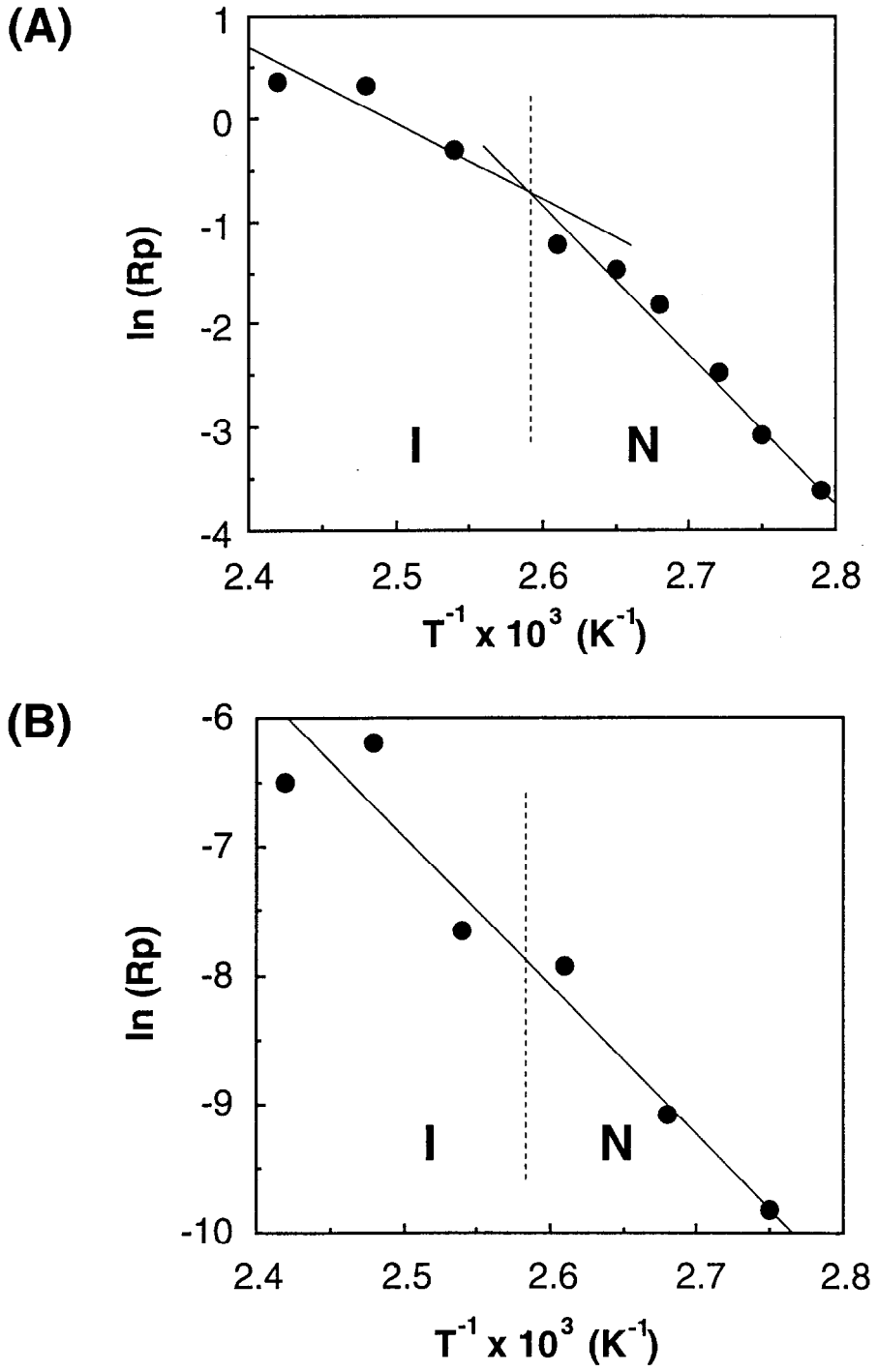

Figure 2-6. Arrhenius plots for the initial rates of polymerization of **ABBA**. (A), thermal polymerization with 2 mol% AIBN; (B), photopolymerization with 2 mol% benzil.

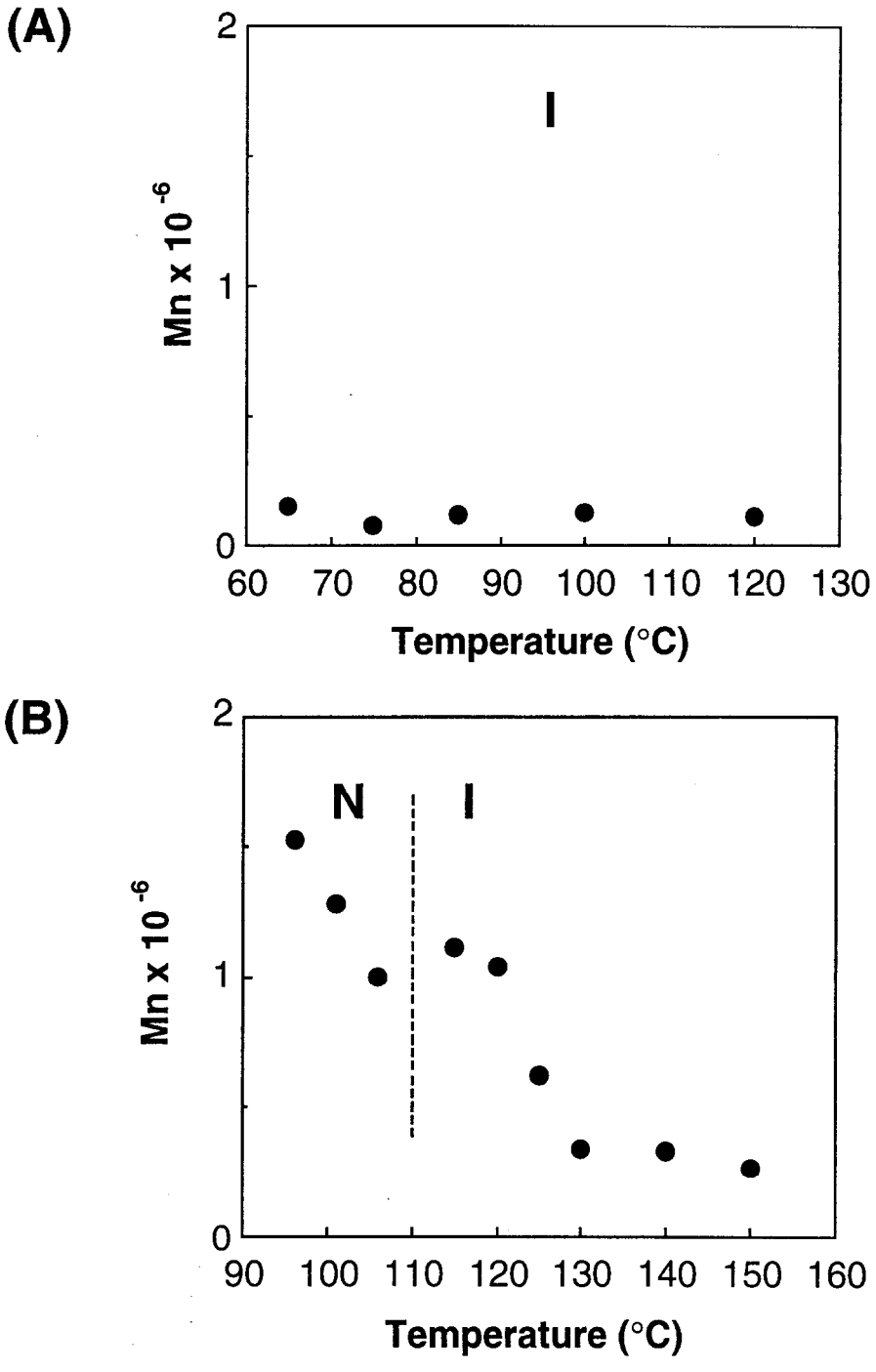

Figure 2-7. Mn of polymers obtained by thermal polymerization at various temperatures. Initiator was not used in the polymerization. (A), **ME**; (B), **MBEA**.

through Sm phase during polymerization of **MBEA**. Based on Figures 2-2, 2-3 and 2-7, it is anticipated that polymerization behavior was affected by diffusion-controlled termination for **ME** and by equilibrium polymerization for **MBEA**. This may account for the difference in Mn of polymers obtained in the I phase between **ME** and **MBEA**. Furthermore, Mn of the polymer obtained by thermal polymerization of **ABBA** was constant at any polymerization temperature examined. It was observed that the polymer produced by thermal polymerization of **ABBA** precipitated during polymerization. Poly(**ABBA**) is not soluble in its monomer, **ABBA**, so that it is expected that poly(**ABBA**) precipitates after the polymer grows to a certain degree of polymerization. This may be an origin of the constant Mn of the polymer of **ABBA** in the thermal polymerization.

Figure 2-8 shows conversion for photopolymerization of **ABBA** with benzil (2 mol%) at 140 °C and gel fraction in the polymer as a function of time. Conversion increased with polymerization time and was saturated at the later stage. Furthermore, gel was produced even at the initial stage of polymerization. It should be noted that the gel fraction in the polymer increased with polymerization time.

The excited triplet state (T_1) of benzil abstracts hydrogen from hydrogen-donating molecules such as polymers produced and monomers.[14] When hydrogens of the polymers are abstracted, polymer radicals are produced and the resulting polymer radicals are readily recombined to form crosslinking. To clarify if this is the case, poly(**ABBA**) synthesized separately by solution polymerization was irradiated at 366 nm in the presence of benzil (2 mol% with respect to the monomer units in the polymer) in the cell. It was found that gel was formed.

2-3-2. Alignment of Polymer Produced

The molecular alignment of the polymers was explored by optical polarizing microscopy. To compare the orientation of polymers produced by thermal polymerization and photopolymerization, **ABBA** was polymerized in the N and I phases in the cells with 20-μm gap. After the polymerization, the cell was opened and

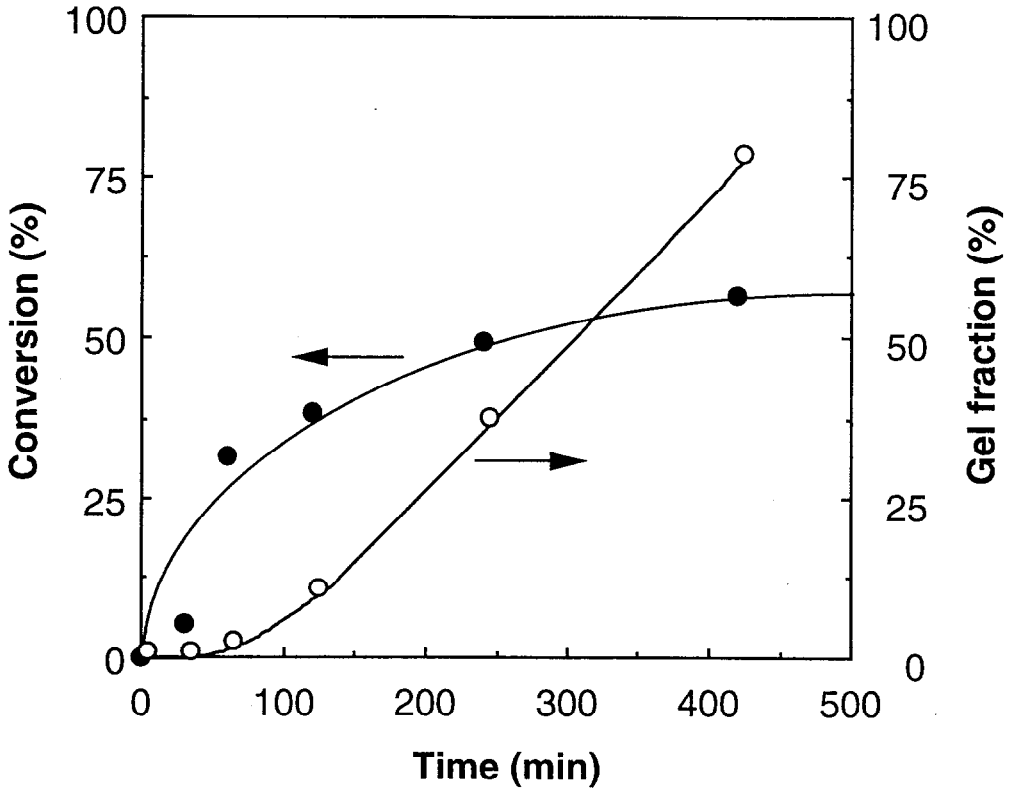

Figure 2-8. Time-conversion curve (●) and gel fraction (○) in the photopolymerization of **ABBA** with benzil (2 mol%) at 140 °C.

the polymerization mixture was thoroughly washed with methanol to remove unreacted monomers and initiator. Washing of the product was repeated until no absorption of the monomer and the initiator was detected in the washings by UV absorption spectroscopy. The sample was then dried and examined with the polarizing microscope on the optical anisotropy.

The polymers produced in the I phase showed no birefringence either in thermal polymerization or in photopolymerization. Surprisingly, however, the polymers prepared in the N phase showed birefringence regardless of the polymerization method. The birefringence was very stable and remained unchanged up to 200 °C in both samples obtained by thermal polymerization and photopolymerization. The optical texture observed after thermal polymerization at 90 °C in the N phase is shown in Figure 2-9(A). The black circular parts were observed in the texture, which resulted presumably from evolution of nitrogen gas by decomposition of AIBN. As is clearly seen, the polymer after polymerization in the N phase partially exhibited LC phase. It must be emphasized here that poly(**ABBA**) obtained by solution polymerization showed no LC phase. This means that poly(**ABBA**) exhibits no LC nature even though its monomer is mesogenic. It is well known that orientation of LC molecules is strongly affected by interface between the LC molecules and the substrate.[15] In fact, in LCD devices, alignment layers (usually PIs) are always employed to obtain better orientation of the mesogens. In the present system, the Schiff-base monomers are aligned due to the LC nature and the orientation is enhanced at the interface. On polymerization of the aligned monomers, mesogens may still be oriented owing to the effect of the interface, although the polymer itself loses the LC nature. If this is the case, the polymer produced by photoirradiation with benzil as the initiator should show better orientation of mesogens because in the photopolymerization one can polymerize the LC monomers after they are completely oriented. As is shown in Figure 2-9(B), the polymer obtained by photopolymerization exhibited much better orientation of mesogens. In the photopolymerized polymer, another factor could enhance further the

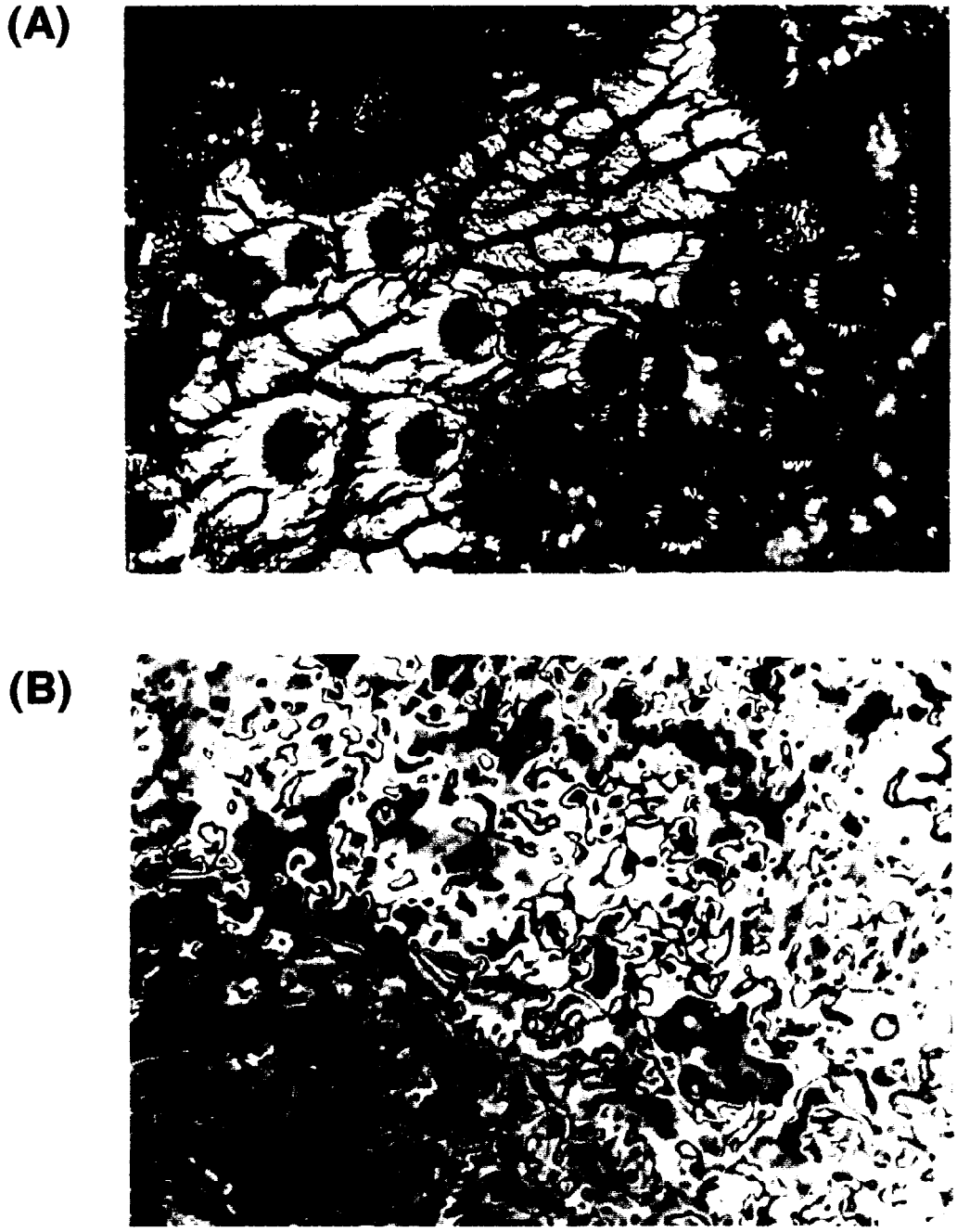

Figure 2-9. Textures observed after polymerization of **ABBA** in the N phase. The sample was thoroughly washed with methanol to remove unreacted monomers and initiator. (A), thermal polymerization; (B), photopolymerization.

orientation. As described before, gel was formed in the photopolymerization. It is highly possible that crosslinking enables the alignment of mesogens more stable.

2-4. Conclusion

Polymerization behavior of the Schiff-base vinyl monomers in bulk was explored and the results showed that the initial rate of polymerization was governed by molecular diffusion and the final conversion may be affected by molecular alignment. It was also found that Mn of the polymer obtained by thermal polymerization in the N phase was higher than that in the I phase. The polymer produced by solution polymerization showed no LC phase. However, very surprisingly, the polymer produced in the N phase exhibited LC phase even after the sample was thoroughly washed with methanol to remove unreacted monomers and initiator. Expectedly, the crosslinked polymer obtained on photoirradiation of **ABBA** was better aligned than that produced in the thermal polymerization.

References

1 (a) Hikmet, R. A. M.; Howard, R. *Phys. Rev. E* **1993**, *48*, 2752. (b) Broer, D. J.; Lub, J.; Mol, G. N. *Nature* **1995**, *378*, 467. (c) Broer, D. J. *Mol. Cryst. Liq. Cryst.* **1995**, *261*, 513. (d) Sahlèn, F.; Andersson, H.; Hult, A.; Gedde, U. W.; Ania, F. *Polymer* **1996**, *37*, 2657.

2 (a) Broer, D. J.; Finkelmann, H.; Kondo, K. *Makromol. Chem.* **1988**, *189*, 185. (b) Broer, D. J.; Mol, G. N. *Makromol. Chem.* **1989**, *190*, 19. (c) Broer, D. J.; Boven, J.; Mol, G. N.; Challa, G. *Makromol. Chem.* **1989**, *190*, 2255. (d) Hikmet, R. A. M.; Lub, J. *J. Appl. Phys.* **1995**, *77*, 6234. (e) He, L.; Zhang, S.; Jin, S.; Qi, Z. *Polym. Bull.* **1995**, *34*, 7. (f) Hoyle, C. E.; Mathias, L. J.; Jariwala, C.; Sheng, D. *Macromolecules* **1996**, *29*, 3182. (g) Guymon, C. A.; Hoggan, E. N.; Clark, N. A.; Rieker, T. P.; Walba, D. M.; Bowman, C. N. *Science* **1997**, *275*, 57.

3 (a) Broer, D. J.; Mol, G. N.; Challa, G. *Polymer* **1991**, *32*, 690. (b) Hoyle, C. E.; Kang, D.; Jariwala, C.; Griffin, A. C. *Polymer* **1993**, *34*, 3070. (c) Hoyle, C. E., Watanabe, T. *Macromolecules* **1994**, *27*, 3790. (d) Hoyle, C. E.; Watanabe, T., Whitehead, J. B. *Macromolecules* **1994**, *27*, 6581. (e) Sahlèn, F.; Trollsås, M.; Hult, A.; Gedde, U. W. *Chem. Mater.* **1996**, *8*, 382.

4 (a) Hellermark, C.; Gedde, U. W.; Hult, A. *Polym. Bull.* **1992**, *28*, 267. (b) Andersson, H.; Gedde, U. W.; Hult, A. *Polymer* **1992**, *33*, 4014.

5 (a) Broer, D. J.; Lub, J.; Mol, G. N. *Macromolecules* **1993**, *26*, 1244. (b) Jahromi, S.; Lub, J.; Mol, G. N. *Polymer* **1994**, *35*, 622.

6 (a) Andersson, H.; Trollsås, M.; Gedde, U. W.; Hult, A. *Macromol. Chem. Phys.* **1995**, *196*, 3667. (b) Williamson, S. E.; Kang, D.; Hoyle, C. E. *Macromolecules* **1996**, *29*, 8656.

7 Paleos, C. M., Labes, M. M. *Mol. Cryst. Liq. Cryst.* **1970**, *11*, 385.

8 (a) Perplies, E.; Ringsdorf, H.; Wendorff, J. H. *Ber. Bunsenges. Phys. Chem.* **1974**, *78*, 921. (b) Perplies, E.; Ringsdorf, H.; Wendorff, J. H. *J. Polym. Sci., Polym. Lett. Ed.* **1975**, *13*, 243.

9 Perplies, E.; Ringsdorf, H.; Wendorff, J. H. *Makromol. Chem.* **1974**, *175*, 553.

10 Ringsdorf, H.; Greber, G. *Makromol. Chem.* **1959**, *1*, 27.

11 Strzelecki, L.; Liebert, L. *Bull. Soc. Chim.* **1973**, 605.

12 (a) Doornkamp, A. T.; Alberda van Ekenstein, G. O. R.; Tan, Y. Y. *Polymer* **1992**, *33*, 2863. (b) Chandra, R.; Soni, R. K. *Polym. Int.* **1993**, *31*, 239.

13 Flory, P. J. *Principles of Polymers Chemistry*; Cornell Univ. Press, Ithaca, New York, 1953; Chapter 4.

14 Rabek, J. F. *Mechanisms of Photophysical Processes and Photochemical Reactions in Polymers (Theory and Applications)*; John Wiley & Sons, 1987; p 306.

15 (a) Iimura, Y.; Kobayashi, N.; Kobayashi, S. *Jpn. J. Appl. Phys.* **1995**, *34*, 1935. (b) Gu, D.-F.; Uran, S.; Rosenblatt, C. *Liq. Cryst.* **1995**, *19*, 427.

Chapter 3

Thermal and Photopolymerization of Liquid-Crystalline Monomers with Biphenyl Moiety

3-1. Introduction

Most of NLCs which showed the LC phase at low temperature were Schiff-base compounds in the early stage of the history of LC materials. However, the LCs having the Schiff-base structure showed some drawbacks in that they tend to be hydrolyzed not only in water but also in organic acids.[1] In contrast, LCs having biphenyl or bicyclohexyl moiety showed several advantages: they are chemically stable, and they show LC phase with a lower viscosity at lower temperature than those of the Schiff-base LC materials. These lead to rapid response of the materials to external stimulus. In addition, the compounds containing the bicyclohexyl structure show no absorption in the UV region, extremely small birefringence and small wavelength dispersion of refractive index. These are advantageous for optical materials.

Many works have recently been reported on polymer films with anisotropic molecular alignment obtained by bulk polymerization of LC monomers.[2-21] These monomers are interesting in view of possibility of studying polymerization kinetics in the mesomorphic phase. The Sm, the N and the I phases differ in the orientation, viscosity and mobility of mesogens. Any orientation and configuration such as a twisted N can be induced by shear stress, electric or magnetic fields and at specially treated surfaces. Orientation of the molecules can also be varied locally, and patterned structures can be prepared.

The effect of LC ordering on the polymerization behavior of mesomorphic vinyl monomers has been examined extensively. There is little agreement concerning the influence of the two basic properties of LC materials, ordering and diffusion, on polymerization behavior. There are at least three types of LC monomers reported previously. First, the polymerization rate of some monomers increased with temperature and the polymerizability in the I phase was higher than that in the LC phase.[22,23] In the second type of the LC monomers, the polymerizability in the LC phase was higher than that in the I phase.[24-29] In the third group of the LC monomers, the polymerization behavior was not affected by phase structure and external forces.[30,31]

The rate of initiation (R_i) changes with temperature in the thermal polymerization, while R_i is constant regardless of temperature in the photopolymerization. Therefore, it is expected that the polymerization behavior is affected by the polymerization method, depending on either thermal polymerization or photopolymerization. In addition, there are some problems regarding the solubility of polymer in monomer. As described in Chapter 2, the Mn of the polymer obtained by polymerization of (4-acryloyloxybenzylidene)-4-butoxyaniline (**ABBA**) was constant at any temperature. It was revealed that poly(**ABBA**) precipitated after the polymer grew to a certain degree of polymerization. In the system where precipitation occurs during polymerization, we could not evaluate the effect of phase structure on polymerization procedure precisely. In order to compare the polymerization behavior, especially Mn of the sample by thermal polymerization and photopolymerization, LC monomers possessing a biphenyl structure, in which the corresponding polymer was soluble in the monomer, were used in this chapter.

3-2. Experimental

3-2-1. Materials

Three monomers, 4-acryloyloxy-4'-cyanobiphenyl (**ACB0**), 4-acryloyloxy-4'-decylbiphenyl (**ADB**), 4-acryloyloxy-4'-butylbicyclohexane (**ABBC**), were used in this chapter and the structure and transition temperatures are shown in Figure 3-1. **ACB0** was synthesized as reported previously (Scheme 3-1).[32,33] The compound was characterized by means of ^{1}H NMR, IR and elemental analysis as described in Chapter 2. **ADB** and **ABBC** were obtained from Dainippon Ink & Chemicals, Inc. The phase transition temperature and the phase structure were determined by DSC (heating and cooling rate, 5 °C/min) and optical polarizing microscopy.

4-Acryloyloxy-4'-cyanobiphenyl (ACB0). 4-Cyano-4'-hydroxybiphenyl (5 g, 0.026 mol), triethylamine (3.0 g, 0.030 mol), and trace amount of hydroquinone were suspended in distilled tetrahydrofuran (THF) (50 mL), and the resulting solution was cooled at 0 °C. With stirring, acryloyl chloride (15 g, 0.17 mol) dissolved in distilled THF (20 mL) was added dropwise to the solution, and the reaction mixture was stirred at room temperature for 24 h. Then, dichloromethane (200 mL) was added. The mixture was poured into saturated aqueous sodium hydrogen carbonate (100 mL x 3) and aqueous sodium chloride (100 mL x 2). The solution was dried over anhydrous sodium sulphate. After the solvent was removed, yellow oil obtained was recrystallized from hexane/ethanol = 5/1 to yield a white crystal.

Yield: 3.7 g (0.015 mol, 58 %)

mp: 101 °C

^{1}H NMR (δ, $CDCl_3$): 7.84-7.46(m, 6H), 7.36-7.12(m, 2H), 6.64(dd, J = 1, 17 Hz, 1H), 6.35(dd, J = 10, 17 Hz, 1H), 6.05(dd, J = 1, 10 Hz, 1H)

IR (KBr, cm^{-1}): 2230, 1730, 1610, 1500, 980

Anal. Calcd for $C_{16}H_{11}NO_2$ (249): C, 77.09; H, 4.45; N, 5.62 %

Found. C, 77.25; H, 4.26; N, 5.56 %

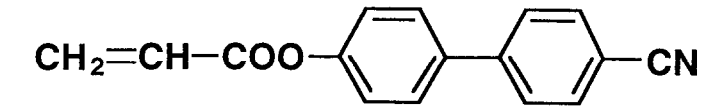

ACB0 **K 101 N 128 I**

ADB **K 53 Sm 73 I**

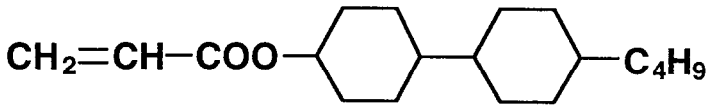

ABBC **K 60 N 91 I**

Figure 3-1. Structures and phase transition temperature of monomers used in this chapter. Abbreviations: K, crystal; Sm, smectic; N, nematic; I, isotropic.

Scheme 3-1. Synthesis of **ACB0**

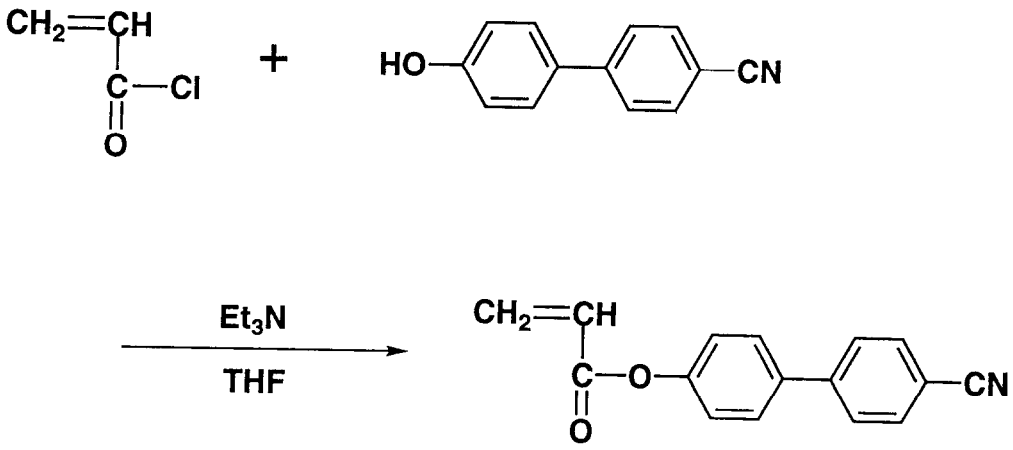

UV: λmax (ethanol) = 273 nm, ε = 1.9 x 10^4

3-2-2. Polymerization Procedure

It was confirmed that spontaneous thermal polymerization occurred during injection of **ACB0** into the glass cell. **ACB0** was thermally polymerized without an initiator. However, no thermal polymerization occurred spontaneously during injection of **ADB** into the glass cell. Therefore, a mixture of **ADB** and an initiator (1 mol%) was prepared by dissolving each component in acetone and subsequent evaporation of the solvent under vacuum. Benzoin was added as a photoinitiator and AIBN was used as a thermal initiator. The I-S phase transition temperature of **ADB** with 1 mol% AIBN and that with 1 mol% benzoin was 71 °C and 68 °C, respectively.

The thermal polymerization of the monomers was carried out isothermally at various temperatures within the range from 55 °C to 150 °C. Monomer samples (9-10 mg) were placed in indented DSC pans and sealed, and they were kept in the I phase for 10 min in the calorimeter. For **ADB**, AIBN (1 mol%) was added in the sample. Then, they were slowly cooled down to polymerization temperature. The conversion was determined by calculating the enthalpies from the area under the DSC curve.[25,34] Initial rate of polymerization was calculated from the initial slope of the time-conversion curve.

Photopolymerization was performed in a glass cell with a gap of 20 μm. Samples for photopolymerization were prepared by injecting **ADB** containing benzoin as a photoinitiator (1 mol%) into the glass cell in the I phase. After the sample was kept in the I phase for 10 min, it was slowly cooled down to polymerization temperature. Photoirradiation was performed at 366 nm (intensity, 3 mW/cm^2) isolated with glass filters from a 500 W high-pressure mercury lamp. The course of the polymerization was followed by GPC as described in Chapter 2.

3-3. Results and Discussion

3-3-1. Polymerization Behavior

Polymerization was performed in three distinct temperature regions: (a) in K phase, (b) in LC phase, and (c) in I phase. No polymerization occurred in K phase of the monomers used in this chapter. The spontaneous thermal polymerization of **ACB0** occurred and the resulting polymer was insoluble in chloroform but soluble in N,N'-dimethylformamide (DMF). Gel was formed after 300-s photoirradiation of **ADB** with 1 mol% benzoin. The excited triplet state (T_1) of benzoin abstracts hydrogen from hydrogen-donating molecules such as polymers produced and monomers.[35] When hydrogens of the polymers are abstracted, polymer radicals are produced and the resulting polymer radicals are readily recombined to form crosslinking. In Chapter 2, when polymer was irradiated in the presence of benzil, gel was formed. However, no gel was produced within 60-s photoirradiation in the present system and then photopolymerization of **ADB** was conducted within 60 s at various temperatures. **ABBC** in the I phase was thermally polymerized without an initiator, although no thermal polymerization of **ABBC** in the N phase occurred spontaneously. Therefore, photopolymerization of **ABBC** could be conducted only in the N phase. However, gel was formed in photopolymerization of **ABBC** in the N phase.

Figure 3-2 shows final conversion of **ACB0** as a function of the polymerization temperature. The final conversion increased with temperature. This is understandable because the propagation process predominates over the termination process such as recombination reaction and disproportionation reaction with rising temperature. In other words, viscosity decreases as temperature increases, then addition of monomers to the propagating radicals becomes favored due to enhanced diffusion of each species. This result suggests that diffusion of monomers affects the polymerization behavior.

The relation between the initial rate of polymerization and the polymerization temperature is shown in Figures 3-3 (**ACB0**) and 3-4 (**ADB**). It was found that the initial rate of polymerization increased monotonously with temperature despite

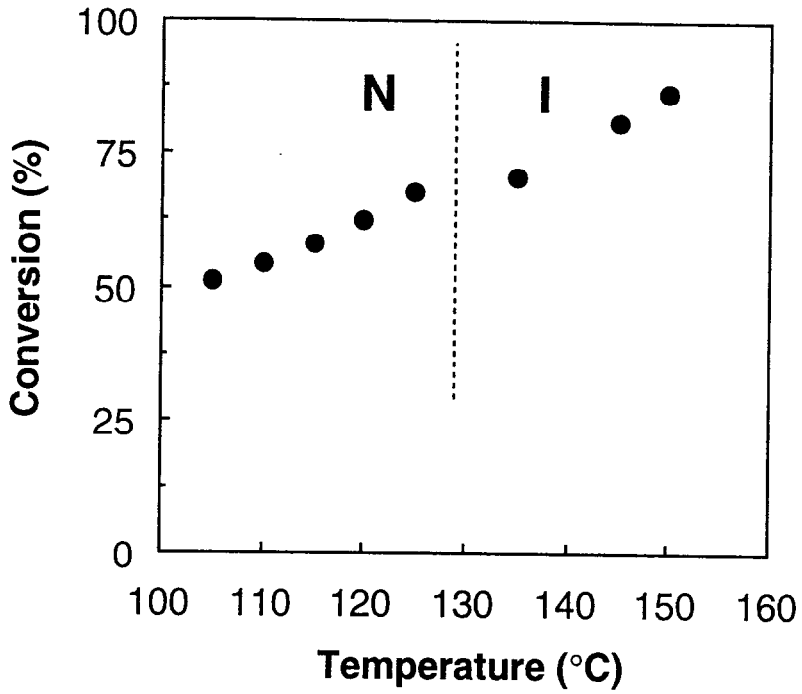

Figure 3-2. Final conversion in thermal polymerization of **ACB0** at various temperatures. Initiator was not used in the polymerization.

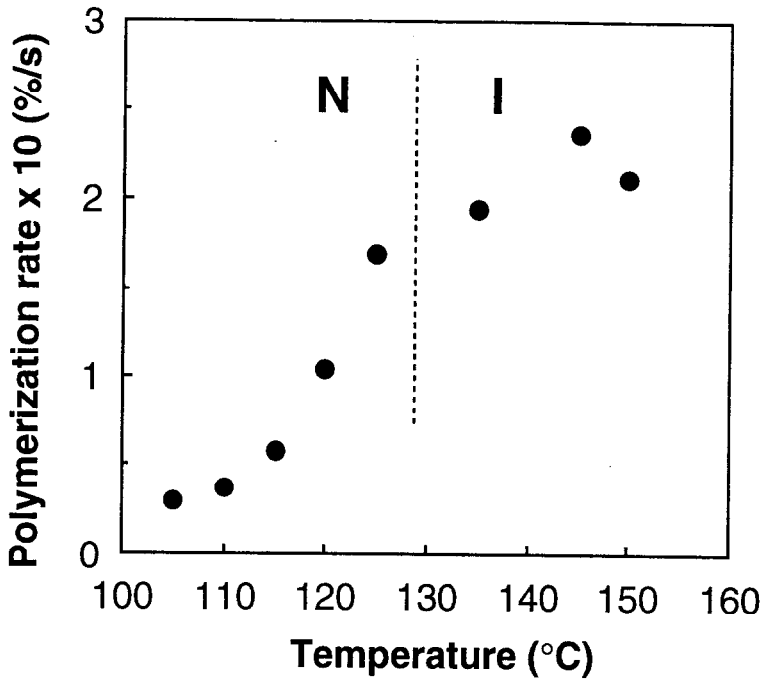

Figure 3-3. Initial rates of thermal polymerization of **ACB0** at various temperatures. Initiator was not used in the polymerization.

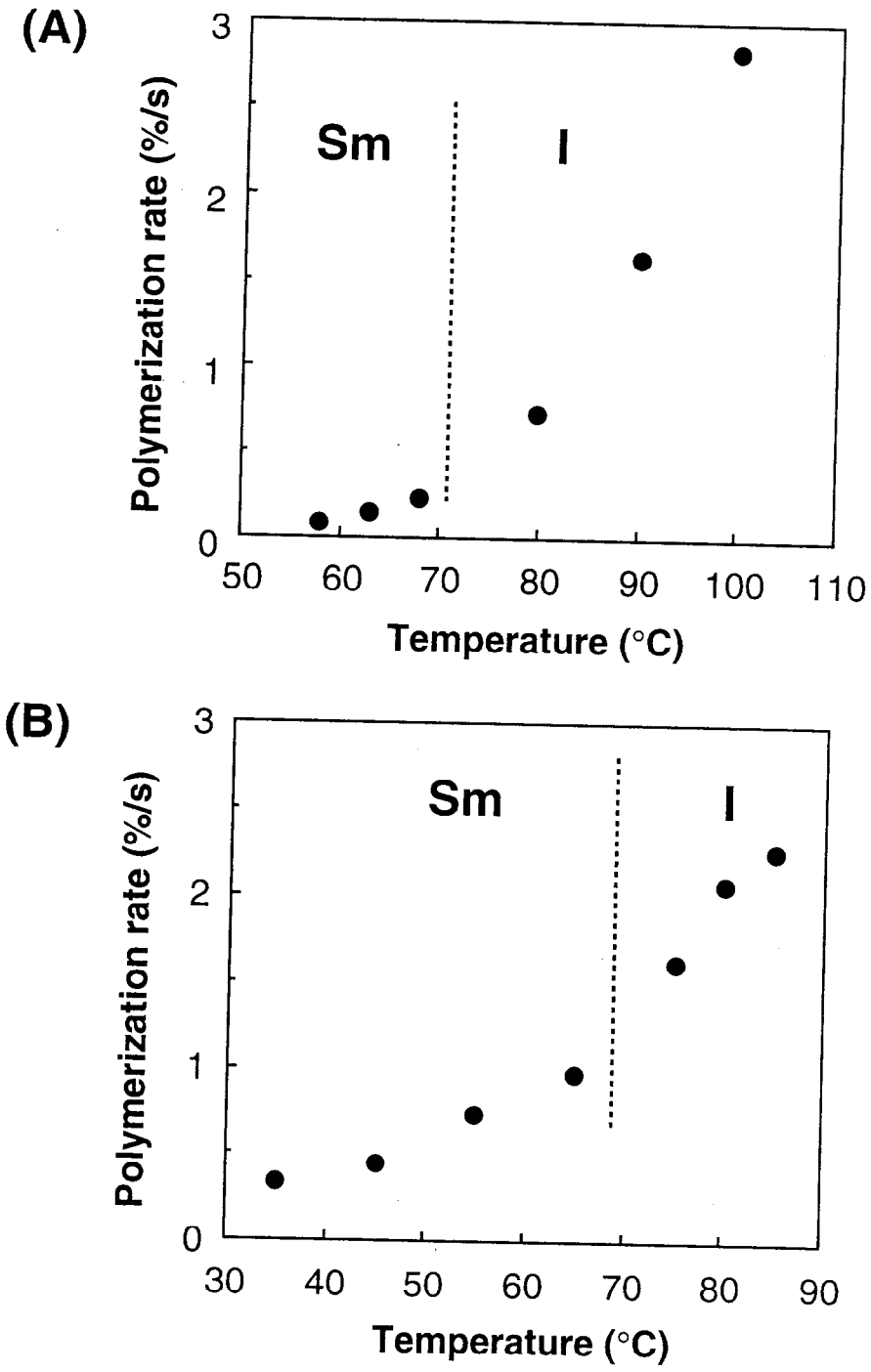

Figure 3-4. Initial rates of polymerization of **ADB** at various temperatures. (A), thermal polymerization with 1 mol% AIBN; (B), photopolymerization with 1 mol% benzoin.

molecular structure of the monomers, phase of the monomers and initiation method, either thermal polymerization or photopolymerization. The rate of polymerization (R_p) is expressed by Equation 2-3,

$$R_p = (k_p/k_t^{1/2}) \times k_i^{1/2} \times [M]^2 \qquad (2\text{-}3)$$

where k_p, k_t and k_i are the rate constants of propagation, termination and initiation, respectively, and [M] is the concentration of monomer. The terms of $k_i^{1/2}$ in the thermal polymerization and k_p are expected to increase with temperature although k_t is not dependent much on temperature. It may be reasonable, therefore, that R_p increased with temperature.

Figures 3-5 and 3-6 show Arrhenius plots for the initial rates of polymerization of **ACB0** and **ADB**, respectively. It was observed that in the thermal polymerization the activation energy was larger in the LC phase than in the I phase (Figures 3-5 and 3-6(A)). The thermal polymerization in the LC phase occurs simultaneously with alignment of monomers, so polymerization competes with the alignment process. It is expected that the alignment process of monomers interferes with propagation process in the polymerization. It is reasonable, therefore, that activation energy of the thermal polymerization in the LC phase is larger than that in the I phase. On the other hand, the activation energy of photopolymerization was constant regardless of the phase structure of monomer (Figure 3-6(B)). This is presumably because photopolymerization can be carried out after the state of the monomer is completely in equilibrium with its intrinsic phase structure. Similar results were obtained for Schiff-base monomers described in Chapter 2.

Figure 3-7 shows the relation between Mn of the polymer obtained and the polymerization temperature. Surprisingly, profiles of Mn vs. temperature in thermal polymerization was different from that in photopolymerization. Mn of polymer produced by thermal polymerization of **ADB** in the Sm phase was higher than that in the I phase (Figure 3-7(A)). In contrast, Mn of the polymer produced by photopolymerization of **ADB** in the Sm phase was lower than that in the I phase, and

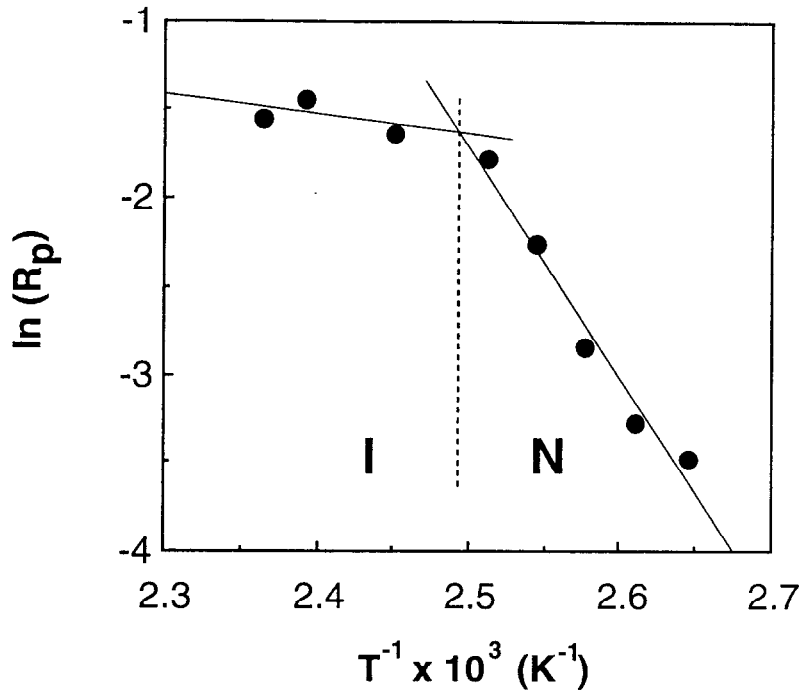

Figure 3-5. Arrhenius plots for the initial rates of thermal polymerization of **ACB0**. Initiator was not used in the polymerization.

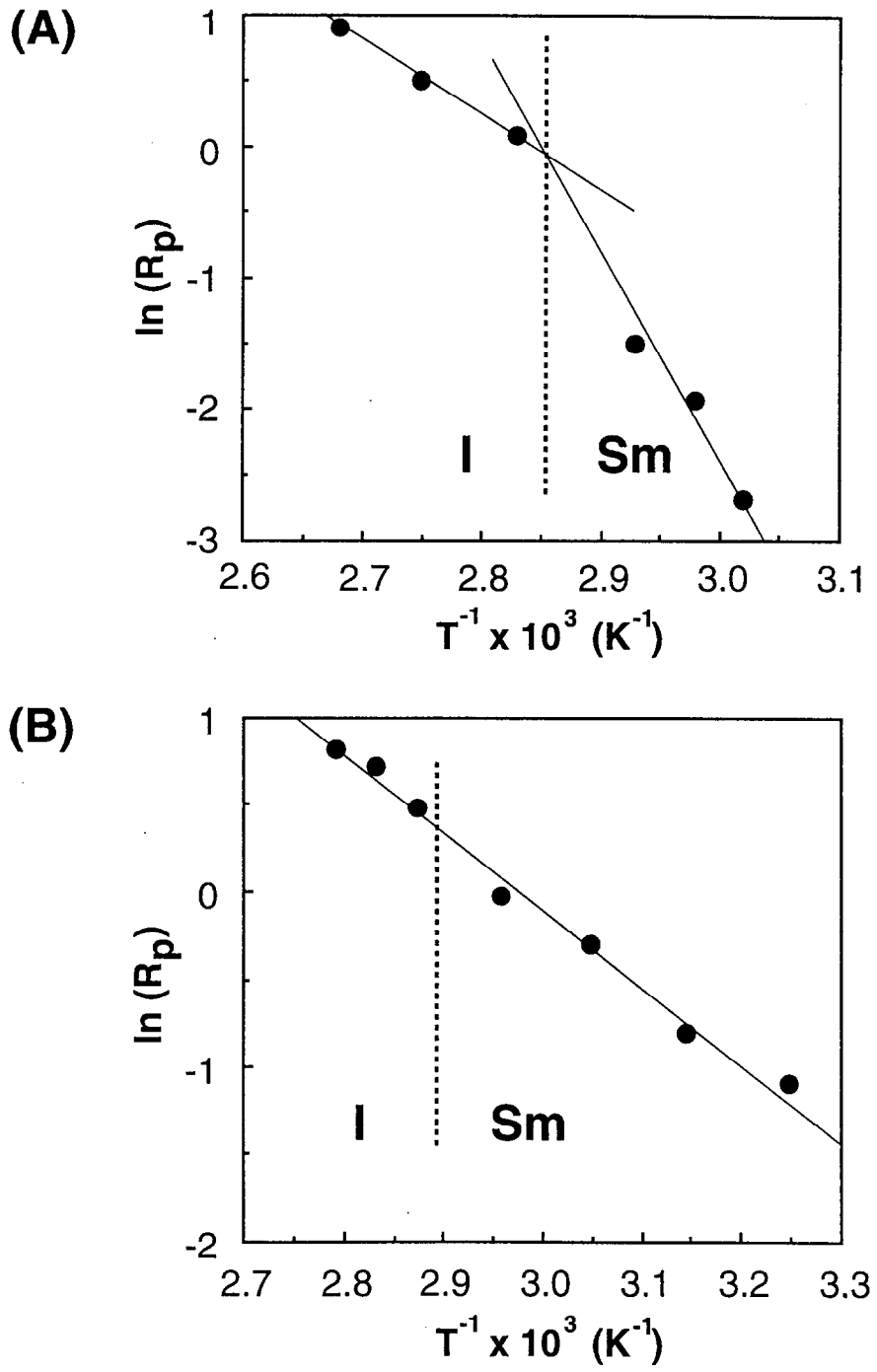

Figure 3-6. Arrhenius plots for the initial rates of polymerization of **ADB**. (A), thermal polymerization with 1 mol% AIBN; (B), photopolymerization with 1 mol% benzoin.

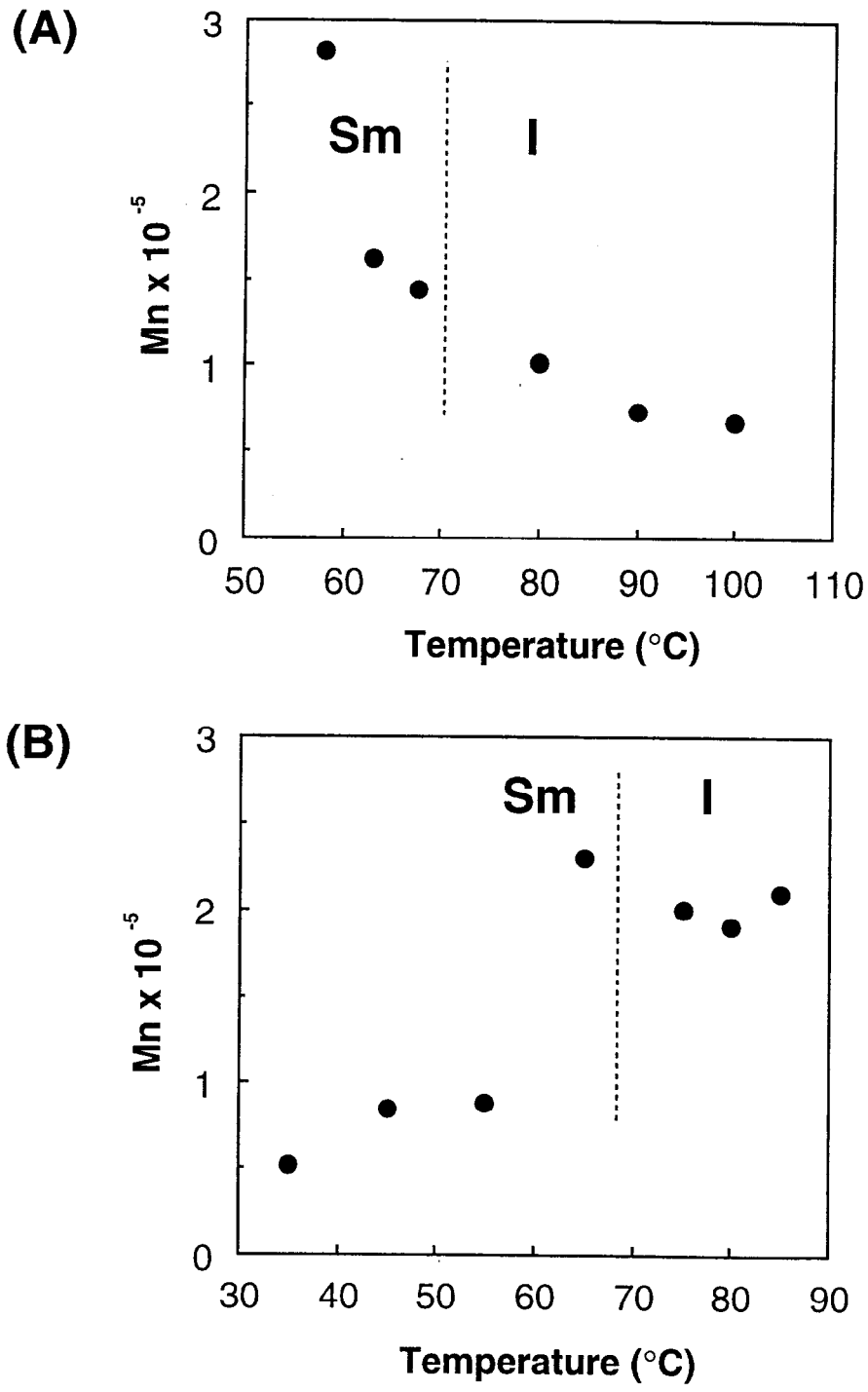

Figure 3-7. Mn of polymers of **ADB** obtained by polymerization with an initiator at various temperatures. (A), thermal polymerization with 1 mol% AIBN; (B), photopolymerization with 1 mol% benzoin.

Mn increased discontinuously at the Sm-I phase transition temperature (Figure 3-7(B)). At the temperature, the orientation of monomer is absent macroscopically, but it remains microscopically, then this microscopic orientation of monomers might be advantageous for the reaction between propagating radicals and monomers.

It is well known that Mn is proportional to kinetic chain length (ν).[36] The term of ν is proportional to R_p and is inversely proportional to R_i. In the photopolymerization, the generation of the radicals is dependent only on the absorbed light, so that R_i is constant at any polymerization temperature. However, R_p increased with temperature as shown in Figure 3-4(A). Therefore, it may be reasonable that Mn increased as temperature increased. On the other hand, since the radicals are thermally produced in the thermal polymerization, the number of radicals produced for a certain period increases with temperature, and then R_i increases with temperature. Although R_p also increased with temperature, it is expected that the rate of increase of R_i is larger than that of R_p in the thermal polymerization. Consequently, Mn decreased as temperature increased.

3-3-2. Alignment of Polymer Produced

The molecular alignment of the polymers was explored by optical polarizing microscopy. To investigate the orientation of polymers produced by photopolymerization, **ADB** was polymerized in the Sm phase in the cells with 20-μm gap. After the polymerization, the cell was opened and the polymerization mixture was thoroughly washed with methanol to remove unreacted monomers and initiator. Washing of the product was repeated until no absorption of the monomer and the initiator was detected in the washings by UV absorption spectroscopy. The sample was then dried and examined with the polarizing microscope on the optical anisotropy.

The optical texture observed before polymerization at 60 °C in the Sm phase is shown in Figure 3-8(A). As is clearly seen, the sample exhibited focal-conic texture. Figure 3-8(B) shows that the polymers prepared in the Sm phase showed the focal-

(A)

(B)

Figure 3-8. Textures observed before and after photopolymerization of **ADB** in the Sm phase. (A), before irradiation; (B), after irradiation. The sample after irradiation was thoroughly washed with methanol to remove unreacted monomers and initiator.

conic texture. It is well known that orientation of LC molecules is strongly affected by interface between the LC molecules and the substrate.[37,38] In the present system, the monomers are aligned due to the LC nature and the orientation is enhanced at the interface. On polymerization of the aligned monomers, mesogens may still be oriented owing to the effect of the interface. The polymer produced by photopolymerization may show good orientation of mesogens because in the photopolymerization one can polymerize the LC monomers after they are completely oriented. Furthermore, gel was formed after 300-s irradiation. It is highly possible that crosslinking produced more stable alignment of mesogens as in Chapter 2.

3-4. Conclusion

Polymerization of vinyl monomers having biphenyl structure was conducted in different phases of monomers in the cells. The final conversion and the initial rate of polymerization of the monomer having biphenyl moiety increased with temperature regardless of phases of the monomer. The Mn of the polymer produced in thermal polymerization in the Sm phase was higher than that in the I phase, whereas that of the polymer obtained by photopolymerization in the Sm phase was lower than that in the I phase. The Mn of the polymer is mainly affected by the initiation method of polymerization.

References

1 Teucher, I.; Paleos, C. M.; Labes, M. M. *Mol. Cryst. Liq. Cryst.* **1970**, *11*, 187.

2 Broer, D. J.; Finkelmann, H.; Kondo, K. *Makromol. Chem.* **1988**, *189*, 185.

3 Broer, D. J.; Mol, G. N. *Makromol. Chem.* **1989**, *190*, 19.

4 Broer, D. J.; Boven, J.; Mol, G. N. Challa, G. *Makromol. Chem.* **1989**, *190*, 2255.

5 Hoyle, C. E.; Chawla, C. P.; Griffin, A. C. *Polymer* **1989**, *60*, 1909.

6 Hikmet, R. A. M.; Howard, R. *Phys. Rev. E* **1993**, *48*, 2752.

7 Broer, D. J.; Lub, J.; Mol, G. N. *Nature* **1995**, *378*, 467.

8 Hikmet, R. A. M.; Lub, J. *J. Appl. Phys.* **1995** *77*, 6234.

9 He, L.; Zhang, S.; Jin, S.; Qi, Z. *Polym. Bull.* **1995**, *34*, 7.

10 Guymon, C. A.; Hoggan, E. N.; Clark, N. A.; Rieker, T. P.; Walba, D. M. C.; Bowman, N. *Science* **1997**, *275*, 57.

11 Broer, D. J.; Mol, G. N.; Challa, G. *Polymer* **1991**, *32*, 690.

12 Hoyle, C. E.; Kang, D.; Jariwala, C.; Griffin, A. C. *Polymer* **1993,** *34*, 3070.

13 Hoyle, C. E.; Watanabe, T. *Macromolecules* **1994**, *27*, 3790.

14 Sahlèn, F.; Trollsås, M.; Hult, A.; U. Gedde, W. *Chem. Mater.* **1996**, *8*, 382.

15 Hellermark, C.; Gedde, U. W.; Hult, A. *Polym. Bull.* **1992**, *28*, 267.

16 Andersson, H.; Gedde, U. W.; Hult, A. *Polymer* **1992**, *33*, 4014.

17 Sahlèn, F.; Andersson, H.; Hult, A.; Gedde, U. W.; Ania, F. *Polymer* **1996**, *37*, 2657.

18 Broer, D. J.; Lub, J.; Mol, G. N. *Macromolecules* **1993**, *26*, 1244.

19 Jahromi, S.; Lub, J.; Mol, G. N. *Polymer* **1994**, *35*, 622.

20 Andersson, H.; Trollsås, M.; Gedde, U. W.; Hult, A. *Macromol. Chem. Phys.* **1995**, *196*, 3667.

21 Williamson, S. E.; Kang, D.; Hoyle, C. E. *Macromolecules* **1996**, *29*, 8656.

22 Perplies, E.; Ringsdorf, H.; Wendorff, J. H. *Makromol. Chem.* **1974**, *175*, 553.

23 Hoyle, C. E.; Mathias, L. J.; Jariwala, C.; Scheng, D. *Macromolecules* **1996**, *29*, 3182.

24 Amerik, Y. B.; Krentsel, B. A. *J. Polym. Sci., Part C* **1967**, *16*, 1383.

25 Doornkamp, A. T.; Alberda van Ekenstein, G. O. R.; Tan, Y. Y. *Polymer* **1992**, *33*, 2863.

26 Hoyle, C. E.; Chawla, C. P.; Kang, D.; Griffin, A. C. *Macromolecules* **1993**, *26*, 758.

27 Hoyle, C. E.; Kang, D.; Jariwala, C.; Griffin, A. C. *Polymer* **1993**, *34*, 3070.

28 Kurihara, S.; Ohta, H.; Nonaka, T. *Polymer* **1995**, *36*, 849.

29 Guymon, C. A.; Bowman, C. N. *Macromolecules* **1997**, *30*, 5271.

30 Paleos, C. M.; Labes, M. M. *Mol. Cryst. Liq. Cryst.* **1970**, *11*, 385.

31 Hoyle, C. E.; Watanabe, T.; Whitehead, J. B. *Macromolecules* **1994**, *27*, 6581.

32 Ringsdorf, H.; Greber, G. *Makromol. Chem.* **1959**, *1*, 27.

33 Strzelecki, L.; Liebert, L. *Bull. Soc. Chim.* **1973**, 605.

34 Chandra, R.; Soni, R. K. *Polym. Int.* **1993**, *31*, 239.

35 Rabek, J. F. *Mechanisms of Photophysical Processes and Photochemical Reactions in Polymers (Theory and Applications)*; John Wiley & Sons, 1987; pp 306.

36 Flory, P. J. *Principles of Polymers Chemistry*; Cornell Univ. Press, Ithaca, New York, 1953; Chapter 4.

37 Iimura, Y.; Kobayashi, N.; Kobayashi, S. *Jpn. J. Appl. Phys.* **1995**, *34*, 1935.

38 Gu, D.-F.; Uran, S.; Rosenblatt, C. *Liq. Cryst.* **1995**, *19*, 427.

Chapter 4

In-Situ Photopolymerization Behavior of a Chiral Liquid-Crystalline Acrylate Monomer Showing a Ferroelectric Phase

4-1. Introduction

Polymerization of LC monomers has been conducted extensively to obtain PLCs.[1] In most of the LC phases such as N or Ch, SmA, and SmC, the symmetry is so high that free rotation around the molecular long axis and head-tail equivalence prevent the occurrence of ferroelectricity (Figure 4-1(A)).[2] In SmC* phase, however, the symmetry is low enough to allow the existence of ferroelectricity induced by chirality. The molecules in each smectic layer still rotate around their long axes, but this rotation is biased in a particular sense along the C_2 axis (Figure 4-1(B)).[2] In-situ photopolymerization of FLC monomers is expected to show specific polymerization behavior. Many studies have been performed so far on polymerization behavior of LC monomers in N, Sm and Ch phases. Photopolymerization of the FLC monomer showing the SmC* phase has been reported on its application to optoelectric materials.[3] In the present chapter, the author used an FLC monomer, which had an acrylate polymerizable unit and a chiral group in terminal aliphatic chain, and evaluated the photopolymerization behavior as well as the molecular alignment before and after photoirradiation.

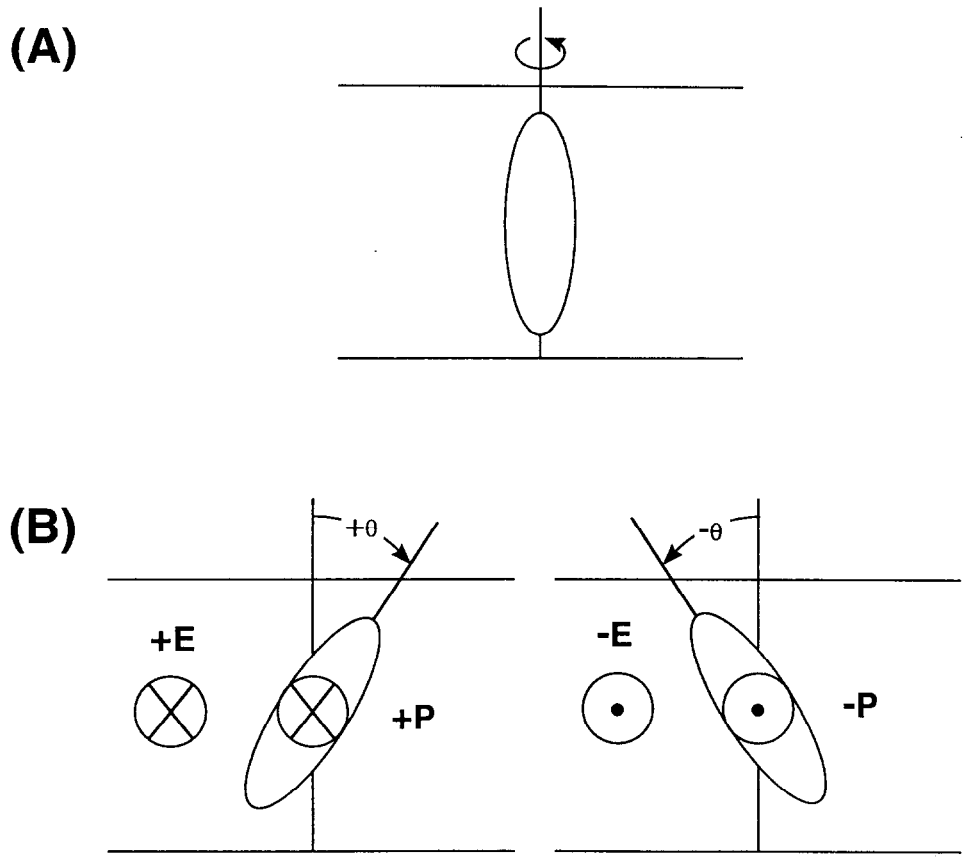

Figure 4-1. Diagrams of rotation around long axis in various phases. (A), free rotation in the N and Sm; (B), restricted rotation in the SmC*.

4-2. Experimental

4-2-1. Materials

Synthesis of FLC Monomer

The structure and phase transition temperature of the FLC monomer {[R]-1-methylheptyl 4'-[4-(ω-acryloyloxyundecyloxy)benzoyloxy]biphenyl-4-carboxylate} (**AS11**) used in this chapter are shown in Figure 4-2. The FLC monomer was prepared according to the synthetic method reported previously (Scheme 4-1).[4] The compound was characterized by means of ^{1}H NMR, IR and elemental analysis as described in Chapter 2. The phase transition temperature and the phase structure were determined by DSC (cooling rate, 1 °C/min) and optical polarizing microscopy. As described in Figure 4-2, the FLC monomer showed various phases with temperature: K, antiferroelectric chiral smectic C (SmC_A*), ferrielectric chiral smectic C ($SmC\gamma$*), ferroelectric chiral smectic C (SmC*), chiral smectic A (SmA*) and I phases.

4-(ω-Hydroxyundecyloxy)benzoic acid. 4-Hydroxybenzoic acid (25 g, 0.18 mol) was dissolved in a mixture of ethanol (60 mL) and potassium hydroxide (27 g, 0.48 mol) in water (30 mL). A trace of potassium iodide was added and the solution was heated and stirred while 11-bromo-1-undecanol (50 g, 0.20 mol) was added slowly. The reaction mixture was heated under reflux for 24 h, then the solvent was removed by evaporation under reduced pressure. Water (300 mL) was added and the mixture was made strongly acidic (pH 2) with the addition of hydrochloric acid. The precipitate was isolated and recrystallized from ethanol (220 mL).

Yield: 23 g (73 mmol, 40 %)

mp: 110-112 °C

^{1}H NMR (δ, DMSO-d_6): 7.92(m, 2H, 2-H, 6-H), 6.90(m, 2H, 3-H, 5-H), 4.01(t, 2H, -CH_2-O-), 3.48(t, 2H, -CH_2-OH), 1.78(m, 2H, -CH_2-CH_2-O-), 1.47-1.28(m, 16H, CH_2)

IR (KBr, cm^{-1}): 3400, 2920, 2850, 1675, 1610, 1250

Anal. Calcd for $C_{18}H_{28}O_4$ (308): C, 70.10; H, 9.15 %

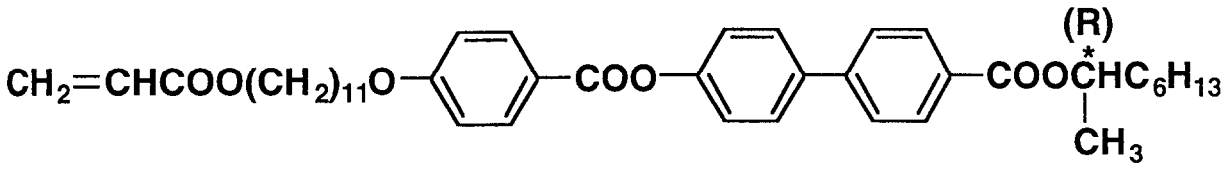

K 3.3 SmC_A^* 38 SmCγ^* 46 SmC* 73 SmA* 87 I

AS11

Figure 4-2. Chemical structure and phase transition temperature of the ferroelectric liquid-crystalline monomer used in this chapter.

Scheme 4-1. Synthetic route for FLC monomer

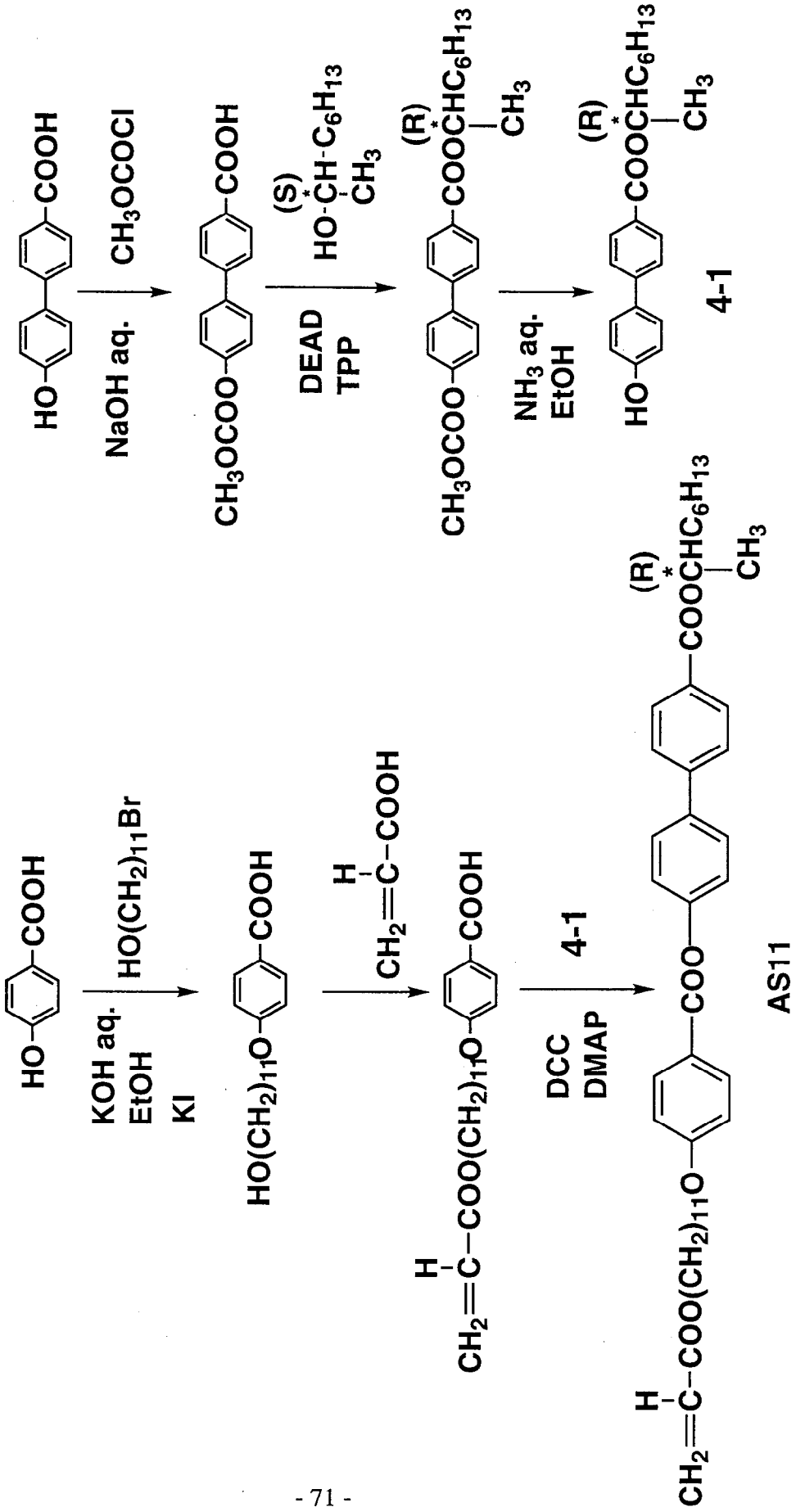

Found: C, 69.77; H, 9.23 %.

4-(ω-Acryloyloxyundecyloxy)benzoic acid. A mixture of 4-(ω-hydroxyundecyloxy)benzoic acid (9.3 g, 0.03 mol), acrylic acid (18 g, 0.25 mol), hydroquinone (1.7 g, 0.02 mol), 4-toluenesulphonic acid-monohydrate (1.7 g, 0.01 mol) and benzene (200 mL) was heated under reflux in a Dean-Stark apparatus for 24 h. A solution of sodium acetate (0.75 g, 0.01 mol) in water was added to neutralize the reaction mixture. The solvent was removed under reduced pressure. The crude product was redissolved in chloroform (400 mL). The solution was filtered, washed with water (300 mL x 4) and dried over anhydrous magnesium sulphate. The solvent was removed very carefully by evaporation under reduced pressure (maximum water bath temperature 40 °C) to prevent the formation of the oligomer. To purify the resulting crude product, it was dissolved in chloroform and precipitated into a large excess of hexane. After the precipitate was dried under vacuum at room temperature, the product was recrystallized from ethanol.

Yield: 3.5 g (9.8 mmol, 32 %)

mp: 90 °C

^{1}H NMR (δ, $CDCl_3$): 8.05(m, 2H, 2-H, 6-H), 6.92(m, 2H, 3-H, 5-H), 6.40(dd, J = 18, 2 Hz, 1H, *trans*-CH_2=CH-), 6.12(dd, J = 18, 10 Hz, 1H, CH_2=CH-), 5.82(dd, J = 10, 2 Hz, 1H, *cis*-CH_2=CH-), 4.15(t, 2H, -COO-CH_2-), 4.02(t, 2H, -CH_2-O-), 1.80(m, 2H, -COO-CH_2-CH_2-), 1.66(m, 2H,-CH_2-CH_2-O-), 1.46-1.27(m, 14H, CH_2)

IR (KBr, cm^{-1}): 3100, 2930, 2860, 1725, 1680, 1610

Anal. Calcd for $C_{21}H_{30}O_5$ (362): C, 69.59; H, 8.34 %

Found. C, 68.90; H, 8.41 %

4-Methoxycarbonoyloxybiphenyl-4'-carboxylic acid. To a solution of sodium hydroxide (10.8 g, 0.27 mol) in water (400 mL), which had been cooled to 0 °C, 4-hydroxybiphenyl-4'-carboxylic acid (19.7 g, 0.09 mol) was added. The reaction

mixture was stirred vigorously and methyl chloroformate (14.7 g, 0.16 mol) was added slowly to the resulting suspension. The reaction mixture was stirred at 0 °C for 4 h and then brought to pH 2 by the addition of 5 N hydrochloric acid. The voluminous white precipitate produced was filtered off and recrystallized from acetic acid (1.5 L).

Yield: 23 g (83 mmol, 90 %)

mp: 255-262 °C

^{1}H NMR (δ, DMSO-d_6): 8.12(m, 2H, 3'-H, 5'-H), 7.63(m, 4H, 2-H, 6-H, 2'-H, 6'-H), 7.28(m, 2H, 3-H, 5-H), 3.93(s, 3H, CH_3-O-COO-)

IR (KBr, cm^{-1}): 2950, 1770, 1615, 830

Anal. Calcd for $C_{15}H_{12}O_5$ (272): C, 66.17; H, 4.44 %

Found: C, 64.93; H, 4.47 %.

(R)-1-Methylheptyl 4-methoxycarbonoyloxybiphenyl-4'-carboxylate. 4-Methoxycarbonoyloxybiphenyl-4'-carboxylic acid (4.0 g, 0.015 mol), (S)-2-octanol (1.95 g, 0.015 mol) and diethyl azodicarbodiimide (DEAD; 2.56 g, 0.015 mol) were dissolved in dry THF (200 mL) at room temperature under a nitrogen atmosphere. Triphenylphosphine (3.85 g, 0.015 mol) dissolved in dry THF (50 mL) was then added to the mixture with stirring. The reaction mixture was stirred at room temperature overnight. After the solid in the mixture was filtered off, THF was removed by evaporation under reduced pressure. The resulting oily crude was purified by column chlomatography (chloroform).

Yield: 5.4 g (14 mmol, 64 %)

^{1}H NMR (δ, $CDCl_3$): 8.11(m, 2H, 3'-H, 5'-H), 7.63(m, 4H, 2-H, 6-H, 2'-H, 6'-H), 7.28(m, 2H, 3-H, 5-H), 5.17(m, 1H, -COO-CH-), 3.94(s, 3H, CH_3-O-COO-), 1.75-1.25(m, 13H, CH_2, CH_3), 0.75(t, 3H, CH_3)

IR (neat, cm^{-1}): 2960, 2930, 2860, 1770, 1720, 1615, 835

(R)-1-Methylheptyl 4-hydroxybiphenyl-4'-carboxylate. (R)-1-Methylheptyl 4-methoxycarbonoyloxybiphenyl-4'-carboxylate (2.80 g, 6.80 mmol) was dissolved in ethanol (100 mL) and then ammonia solution (25 %) (15 mL) was added with stirring at room temperature. The reaction mixture was stirred at room temperature for 2 days. The solvent was removed by evaporation under reduced pressure. The residue was redissolved in diethyl ether, washed with water and dried over anhydrous magnesium sulphate. The solvent was removed by evaporation under reduced pressure to yield an product.

Yield: 4.0 g (12 mmol, 92 %)

mp: 85 °C

^{1}H NMR (δ, $CDCl_3$): 8.08(m, 2H, 3'-H, 5'-H), 7.55(m, 4H, 2-H, 6-H, 2'-H, 6'-H), 6.93(m, 2H, 3-H, 5-H), 5.27(s, 1H, OH), 5.17(m, 1H, -COO-CH-), 1.74-1.25(m, 13H, CH_2, CH_3), 0.87(t, 3H, CH_3)

IR (KBr, cm^{-1}): 3400, 2930, 2860, 1715, 1610, 835

Anal. Calcd for $C_{21}H_{26}O_3$ (326): C, 77.27; H, 8.03 %

Found. C, 76.71; H, 7.88 %.

(R)-1-Methylheptyl 4'-(4"-(ω-acryloyloxyundecyloxy)benzoyloxy)biphenyl-4-carboxylate (AS11). 4-(ω-Acryloyloxyundecyloxy)benzoic acid (1.1 g, 3.1 mmol), (R)-1-methylheptyl 4-hydroxybiphenyl-4'-carboxylate (1.0 g, 3.1 mmol) and 4-dimethylaminopyridine (DMAP; 0.03 g, 0.3 mmol) were dissolved in dry chloroform (15 mL). Dicyclohexylcarbodiimide (DCC; 1.28 g, 6.2 mmol) was added and the solution was stirred at room temperature for 2 days. After filtration to remove precipitated material, the filtrate was washed with water and dried over magnesium sulphate. After removal of the solvent, the product was purified by column chromatography (chloroform/hexane = 9/1) and recrystallized from ethanol (50 mL).

Yield: 2.1 g (3.1 mmol, 50 %)

mp: 56 °C

^{1}H NMR (δ, $CDCl_3$): 8.15(m, 4H, 3-H, 5-H, 2"-H, 6"-H), 7.67(m, 4H, 2-H, 6-H, 2'-H, 6'-H), 7.31(m, 2H, 3'-H, 5'-H), 6.98(m, 2H, 3"-H, 5"-H), 6.41(dd, *J* = 17, 2 Hz, 1H, *trans*-CH_2=CH-), 6.12(dd, *J* = 17, 10 Hz, 1H, CH_2=CH-), 5.82(dd, *J* = 10, 2 Hz, 1H, *cis*-CH_2=CH-), 5.18(m, 1H), 4.16(t, 2H, -COO-CH_2-), 4.05(t, 2H, -CH_2-O-), 1.85-1.27(m, 31H, CH_2, CH_3), 0.89(t, 3H, CH_3)

IR (KBr, cm^{-1}): 2930, 2850, 1735, 1710, 1610, 840

Anal. Calcd for $C_{42}H_{54}O_7$ (670): C, 75.19; H, 8.11 %

Found. C, 75.13; H, 8.14 %

Preparation of PLCs by Means of Solution Polymerization. A solution of the monomer (0.3 g) and 1 mol% of AIBN in distilled DMF (3 mL) was degassed by several freeze-pump-thaw cycles, and stirred in a sealed tube at 60 °C for 48 h. The resulting solution was cooled to room temperature and poured into 100 mL of methanol with vigorously stirring to precipitate the polymer. To purify the polymer, it was dissolved in chloroform and precipitated into methanol. The purification was repeated until no monomer was detected by GPC. The polymer was dried under vacuum for 48 h at room temperature.

4-2-2. Preparation of Phase Diagram

Before evaluation of the in-situ photopolymerization behavior of the monomeric FLCs, the author evaluated the phase transition behavior during polymerization. It is assumed that during photoirradiation, accumulation of the polymer produced in the LC phase is accompanied by changes in the phase transition temperatures due to change in composition of monomer-polymer mixture. To prepare the phase diagram in the binary mixture of the polymer and the monomer, the FLC polymer was synthesized as described in the previous section. The phase transition temperature and the phase structure were determined by DSC (10 °C/min) and optical polarizing microscopy. The polymer exhibited glassy (G), SmC_A*, SmA* and I phases (Figure 4-3).

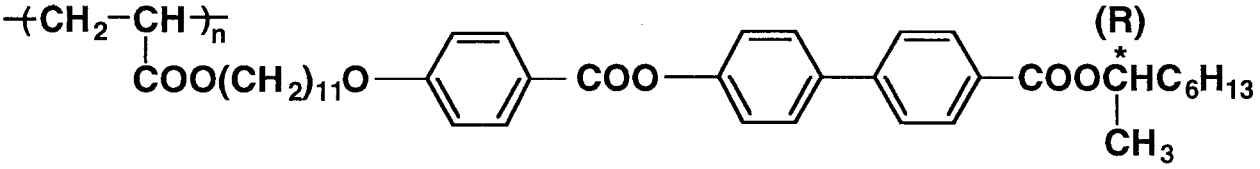

G 37 SmC_A^* 149 SmA* 162 I

Mn = 1.8 x 10^4

Mw/Mn = 1.6

Figure 4-3. Structure and characteristic of the polymer obtained by solution polymerization of the ferroelectric liquid-crystalline monomer.

4-2-3. Preparation of Liquid-Crystal Cell

Materials

3,3',4,4'-Biphenyltetracarboxylic dianhydride (BPDA) and 4,4'-diaminodiphenylmethane (DPM) were purchased from Tokyo Chemical Industry Co., Ltd. N-Methyl-2-pyrrolidinone (NMP) and 4-butyrolactone were purchased from Kanto Chemical Co., Inc.

Synthesis of PI Precursor

PI precursor, poly(amic acid), was synthesized by slowly adding a stoichiometric amount of dianhydride powder to DMF solution of diamine with continuous stirring at room temperature in nitrogen atmosphere. After 24 h, the solution was poured into a large excess of methanol with vigorously stirring to precipitate the polymer. The polymer obtained was purified by reprecipitation from DMF into a large excess of methanol and dried under vacuum for 48 h. The poly(amic acid) solution was prepared at a concentration of 3 wt% with a mixed solvent of NMP and 4-butyrolacton (the ratio of NMP and 4-butyrolacton was 1 to 2) before use.

Preparation of PI Alignment Film

Indium-tin-oxide (ITO) coated glass substrates, with dimension of 25 x 20 mm^2, were washed with neutral detergent, distilled water and isopropyl alcohol in an ultrasonic bath and then dried at room temperature. The clean substrates were spin-coated with 3 wt% poly(amic acid) solutions at 500 rpm for 5 s and at 4300 rpm for 35 s. Then, the surface-treated substrates were soft-baked at 100 °C for 1 h and hard-baked at 250 °C for 2 h to remove solvent and cure. Then, polyimide layers were rubbed and cells were prepared with the rubbing direction of antiparallel. The chemical structure of the PI used in this chapter is shown in Figure 4-4.

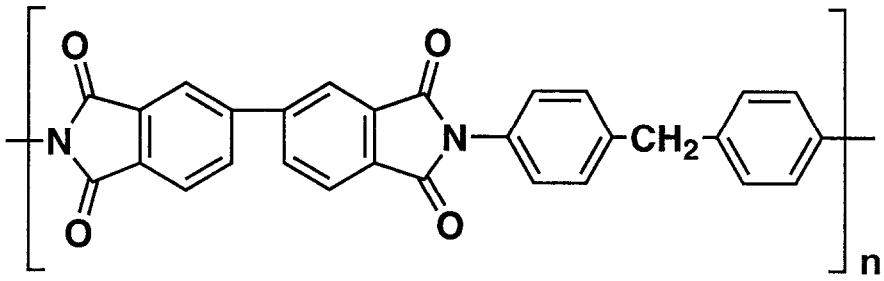

Figure 4-4. Structure of polyimide for alignment layer.

4-2-4. In-Situ Photopolymerization Procedure

Photopolymerization was performed in a glass cell with a gap of 2 μm without an electric field or under 3 V/μm dc electric field. The glass cell was composed of two glass substrates with ITO electrodes and rubbed PI alignment layers (Figure 4-5). Samples for photopolymerization were prepared by injecting the FLC monomer, containing benzoin as a photoinitiator (2 mol%), into the glass cell in the I phase at 90 °C using capillary action. Here the author confirmed that the concentration of the photoinitiator was small enough not to destabilize the LC phases and no spontaneous thermal polymerization occurred during injection of the FLC monomers into the glass cell. Furthermore, it was also confirmed that without the photoinitiator, the photopolymerization could not be induced even after prolonged photoirradiation at 366 nm. After the samples were prepared, they were cooled down slowly (0.5 °C/min) to a temperature at which photopolymerization was attempted. Photoirradiation was performed at 366 nm (intensity, 1 mW/cm^2) isolated with glass filters from a 500 W high-pressure mercury lamp. In the photopolymerization under an electric field, the samples were cooled down slowly under ac electric field (1 Hz, 3 V_{pp}/μm) to a temperature for photopolymerization. The quality of the alignment obtained by cooling under ac fields was better than that under dc fields.[5] After obtaining a ferroelectric monodomain structure at the temperatures for which the ferroelectric electrooptic response in the SmC* phase was fully developed, the cell was irradiated at 366 nm with the dc electric field of 3 V/μm during polymerization.

The course of the polymerization was followed by gel permeation chromatography (GPC, JASCO GULLIVER SERIES; column, Shodex GPC K802 + K803 + K804 + K805; eluent, chloroform) calibrated with standard polystyrenes using UV-Vis detector (λ = 254 nm). The conversion was estimated as described in Chapter 2. Each GPC measurement was repeated three times, and the reproducibility of the conversion and the molecular weight was invariably good. This fact was verified by the interval estimation of each data point which was mean for triplicate runs. The

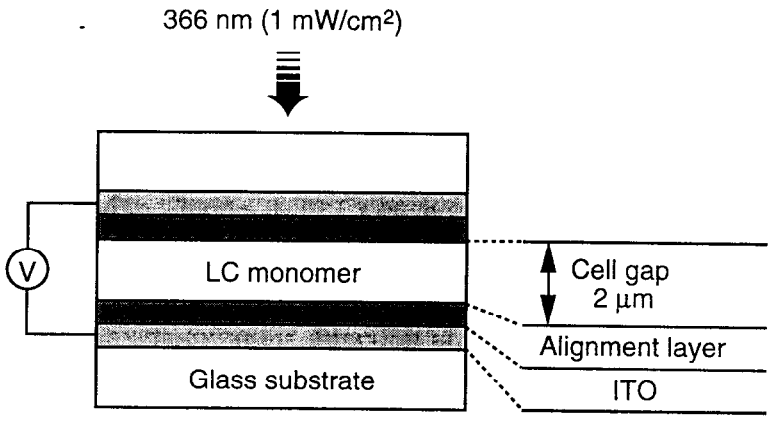

Figure 4-5. Ferroelectric liquid crystal cell used for evaluation of in-situ photopolymerization behavior.

statistics showed that the 95 % confidence limits analyzed from the sample mean and the sample standard deviation on the repeated runs were within ±3 % and ±5,600 for conversion and molecular weight, respectively. These results indicate clearly that the GPC method is reproducible and the resulting experimental data are reliable.

4-2-5. Evaluation of Alignment of Polymerized FLC

The degree of alignment of the polymerized FLC after photoirradiation with and without electric field in the 2-μm-gap cell was explored by means of optical polarizing microscopy. The molecular alignment was evaluated from the angular dependence of the transmittance of linearly polarized light through the sample cell.

As described in Chapter 1, FLCs have a spontaneous polarization in the surface-stabilized state due to the alignment of dipoles into one direction, and they exhibit bistable states via inversion in the direction of the spontaneous polarization. When an electric field with reverse polarity is applied across the cell, the polarization flips into opposite direction and simultaneously the aligning direction of the long axis of each FLC molecule changes. In the polymerized FLC, the author examined if the polarization flipped by changing the polarity of the applied electric field and evaluated the difference in electric response between the irradiated and the unirradiated site in a sample cell.

4-3. Results and Discussion

4-3-1. In-Situ Photopolymerization Behavior

It is important to investigate the changes in the phase transition temperature due to changes in composition of the monomer-polymer mixture.[6] Several samples were prepared in which the mixing ratio of the monomeric and the polymeric FLC was altered, and the binary mixtures were subjected to DSC and microscopic observation to explore phase transition. The phase diagram is shown in Figure 4-6. In the region with a low polymer content (less than 10 wt%), the phase transition temperature changed

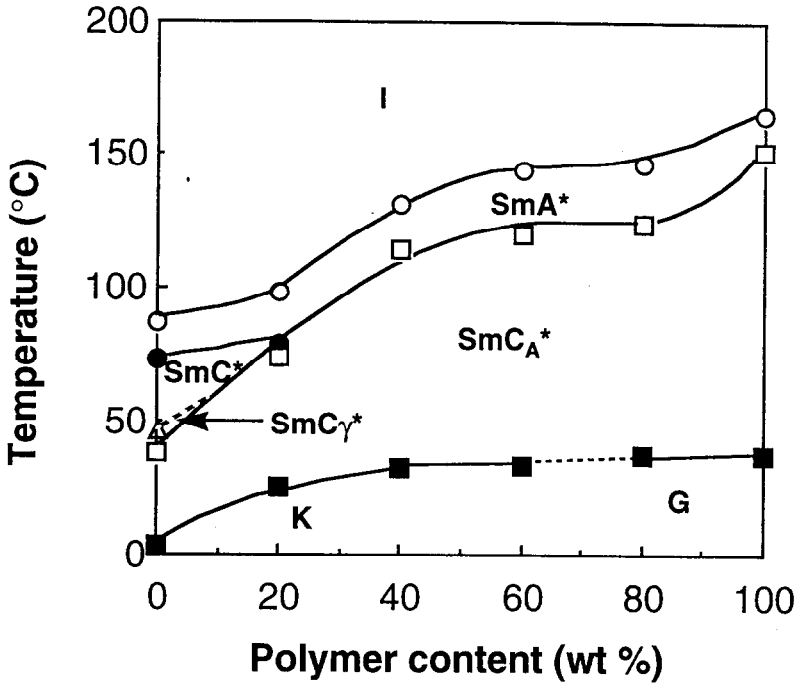

Figure 4-6. Phase diagram for mixtures of monomer and polymer.

only slightly. This result demonstrates that the change in the phase structure could be negligible during the early stages of polymerization. The phase transition temperature of the mixtures was, however, shifted to higher temperatures as the polymer content increased, and the temperature range of the SmC_A* phase increased considerably.

Effect of the irradiation time on the FLC monomer conversion was investigated. The samples were irradiated at 366 nm at different temperatures without or with an electric field. The time-conversion curve obtained by photoirradiation at the light intensity of 1 mW/cm^2 is shown in Figure 4-7. The conversion showed a tendency to increase with increasing the irradiation time, irrespective of the polymerization temperature. The time course of the photopolymerization was similar to that of the general thermal polymerization in solution.[7] A similar trend was observed for a sample under an electric field. On the basis of the phase diagram shown in Figure 4-6, it is assumed that no phase transition occurs at least on 5-s irradiation due to low content of the polymer produced. On the other hand, after 60-s irradiation the conversions reached to above 50 % irrespective of polymerization temperature. Under such condition the in-situ photopolymerization may be accompanied by changes in the phase structure of the polymerization mixture. The author therefore used the conversions after 5-s and 60-s irradiations as a measure to explore the in-situ photopolymerization behavior of the FLC monomer.

Polymerization Behavior in Early Stage of Polymerization

The open symbols in Figure 4-8 show plots of conversion after 5-s irradiation versus temperature without an electric field. The conversion was high below 50 °C at which the FLC monomer shows SmC_A*, SmCγ* and SmC* phases. This result suggests that the enhancement of polymerizability is due to the proximity of the polymerizable groups in highly ordered systems. It is expected that the initial polymerization rate would be enhanced significantly when the FLC monomers are highly aligned by application of the electric field. Such effects of the external electric

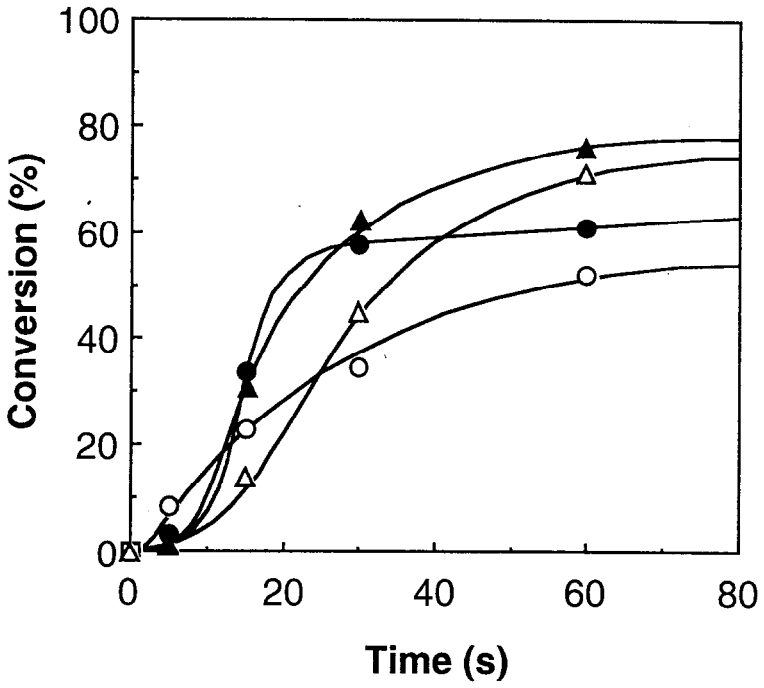

Figure 4-7. Time-conversion curves for photopolymerization at various temperatures in glass cell with a gap of 2 μm. (○ and ●), 40 °C; (△ and ▲), 80 °C; (○ and △) without an electric field; (● and ▲), with an electric field of 3 V/μm.

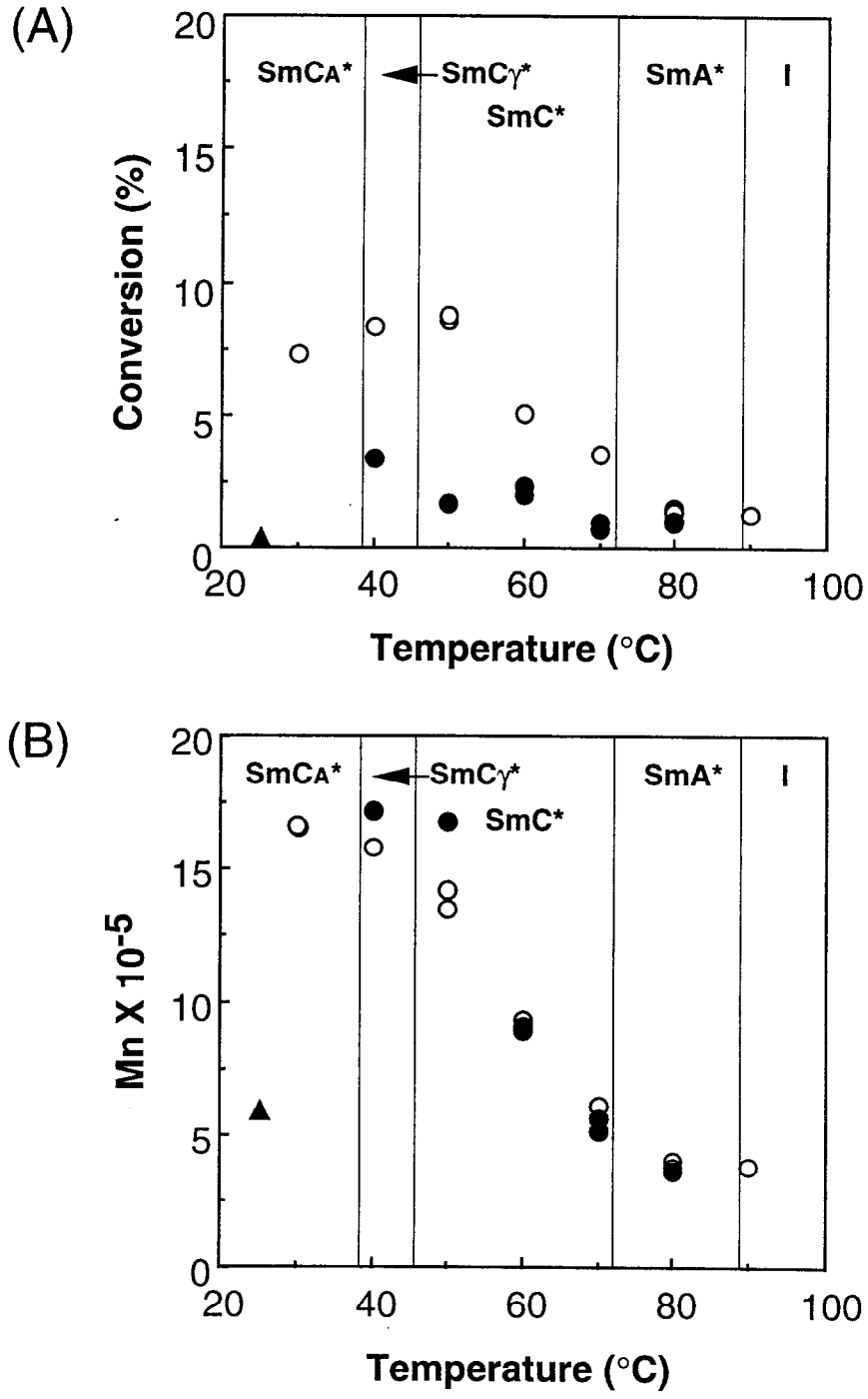

Figure 4-8. Polymerization behavior after 5-s photoirradiation at various temperatures in a glass cell. (A), conversion; (B), number-average molecular weight; O, without an electric field; ●, with an electric field of 3 V/μm; ▲, K phase at 25 °C for 24 h after cooling.

field on the polymerization rate have been investigated also for the chiral LC monomer showing SmA phase and the polymerization rate seems to be dependent on the efficient collision between polymerizable groups.[8] Therefore, the enhancement of polymerizability may be due to the proximity of the polymerizable groups in the surface-stabilized state in which the distance between the polymerizable groups is very small in each layer of the SmC* phase. It has been also reported that the macroscopic alignment of the LC monomers does not affect the polymerization kinetics.[2j] Unfortunately, the conversions obtained by photoirradiation for 5 s with the dc electric field were much smaller than those obtained without the electric field (closed symbols in Figure 4-8(A)).

The FLCs have a helicoidal structure in the bulk. This helical structure arises from two kinds of molecular interactions: one is a spontaneous bend which is a result of the polar symmetry.[9] Injection of FLCs into a glass cell with a narrow gap (1~2 μm) suppresses the helix formation by surface stabilization. The FLCs become highly aligned, in principle, in a 2-μm-gap cell, however, it was difficult to align completely the FLC monomer used in this chapter even in the 2-μm-gap cell. Practically, even when the FLC monomer showed the surface-stabilized state in the presence of an external field, relaxation of the molecules was observed when the application of the electric field was ceased. From viewpoint of molecular alignment, therefore, the polymerization under an electric field is more favored than that without an electric field. Although the author expected that the polymerizability in the presence of an electric field was superior to that in the absence of an electric field, the result obtained was contrary to the prediction. One possible explanation is that the photopolymerization behavior depends not only on molecular alignment, but also on kinetic factors such as mobility, diffusion and molecular rearrangement of FLC monomers in the LC phase. In fact, in K phase in which the FLC molecules show no mobility, the conversion was only 0.13 % and their polymerizability was extremely low (triangular symbol in Figure 4-8(A)). Consequently, the polymerizability of the FLC

monomers in early stage of polymerization is governed by their molecular alignment as well as their mobility in the LC phase.

The relation between molecular weight of the polymer produced and polymerization temperature is shown in Figure 4-8(B). The values of number-average molecular weight were larger in low temperature region (SmC_A*, SmC_γ* and SmC* phase). This is presumably due to decrease in termination rate, resulting from lower mobility of the FLC molecules in highly ordered systems. Furthermore, the molecular weight of the polymer in the K phase was low. These results indicate that the molecular mobility as well as the orientation are needed to obtain high molecular weight polymers.

Polymerization Behavior in Late Stage of Polymerization

The polymerization behavior on 60-s irradiation was different from that on 5-s irradiation. As shown in Figure 4-9(A), the conversion increased monotonically with temperature. This result demonstrates that the polymerization behavior in late stage of polymerization was not affected by the initial molecular alignment of the FLC monomer. On the basis of the phase diagram and the time-conversion curve shown in Figures 4-6 and 4-7, respectively, during 60-s irradiation the initial phase structure is assumed to change to SmC_A* in the wide temperature region. Thus, the observed polymerization behavior may be ascribed to the change in the phase structure during photoirradiation. This is also evident from the fact that the molecular weights are almost the same irrespective of the initial phase structure (Figure 4-9(B)). A similar phase transition during photoirradiation has been reported by Hoyle et al.[6] Photopolymerization behavior has been affected by phase changes during polymerization.[4i,4h,10] In addition, by applying the electric field during polymerization the conversion increased slightly at any temperature (closed symbols in Figure 4-9(A)). These results suggest that in the late stage of polymerization, the polymerization

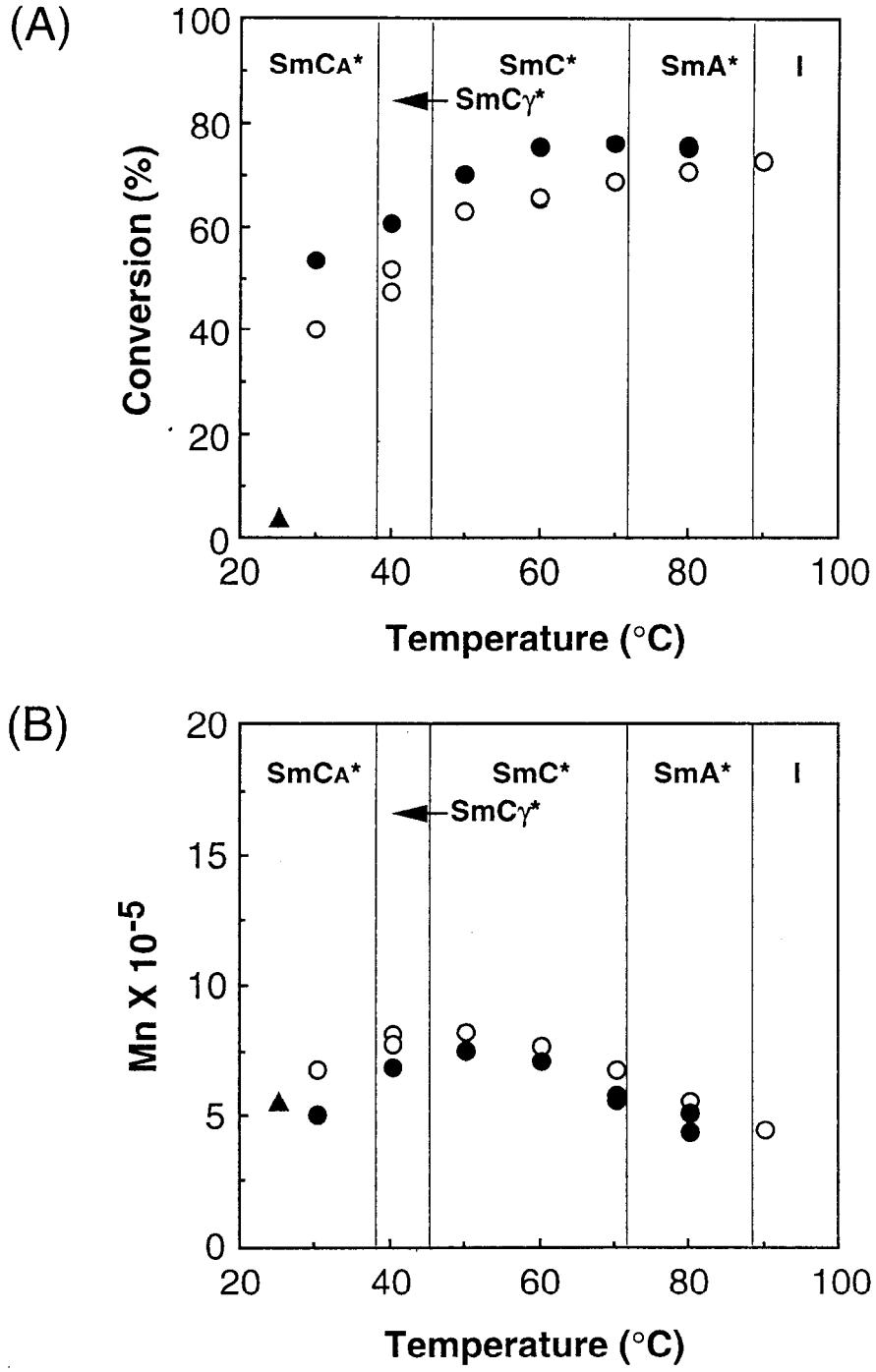

Figure 4-9. Polymerization behavior after 60-s photoirradiation at various temperatures in a glass cell. (A), conversion; (B), number-average molecular weight; ○, without an electric field; ●, with an electric field of 3 V/μm; ▲, K phase at 25 °C for 24 h after cooling.

behavior of the FLC monomers is governed by molecular diffusion as described above rather than their alignment.

4-3-2. Alignment of Photopolymerized FLC.

The molecular alignment of the FLCs was explored by optical polarizing microscopy after the photopolymerization was conducted in the 2-μm-gap cell at 60 °C in the SmC* phase. Figure 4-10 shows the optical textures of the FLC after photoirradiation in the absence of the electric field, where the left and the right half of each micrograph shows the irradiated and the unirradiated site, respectively, In the unirradiated site, when the alternating electric field of ±3 V/μm was applied across the cell, the dark and the bright view of birefringent texture was observed alternatively according to the polarity of the electric field (Figure 4-10(A) and 4-10(B)). This result implies that the polarization flipped from one direction to the opposite direction. In contrast, in the irradiated site, such a change in the texture was not observed. Furthermore, when the sample was heated to 90 °C which was higher than the SmA*-I phase transition temperature of the monomeric FLC, the optical texture disappeared only in the unirradiated site, irrespective of the polarity of the electric field (Figure 10(C)). Therefore, in the unirradiated site the polymerization was not initiated, while in the irradiated site the initial aligned state was stabilized by the photopolymerization even in the absence of the electric field.

Figure 4-11 shows the polarized optical micrographs of the sample before and after photopolymerization in the presence of 3 V/μm dc voltage. Before photoirradiation, the polarization flip was confirmed at first to occur by application of the alternating electric field (Figure 4-11(A) and 4-11(B)). The optical texture after photoirradiation was the same as that before photoirradiation (Figure 4-11(C)), but the polymerized FLC showed no response to the electric field (0.1 Hz - 1 kHz, 10 V_{pp}). This immobilization of molecular alignment could be attributed to low mobility of mesogens of the polymerized FLC. It is known that the general vinyl monomers are

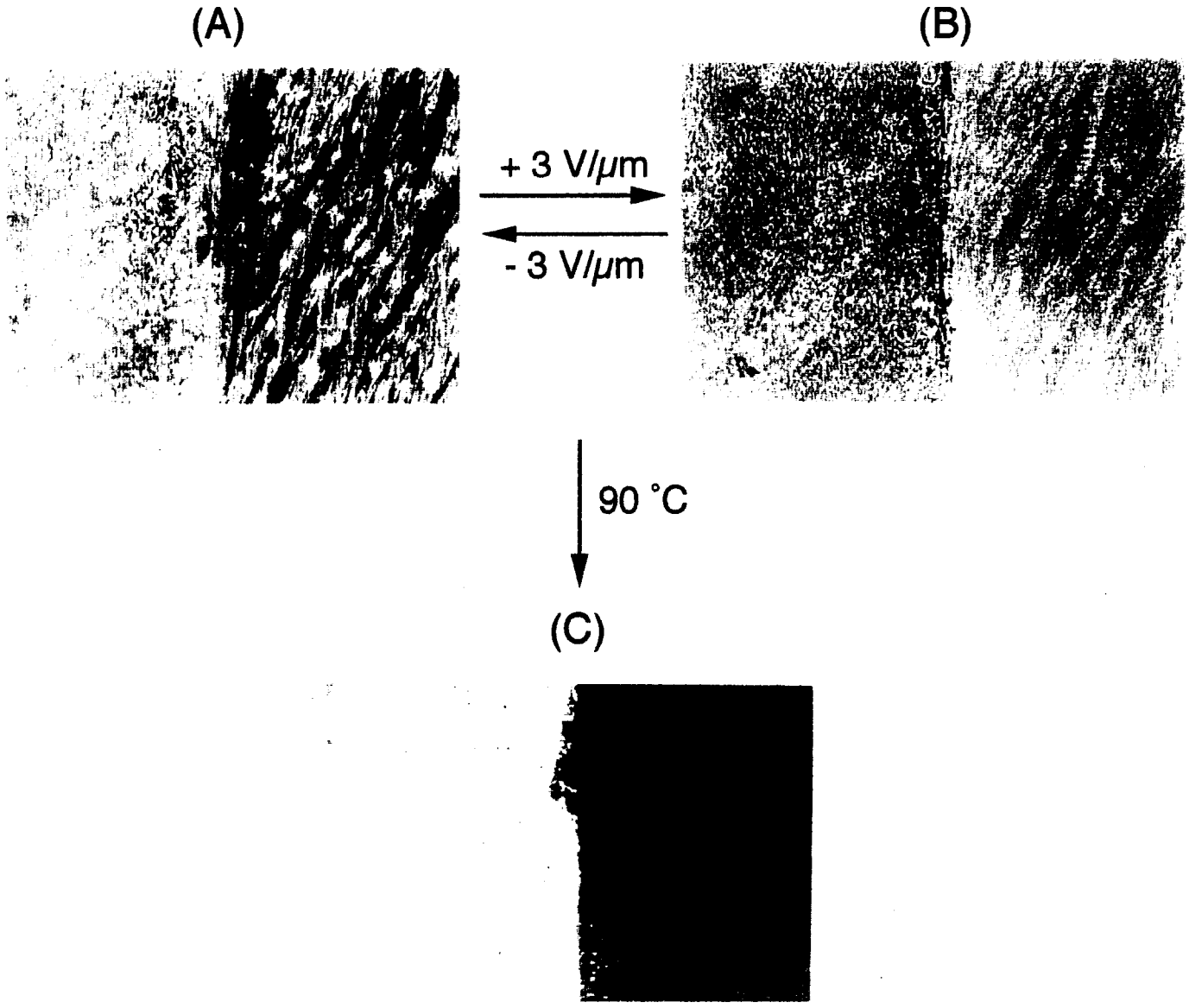

Figure 4-10. Polarized optical micrographs of the texture observed in the 2-μm-gap cell after 60-s photoirradiation of FLC monomer without an electric field at 60 °C in the SmC* phase. The left and the right half of the figures corresponds to irradiated and unirradiated site, respectively. (A), texture obtained on application of an electric field of -3 V/μm; (B), texture observed on application of an opposite electric field (3 V/μm); (C), texture obtained after heating to 90 °C at which the FLC monomer shows an I phase.

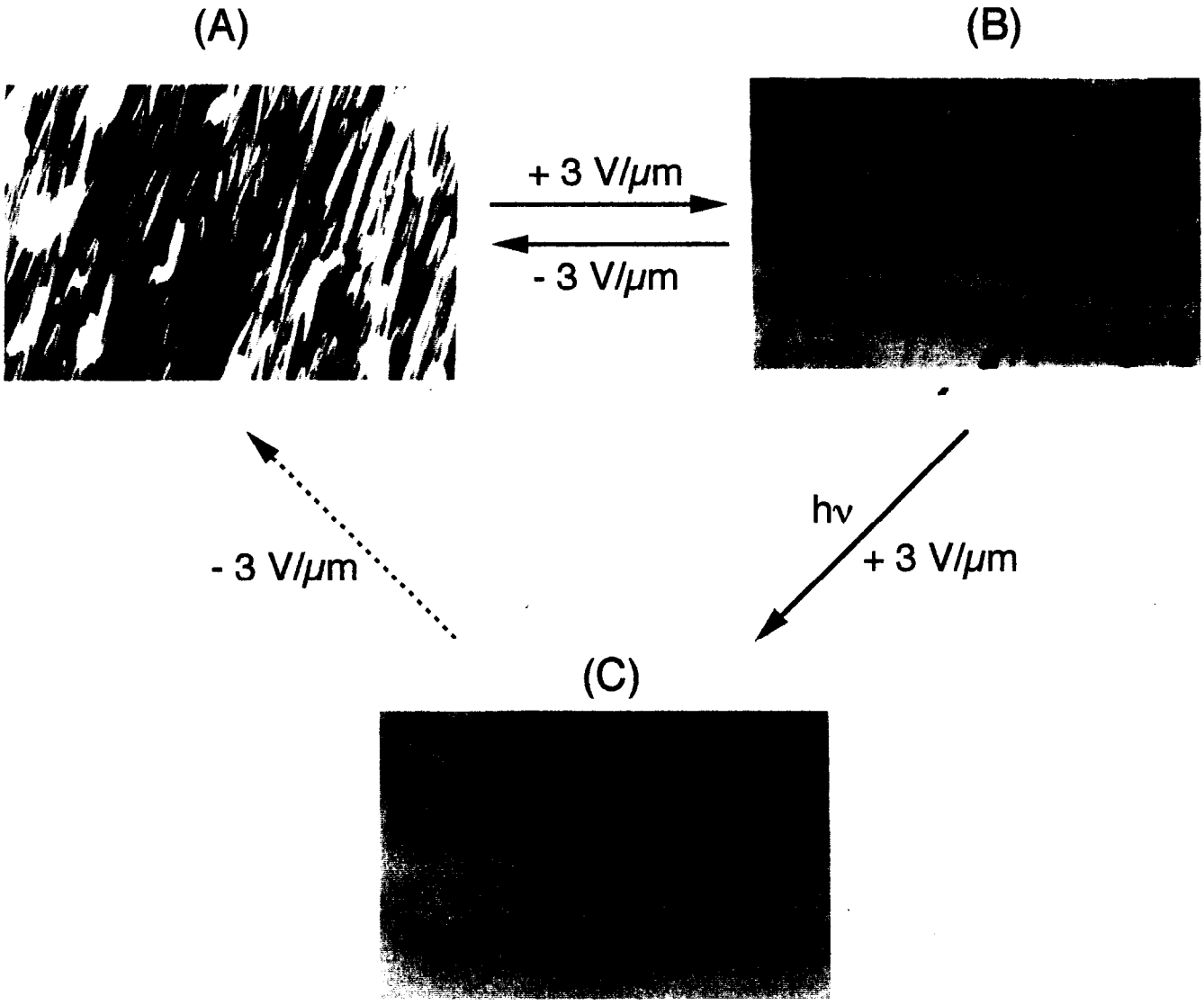

Figure 4-11. Optical textures observed in the 2-μm gap cell before and after photopolymerization of FLC monomer under the constant electric field of 3 V/μm. Photoirradiation was carried out at 60 °C for 60 s. (A), dark view with an electric field of -3 V/μm before polymerization; (B), bright view on application of an opposite electric field (3 V/μm); (C), texture obtained after polymerization.

accompanied by volume shrinkage on polymerization and the degree of the volume shrinkage is approximately 15-35 %,[10] whereas degree of the volume shrinkage in the polymerization in molecular alignment is approximately 5 %.[11] The shrinkage during the polymerization, practically, was observed for the LC monomer showing Sm and N phases.[4j] Since the mobility of LC molecules could be affected significantly by change in environmental conditions, the mobility of the FLC molecules linked to a polymer backbone may decrease in comparison with that of free FLC molecules. It is reasonable that the decrease of the mobility of mesogens by the polymerization results in no change in the molecular alignment even in the presence of the external field.

The effect of electric field on the alignment of mesogens of the polymerized FLCs was investigated in more detail. The optical textures observed at the ITO electrode-glass substrate interface in the LC cell are shown in Figure 4-12. The left side of each figure shows the texture of the polymerized FLC obtained with the electric field, and the right side shows that obtained without the electric field. The angular dependence of the transmittance of linearly polarized light through the FLC cell was significantly different between the left and right sides. As shown in Figure 4-12, the position of the sample cell between the crossed polarizers was adjusted at first so as to transmit thoroughly the linearly polarized light. When the sample cell was rotated with respect to the polarizers, only the left side became dark. The contrast between the dark and the bright view in the left side was found to be highest at every 45 ° interval. This is because tilt angle of the FLC monomer at 60 °C is 22.5 °. On the other hand, in the right side brightness of the optical texture was almost independent of the rotation of the cell. These results clearly indicate that the application of the external electric field to the sample results in appearance of the immobilized SmC* phase in which all mesogens of the polymerized FLC are aligned into one direction to form a monodomain of LC phase. Such immobilization of the SmC* phase is quite favorable from viewpoint of optical applications.

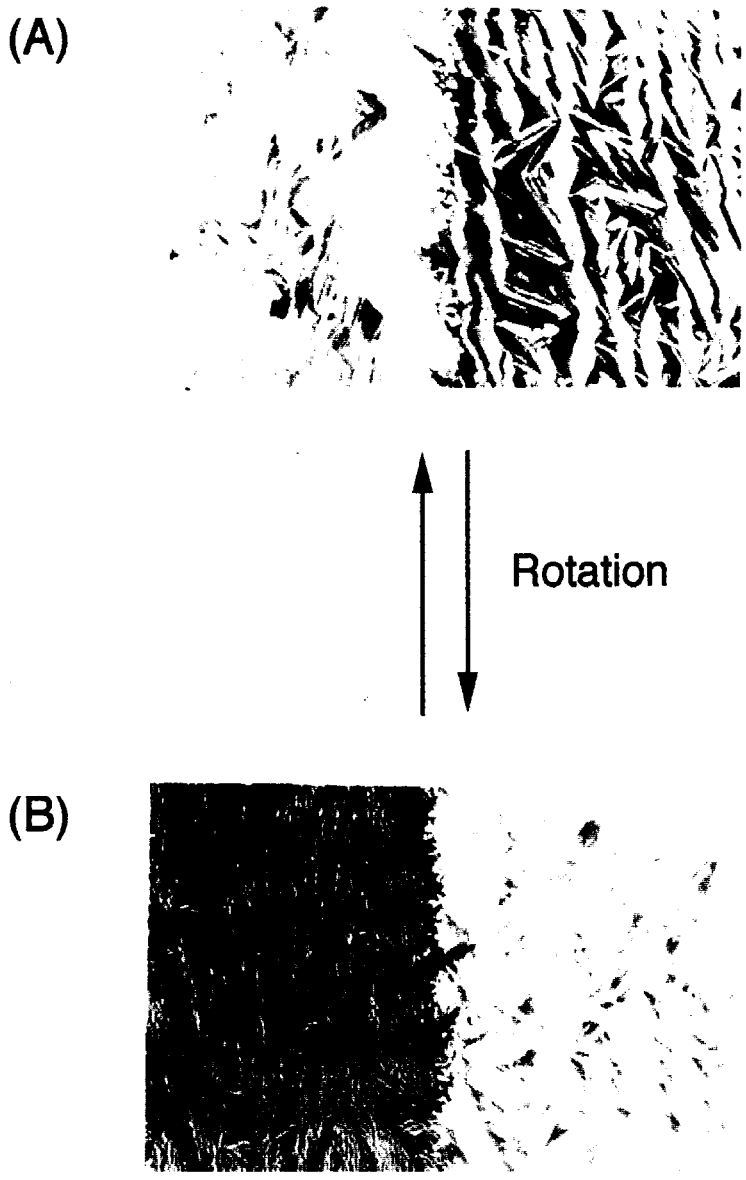

Figure 4-12. Angular dependence of the transmittance of linearly polarized light through a 2-μm-gap FLC cell. The left-hand side texture of each figure was observed by photopolymerization at 60 °C for 60 s under an electric field of 3 V/μm, and the right-hand side texture was obtained without the electric field. (A), texture of the polymerized FLC adjusted so as to show the maximum brightness; (B), texture observed when the FLC cell was rotated at 45 ° with respect to the initial position.

4-4. Conclusion

The author used a chiral LC monomer showing a ferroelectric phase and evaluated its in-situ photopolymerization behavior on the basis of molecular alignment in the LC phase. The initial polymerization rate was affected strongly by molecular alignment, and polymerizability of the FLCs was highest in the SmC* phase in the absence of an external electric field. When the FLC monomers were highly ordered by the external electric field, however, the conversions obtained were much smaller than those obtained without the electric field irrespective of polymerization temperature (i.e., phase structure). These results suggest that in the early stage of polymerization the polymerizability of the monomeric FLCs is dependent on both the molecular alignment and the molecular diffusion. Conversely, in the late stage of polymerization, the polymerization behavior of the FLC monomers was governed by their diffusion rather than their alignment. The conversion monotonically increased with temperature. This may be ascribed to the change in the phase structure during in-situ polymerization. In addition, the alignment of the photopolymerized FLC was evaluated by optical polarizing microscopy. It was found that the FLCs polymerized under the electric field formed the immobilized SmC* phase retaining the monodomain of the LC phase before photopolymerization.

References

1 (a) Broer, D. J.; Finkelmann, H.; Kondo, K. *Makromol. Chem.* **1988**, *189*, 185. (b) Hoyle, C. E.; Chawla, C. P.; Griffin, A. C. *Mol. Cryst. Liq. Cryst.* **1988**, *157*, 639. (c) Broer, D. J.; Mol, G. N. *Makromol. Chem.* **1989**, *190*, 19. (d) Broer, D. J.; Boven, J.; Mol, G. N. *Makromol. Chem.* **1989**, *190*, 2255. (e) Broer, D. J.; Hikmet, R. A. M.; Challa, G. *Makromol. Chem.* **1989**, *190*, 3201. (f) Hoyle, C. E.; Chawla, C. P.; Griffin, A. C. *Polymer* **1989**, *60*, 1909. (g) Broer, D. J.; Mol, G. N. *Makromol. Chem.* **1991**, *192*, 59. (h) Hoyle, C. E.; Kang, D.; Chawla, C. P.; Griffin, A. C. *Polym. Eng. Sci.* **1992**, *32*, 1490. (i) Hoyle, C. E.; Kang, D.; Jariwala, C.; Griffin, A. C. *Polymer* **1993**, *34*, 3070. (j) Hoyle, C. E.; Watanabe, T.; Whitehead, J. B. *Macromolecules* **1994**, *27*, 6581. (k) Broer, D. J.; Lub, J.; Mol, G. N. *Nature* **1995**, *378*, 467. (l) Kurihara, S.; Ohta, H.; Nonaka, T. *Polymer* **1995**, *36*, 849. (m) He, L.; Zhang, S.; Jin, S.; Qi, Z. *Polym. Inter.* **1995**, *38*, 211. (n) Guymon, C. A.; Hoggan, E. N.; Clark, N. A.; Rieker, T. P.; Walba, D. M.; Bowman, C. N. *Science* **1997**, *275*, 57.

2 Fukuda, A.; Takanishi, Y.; Isozaki, T.; Ishikawa, K.; Takezoe, H. *J. Mater. Chem.* **1994**, *4*, 997.

3 (a) Kondo, K.; Takezoe, H.; Fukuda, A.; Kuze, E. *Jpn. J. Appl. Phys.* **1983**, *22*, L85. (b) Ishikawa, K.; Ouchi, Y.; Uemura, T.; Tsuchiya, T.; Takezoe, H.; Fukuda, A. *Mol. Cryst. Liq. Cryst.* **1985**, *122*, 175. (c) Haramoto, Y.; Kamogawa, H.; *Mol. Cryst. Liq. Cryst.* **1989**, *173*, 89. (d) Parfenov, A. V.; Chigrinov, V. G. *Liq. Cryst.* **1990**, *7*, 131. (e) Loos-Wildenauer, M.; Kunz, S.; Voigt-Martin, I. G.; Yakimanski, A.; Wischerhoff, E.; Zentel, R.; Tschierske, C.; Müller, M. *Adv. Mater.* **1995**, *7*, 170. (f) Hikmet, R. A. M.; Lub, J. *J. Appl. Phys.* **1995**, *77*, 6234.

4 Nishiyama, I.; Goodby, J. W. *J. Mater. Chem.* **1993**, *3*, 169.

5 Jákli, A.; Saupe, A. *J. Appl. Phys.* **1997**, *82*, 2877.

6 Hoyle, C. E.; Watanabe, T. *Macromolecules* **1994**, *27*, 3790.

7 Billmeyer, F. W. *Textbook of Polymer Science*; Wiley: New York, 1984; pp 49-81.

8 He, L.; Zhang, S.; Jin, S.; Qi, Z. *Polym. Bull.* **1995**, *34*, 7.

9 Skarp, K.; Handschy, M. A. *Mol. Cryst. Liq. Cryst.* **1988**, *165*, 439.

10 Endo, T.; Ogasawara, T. *Netsukoukaseijushi* **1984**, *5*, 30.

11 Hikmet, R. A. M.; Zwerver, B. H.; Broer, D. J. *Polymer* **1992**, *33*, 89.

Chapter 5

In-Situ Photopolymerization Behavior of Chiral Liquid-Crystalline Methacrylate Monomers and Image Storage Using Ferroelectric Properties

5-1. Introduction

In Chapter 4, in-situ photopolymerization behavior of FLC monomer possessing a long spacer was investigated. However, photopolymerization behavior of FLC monomers which have a short spacer has not yet been reported. If an alkyl spacer attached to the functional group is long, the orientation of polymerizable groups between LC molecules is disordered even though the core part of mesogens is highly aligned. On the other hand, for monomers with short spacer, the orientation of mesogens affects that of polymerizable groups, improving molecular packing in an LC phase.[1] In this chapter, chiral LC vinyl monomers with methacrylate group attached to the rigid core through a short methylene spacer (carbon number of 2) and a long methylene spacer (carbon number of 11) were synthesized to explore the effect of molecular packing of the LC monomers on polymerization behavior. Furthermore, image storage was examined by means of in-situ photopolymerization under dc electric field.

5-2. Experimental

5-2-1. Materials

The structures of the two FLC monomers, [R]-1-methylheptyl 4'-[4-(ω-methacryloyloxyundecyloxy)benzoyloxy]biphenyl-4-carboxylate (**MS11**), [R]-1-methylheptyl 4'-[4-(ω-methacryloyloxyethoxy)benzoyloxy]biphenyl-4-carboxylate (**MS2**), used in this chapter are shown in Figure 5-1. The FLC monomers were prepared according to the synthetic method reported previously (Scheme 5-1).[2] 4-(ω-Hydroxyundecyloxy)benzoic acid, 4-methoxycarbonoyloxybiphenyl-4'-carboxylic acid, (R)-1-methylheptyl 4-methoxycarbonoyloxybiphenyl-4'-carboxylate, (R)-1-methylheptyl 4-hydroxybiphenyl-4'-carboxylate, and PLCs by means of solution polymerization were prepared as decribed in Chapter 4. The compounds were characterized by means of ^{1}H NMR, IR and elemental analysis as described in Chapter 2. The phase transition temperature and the phase structure were determined by DSC (cooling rate, 1 °C/min) and optical polarizing microscopy.

4-(ω-Hydroxyethoxy)benzoic acid. 4-Hydroxybenzoic acid (25 g, 0.18 mol) was dissolved in a mixture of ethanol (60 mL) and potassium hydroxide (25 g, 0.45 mol) in water (30 mL). A trace of potassium iodide was added and the solution was heated and stirred while 2-bromoethanol (25 g, 0.20 mol) was added slowly. The reaction mixture was heated under reflux for 24 h, then the solvent was removed by evaporation under reduced pressure. Water (300 mL) was added and the mixture was made strongly acidic (pH 2) with the addition of hydrochloric acid. The precipitate was isolated and recrystallized from ethanol (200 mL).

Yield: 13 g (0.072 mol, 40 %)

mp: 173-180 °C

^{1}H NMR (δ, DMSO-d_6): 7.85(m, 2H, 2-H, 6-H), 7.00(m, 2H, 3-H, 5-H), 4.04(t, 2H, -CH_2-O-), 3.71(t, 2H, -CH_2-OH)

IR (KBr, cm^{-1}): 3400, 2920, 2850, 1675, 1610, 1250

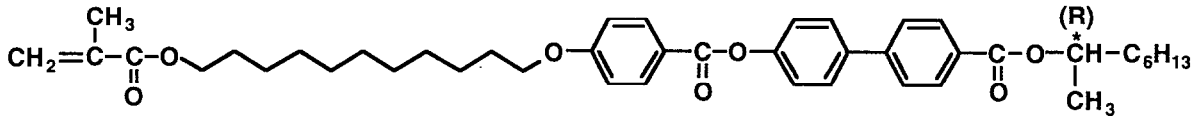

MS11

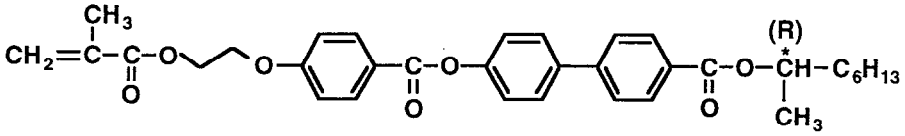

MS2

Figure 5-1. Chemical structures of the FLC monomers used in this chapter.

Scheme 5-1. Synthetic route for FLC monomers

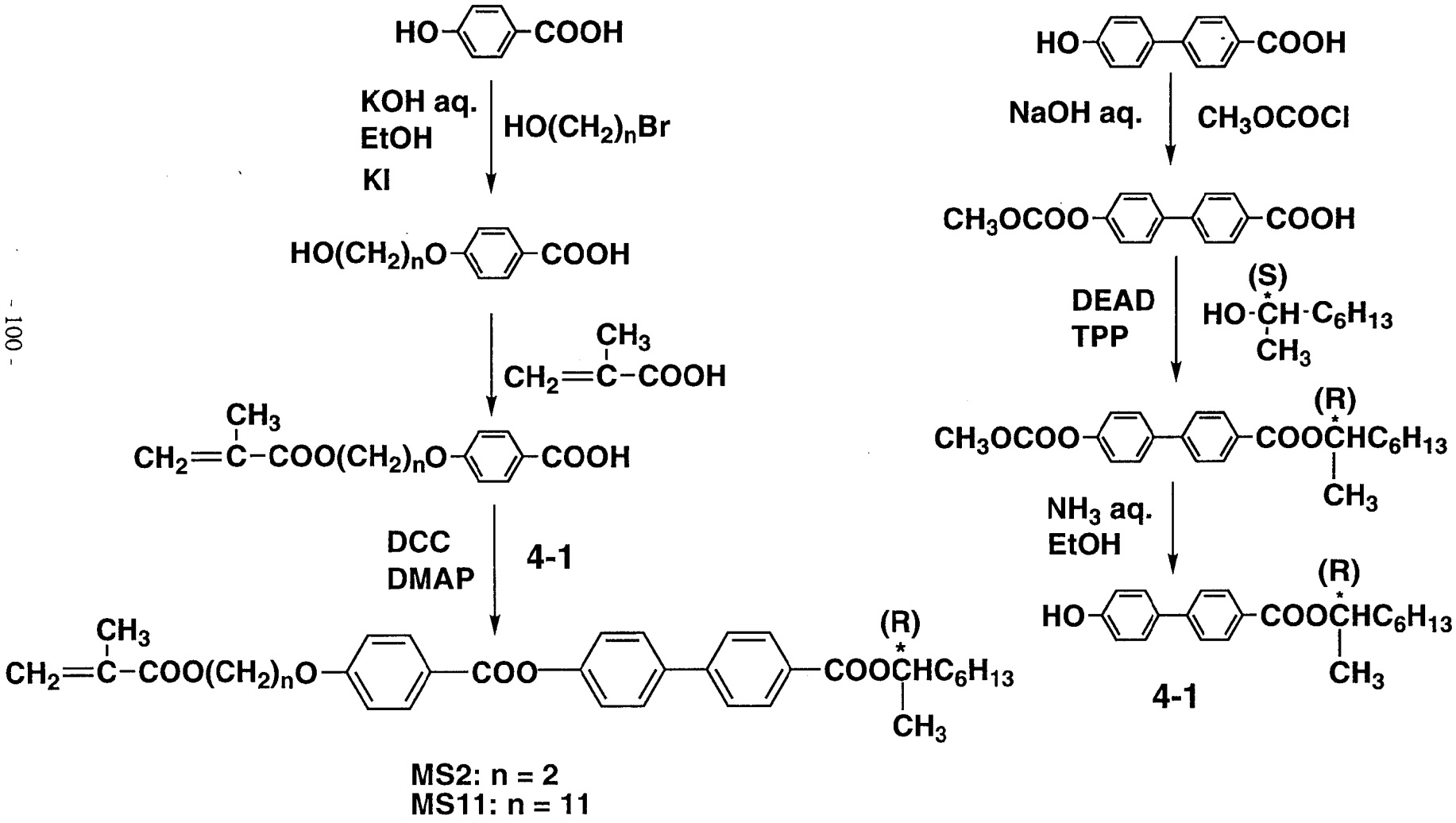

Anal. Calcd for $C_9H_{10}O_4$ (182): C, 59.34; H, 5.53 %

Found: C, 59.14; H, 5.32 %.

4-(ω-Methacryloyloxyundecyloxy)benzoic acid. A mixture of 4-(ω-hydroxyundecyloxy)benzoic acid (9.3 g, 0.03 mol), methacrylic acid (22 g, 0.25 mol), hydroquinone (1.7 g, 0.02 mol), 4-toluenesulphonic acid monohydrate (1.7 g, 0.01 mol) and benzene (200 mL) was heated under reflux in a Dean-Stark apparatus for 24 h. A solution of sodium acetate (0.75 g, 0.01 mol) in water was added to neutralize the reaction mixture. The solvent was removed under reduced pressure. The crude product was redissolved in chloroform (400 mL). The solution was filtered, washed with water (300 mL x 4) and dried over anhydrous magnesium sulphate. The solvent was removed very carefully by evaporation under reduced pressure (maximum water bath temperature 40 °C). To purify the resulting crude product, it was dissolved in chloroform and precipitated into a large excess of hexane. After the precipitate was dried under vacuum at room temperature, the product was recrystallized from ethanol.

Yield: 4.7 g (13 mmol, 42 %)

mp: 102 °C

^{1}H NMR (δ, $CDCl_3$): 8.05(m, 2H, 2-H, 6-H), 6.92(m, 2H, 3-H, 5-H), 6.10(s, 1H, *trans*-CH_2=C(CH_3)-), 5.54(s, *cis*-CH_2=C(CH_3)-), 4.13(t, 2H, -COO-CH_2-), 4.02(t, 2H, -CH_2-O-), 1.94(s, 3H, CH_2=C(CH_3)-), 1.80-1.27(m, 18H, CH_2)

IR (KBr, cm^{-1}): 3100, 2930, 2860, 1725, 1680, 1610

Anal. Calcd for $C_{22}H_{32}O_5$ (376): C, 70.19; H, 8.57 %

Found. C, 70.05; H, 8.48 %

4-(ω-Methacryloyloxyethoxy)benzoic acid. The title compound was prepared by the same procedure as 4-(ω-methacryloyloxyundecyloxy)benzoic acid.

Yield: 6.1 g (0.024 mmol, 81 %)

mp: 135-138 °C

^{1}H NMR (δ, $CDCl_3$): 8.05(m, 2H, 2-H, 6-H), 6.96(m, 2H, 3-H, 5-H), 6.14(s, 1H, *trans*-CH_2=C(CH_3)-), 5.60(s, *cis*-CH_2=C(CH_3)-), 4.52(t, 2H, -COO-CH_2-), 4.30(t, 2H, -CH_2-O-), 1.95(s, 3H, CH_2=C(CH_3)-)

IR (KBr, cm^{-1}): 3100, 2930, 2860, 1725, 1680, 1610

Anal. Calcd for $C_{13}H_{14}O_5$ (250): C, 62.40; H, 5.64 %

Found. C, 62.30; H, 5.82 %

(R)-1-Methylheptyl 4'-(4''-(ω-methacryloyloxyundecyloxy)benzoyloxy)biphenyl-4-carboxylate (MS11). 4-(ω-Methacryloyloxyundecyloxy)benzoic acid (1.1 g, 3.1 mmol), (R)-1-methylheptyl 4-hydroxybiphenyl-4'-carboxylate (1.0 g, 3.1 mmol) and DMAP (0.03 g, 0.3 mmol) were dissolved in dry chloroform (15 mL). DCC (1.38 g, 6.8 mmol) was added and the solution was stirred at room temperature for 2 days. After filtration to remove precipitated material, the filtrate was washed with water and dried over magnesium sulphate. After removal of the solvent, the product was purified by column chromatography (chloroform/hexane = 9/1) and recrystallized from ethanol (50 mL).

Yield: 1.0 g (1.5 mmol, 50 %)

mp: 50 °C

^{1}H NMR (δ, $CDCl_3$): 8.15(m, 4H, 3-H, 5-H, 2''-H, 6''-H), 7.67(m, 4H, 2-H, 6-H, 2'-H, 6'-H), 7.31(m, 2H, 3'-H, 5'-H), 6.98(m, 2H, 3''-H, 5''-H), 6.10(s, 1H, *trans*-CH_2=C(CH_3)-), 5.54(s, 1H, *cis*-CH_2=C(CH_3)-), 5.18(m, 1H), 4.14(t, 2H, -COO-CH_2-), 4.05(t, 2H, -CH_2-O-), 1.94(s, 3H, CH_2=C(CH_3)-), 1.80-1.27(m, 31H, CH_2, CH_3), 0.88(t, 3H, CH_3)

IR (KBr, cm^{-1}): 2930, 2850, 1735, 1710, 1610, 850

Anal. Calcd for $C_{43}H_{56}O_7$ (684): C, 75.41; H, 8.24 %

Found. C, 75.41; H, 8.08 %

(R)-1-Methylheptyl 4'-(4"-(ω-methacryloyloxyethoxy)benzoyloxy)biphenyl-4-carboxylate (MS2). 4-(ω-Methacryloyloxyethoxy)benzoic acid (0.8 g, 3.2 mmol), (R)-1-methylheptyl 4-hydroxybiphenyl-4'-carboxylate (1.1 g, 3.4 mmol) and DMAP (0.04 g, 0.33 mmol) were dissolved in dry chloroform (20 mL). DCC (1.0 g, 4.9 mmol) was added and the solution was stirred at room temperature for 2 days. After filtration to remove precipitated material, the filtrate was washed with water and dried over magnesium sulphate. After removal of the solvent, the product was purified by column chromatography (chloroform) and recrystallized from ethanol (50 mL).

Yield: 0.90 g (1.6 mmol, 50 %)

mp: 50 °C

^{1}H NMR (δ, $CDCl_3$): 8.14(m, 4H, 3-H, 5-H, 2"-H, 6"-H), 7.68(m, 4H, 2-H, 6-H, 2'-H, 6'-H), 7.29(m, 2H, 3'-H, 5'-H), 7.02(m, 2H, 3"-H, 5"-H), 6.16(s, 1H, *trans*-CH_2=C(CH_3)-), 5.61(s, 1H, *cis*-CH_2=C(CH_3)-), 5.16(m, 1H), 4.55(t, 2H, -COO-CH_2-), 4.33(t, 2H, -CH_2-O-), 1.97(s, 3H, CH_2=C(CH_3)-), 1.80-1.28(m, 13H, CH_2, CH_3), 0.88(t, 3H, CH_3)

IR (KBr, cm^{-1}): 2930, 2850, 1735, 1710, 1610, 850

Anal. Calcd for $C_{34}H_{38}O_7$ (559): C, 73.10; H, 6.86 %

Found. C, 73.41; H, 6.74 %

5-2-2. Preparation of Phase Diagram

Before evaluation of the in-situ photopolymerization behavior of the monomeric FLCs, the phase transition behavior during polymerization was investigated, since during photoirradiation, phase transition temperature changed with the change in composition of the monomer-polymer mixture as described in Chapter 4. To prepare the phase diagram in the binary mixture of the polymer and the monomer, the FLC polymers were synthesized by the conventional solution polymerization as mentioned in Chapter 4. The Mn and polydispersity (Mw/Mn) were determined by GPC

calibrated with standard polystyrenes. The phase transition temperature and the phase structure were identified by DSC (10 °C/min) and optical polarizing microscopy.

5-2-3. In-Situ Photopolymerization Procedure

As in Chapter 4, photopolymerization was performed in a glass cell with a gap of 2 μm without an electric field or under dc electric field of 3 V/μm. The glass cell was composed of two ITO glass substrates with PI alignment layers rubbed in an antiparallel direction. Samples for photopolymerization were prepared by injecting the FLC monomer containing 1-hydroxycyclohexyl phenyl ketone as a photoinitiator (2 mol%) into the glass cell in the I phase at 85 °C using capillary action.

5-3. Results and Discussion

5-3-1. Phase Transition Behavior of FLC Monomers and Polymers

Before exploring the polymerization behavior, the phase transition behavior of monomers was investigated. Figure 5-2 shows the DSC thermograms of the FLC monomers. The FLC monomers exhibited several sharp endothermic (heating) and exothermic (cooling) peaks. Referring to the optical microscopic observation, the phases could be assigned to K, SmC_A*, SmC*, SmA* and I phases. The temperatures and enthalpies for each phase transition are summarized in Table 5-1.

Table 5-2 summarizes the Mn, Mw/Mn and phase transition temperature of each polymer obtained by solution polymerization.

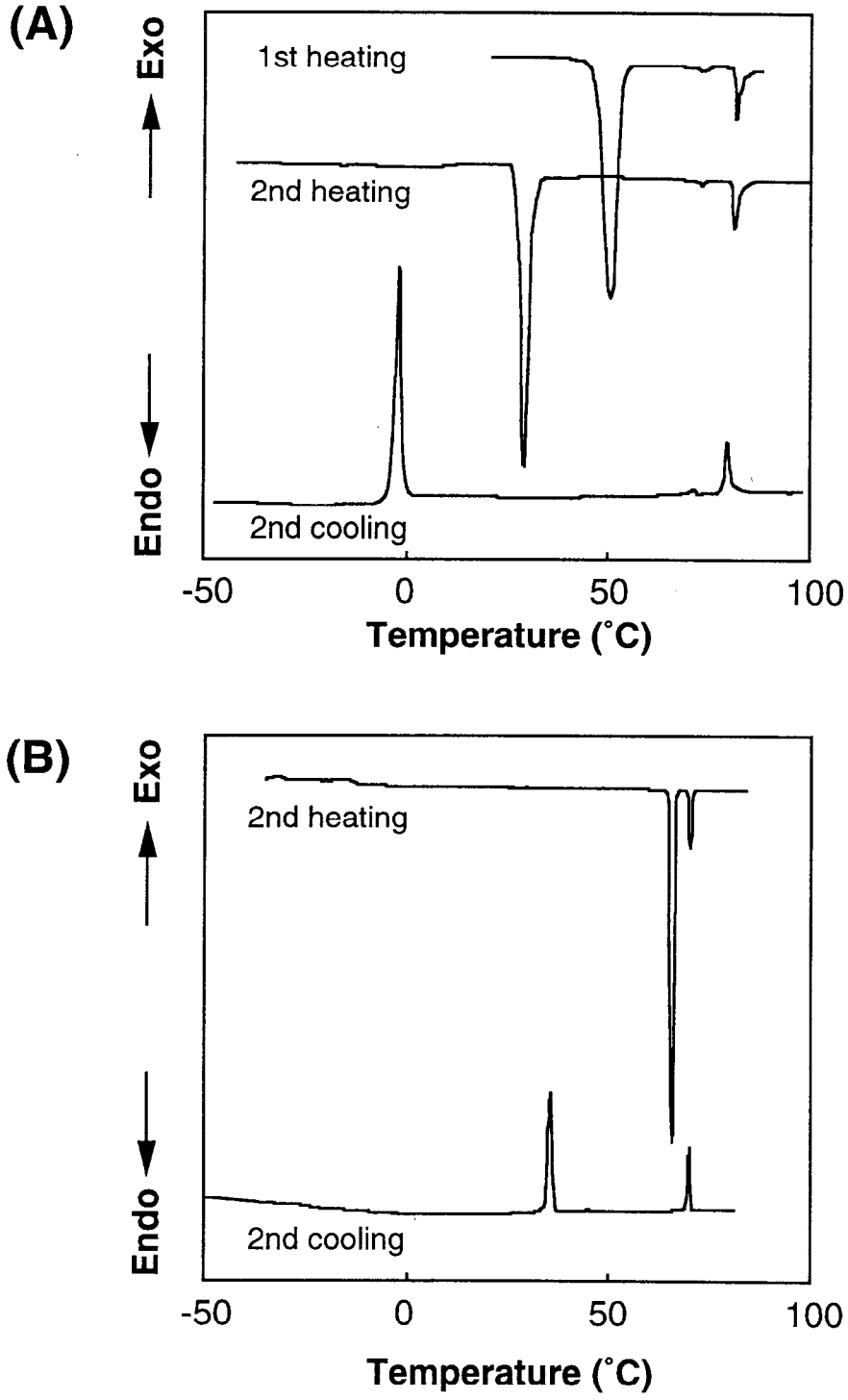

Figure 5-2. DSC thermograms of FLC monomers at heating and cooling rate of 1 °C/min. (A), **MS11**; (B), **MS2**.

Table 5-1. Phase transition temperature[a] and change in enthalpy[b] of transition of FLC monomers

Compd		Phase transition temperature (°C)
MS11	1st heating	K 50 (45) SmC* 73 (0.55) SmA* 81 (3.4) I
	2nd heating	K 29 (48) SmC* 73 (0.48) SmA* 81 (4.3) I
	2nd cooling	I 80 (3.7) SmA* 72 (0.55) SmC* 55 (-[c]) SmC_A* -1.7 (21) K
MS2	2nd heating	K 66 (29) SmA* 70 (3.5) I
	2nd cooling	I 70 (3.0) SmA* 47 (0.50) SmC* 35 (13) K

[a] Key: K, crystal; SmC_A*, antiferroelectric chiral smectic C; SmC*, ferroelectric chiral smectic C; SmA*, chiral smectic A; I, isotropic.

[b] The values in parentheses give change in enthalpy of transition in kJ/mol.

[c] The change in enthalpy of SmC*-SmC_A* transition was too small to be evaluated.

Table 5-2. Mn, Mw/Mn and phase transition temperature[a] of polymer by solution polymerization

Compound	Mn	Mw/Mn	Phase transition temperature (°C)
Poly(MS11)	6.4 x 10^4	3.5	G 37 SmC_A* 150 SmA* 161 I
Poly(MS2)	6.3 x 10^4	4.1	G 138 SmA* 220 Decomposition

[a] Key: G, glassy; SmC_A*, antiferroelectric chiral smectic C; SmA*, chiral smectic A; I, isotropic.

Figure 5-3 shows X-ray diffraction patterns observed for **MS11** and **MS2** at various temperatures. The reflections in small-angle region (< 10 °) correspond to those of the interlayer spacing. The numbers shown in Figure 5-3 are layer spacing and temperature, respectively. Tilt angles determined by optical measurement and X-ray diffraction were 22.5 ° and 18.2 ° for **MS11** at 60 °C. Optical measurement depends on the delocalized electrons which show strong interaction with light and determines the tilt angle of skeleton, whereas in X-ray diffraction the electron density is important and the tilt angle of the whole molecule is determined. Materials whose molecules have longer alkyl tails exhibit a systematic difference between the values of the tilt angle obtained from the optical and X-ray measurements ($\theta^{opt} > \theta^{X\text{-}ray}$). This indicates that possible packing of molecules approximates the molecule by the zigzag structure

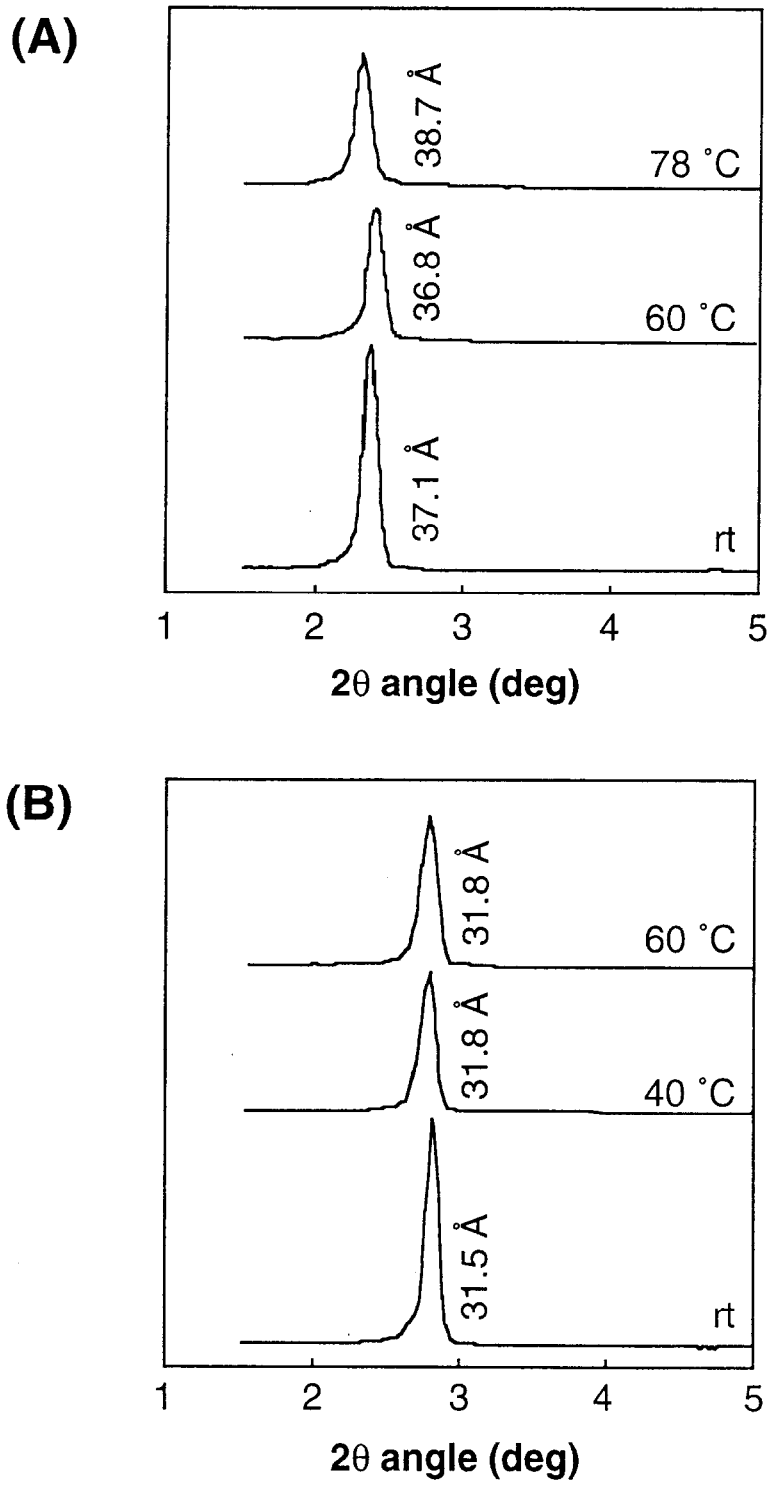

Figure 5-3. X-ray diffraction patterns measured at various temperatures. (A), **MS11** monomer; (B), **MS2** monomer.

shown in Figure 5-4.[3] On the other hand, the tilt angle for **MS2** was 15 ° at 40 °C. However, it was not possible to obtain X-ray diffraction data for **MS2** in the SmC* phase because the mesophase tended to transform to crystal when left at constant temperature.

5-3-2. In-Situ Photopolymerization Behavior

It is important to evaluate the changes in the phase transition temperature due to changes in composition of the monomer-polymer mixture as in Chapter 4.[4] Several samples were prepared in which the mixing ratio of the monomer and the polymer was altered, and the binary mixtures were subjected to DSC and microscopic observation to explore the phase behavior. The phase diagram is shown in Figure 5-5. In both systems, phase transition occurred as the ratio of the monomer to polymer changed. In the case of **MS11** with a relatively low polymer content (less than 20 wt%), the phase transition temperature changed only slightly. This result demonstrates that the change in the phase structure could be negligible during the early stage of polymerization. The phase transition temperature of the mixtures was, however, shifted to higher temperature as the polymer content increased, and the temperature range of the SmC_A* phase increased considerably. For **MS2** with a relatively low polymer content, the phase transition temperature changed, but to less extent. On the other hand, the phase structure changed considerably as the polymer content increased.

The time-conversion curve obtained by photoirradiation of **MS11** at a light intensity of 1 mW/cm^2 is shown in Figure 5-6(A) and that of **MS2** at 0.1 mW/cm^2 in Figure 5-6(B). The conversion showed a tendency to increase with increasing the irradiation time, irrespective of the polymerization temperature. A similar trend was observed for a sample under an electric field. However, time-conversion profiles were considerably different by condition of applied electric field. These differences in polymerization behavior in the SmC* phase by the condition of applied electric field is discussed in detail in Chapter 6. On the basis of the phase diagram shown in Figure 5-

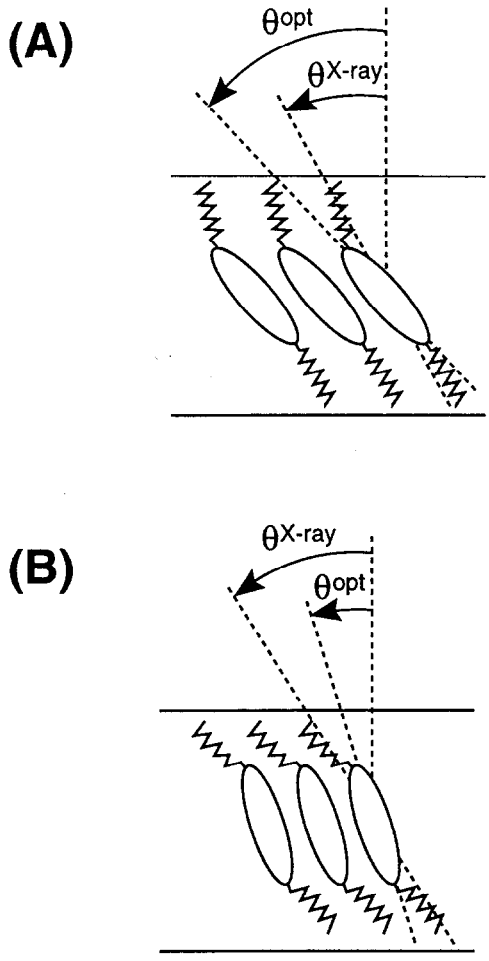

Figure 5-4. Possible packing of molecules (zigzag model) in the ferroelectric SmC* phase.

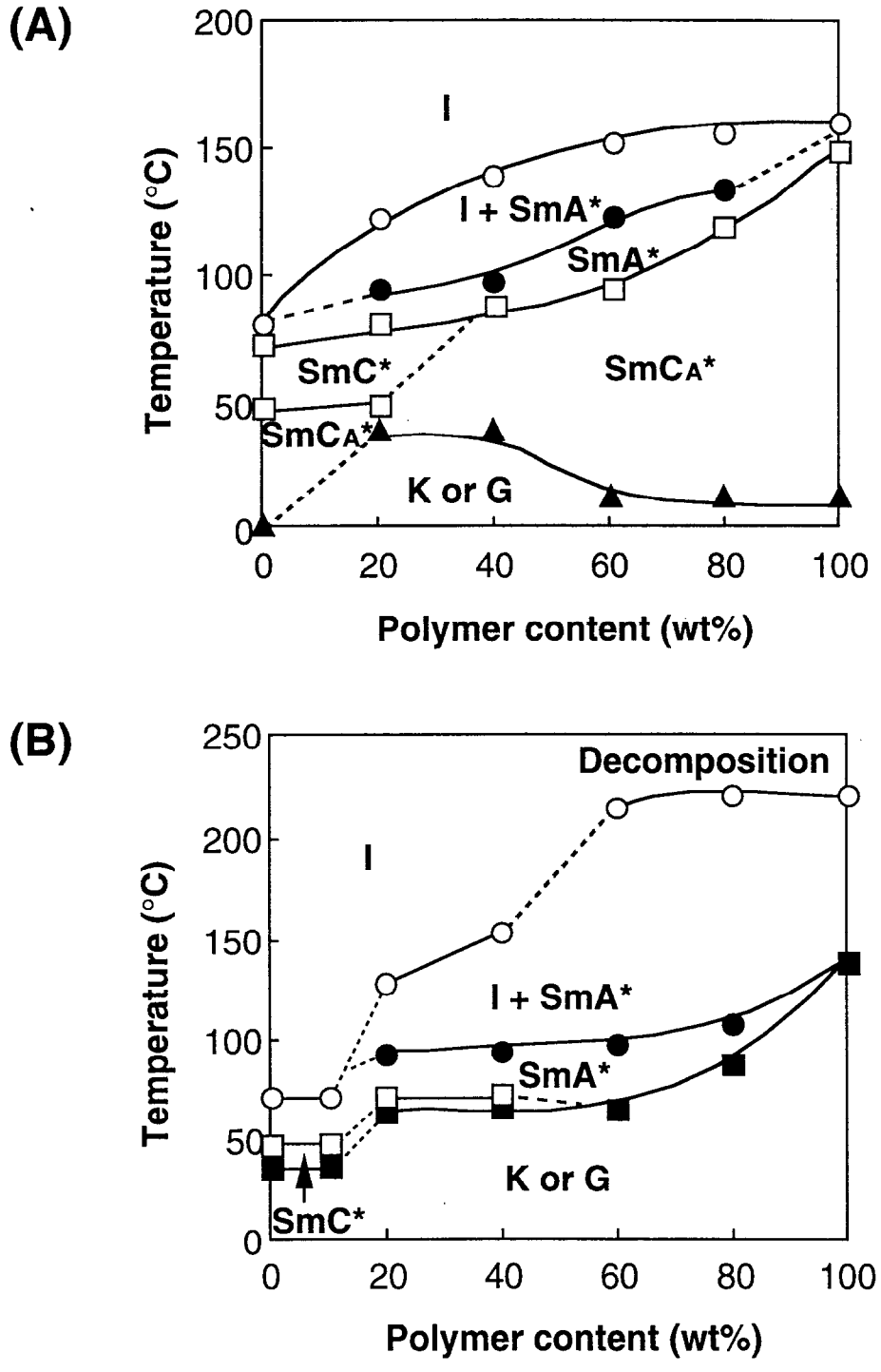

Figure 5-5. Phase diagrams for mixtures of monomer and polymer. (A), **MS11**; (B), **MS2**.

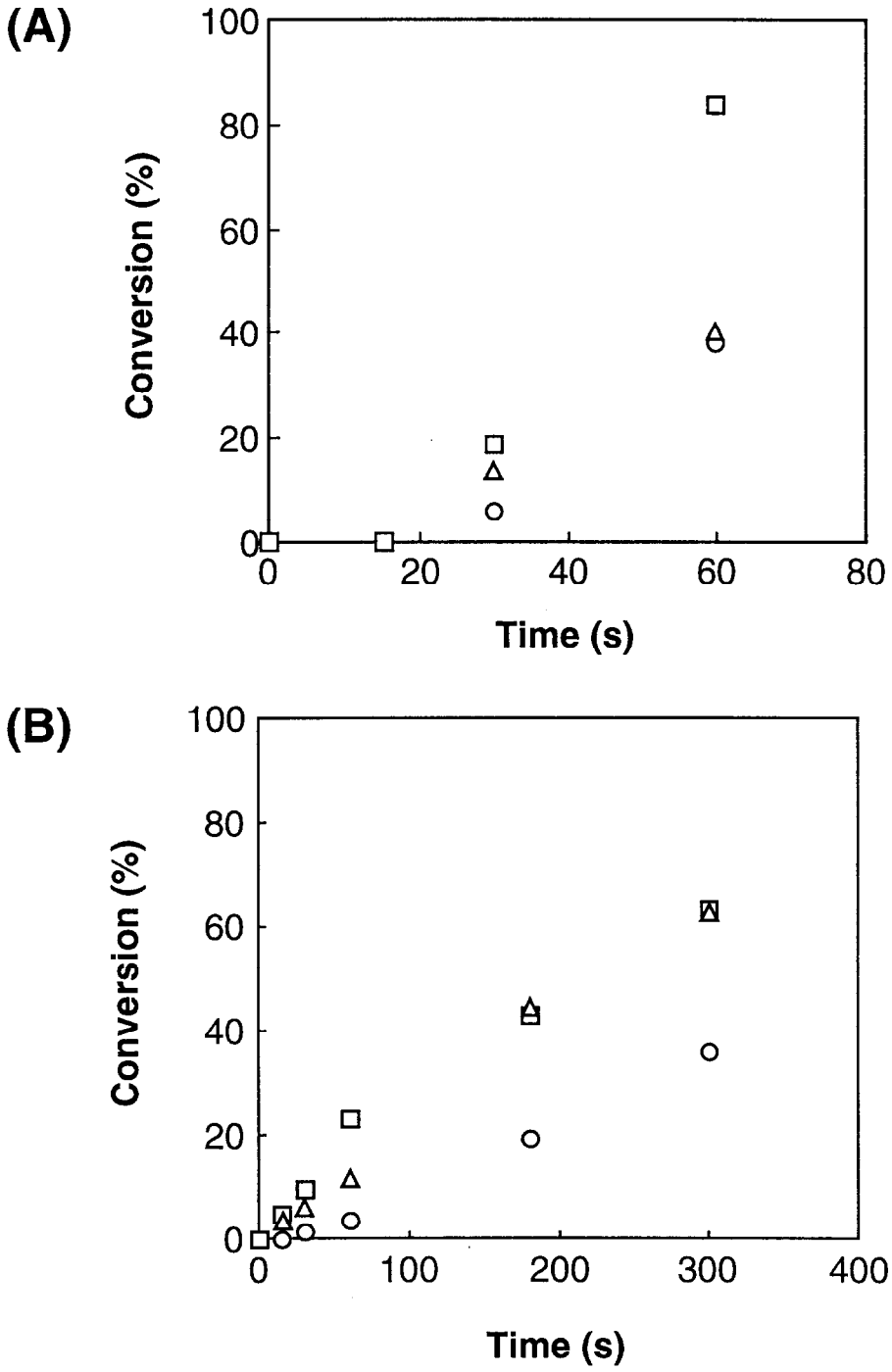

Figure 5-6. Time-conversion curves for photopolymerization at various temperatures in glass cell with a gap of 2 μm. (A), on photoirradiation (1 mW/cm^2) of **MS11**; (B), on photoirradiation (0.1 mW/cm^2) of **MS2**; ○, 40 °C; □, 60 °C; △, 80 °C.

5, it is assumed that no phase transition occurs at least on 30-s irradiation of **MS11** due to low content of the polymer produced. The author therefore used the conversions after 30-s irradiation as a measure to explore the in-situ photopolymerization behavior of the **MS11** monomer. On the other hand, for **MS2** which has a short spacer the conversions after photoirradiation at 1 mW/cm^2 were high and it is assumed that phase transition occurred during polymerization. At 0.1 mW/cm^2, conversions after 60-s irradiation were relatively low, which resulted in no phase transition during polymerization.

Polymerization Behavior of MS11 Monomer

Figure 5-7(A) shows GPC charts of samples after photopolymerization of **MS11** in the SmC* phase at 60 °C. At low conversion (19 % conversion), a monomodal peak of polymer was observed, although at higher conversion (84 % conversion) the peak showed a shoulder. It has been reported that phase transition occurred during polymerization and the peak in the lower molecular weight fractions appeared in the GPC chart.[5] The formation of the polymer with the lower molecular weight is related to the extremely small rate constant of propagation due to high viscosity of the system. It can therefore be presumed that polymerization behavior changed at high conversion because of phase transition to SmC_A* phase during polymerization.

The relation between conversion and temperature in photopolymerization of **MS11** is shown in Figure 5-8. Conversions after 30-s irradiation were plotted as a function of temperature. Without electric field, conversion was highest after irradiation in the SmC* phase (Figure 5-8(A), O). The distances between polymerizable groups become small when monomer shows high orientation. From the standpoint of the kinetics, in the SmC* phase the rate constant of propagation (k_p) is smaller, while the rate constant of termination (k_t) is much smaller because of high viscosity with small mobility. Therefore, it is anticipated that polymerization is fast. The conversion of corresponding acrylate in the SmC_A* phase was as high as that in the SmC* phase in

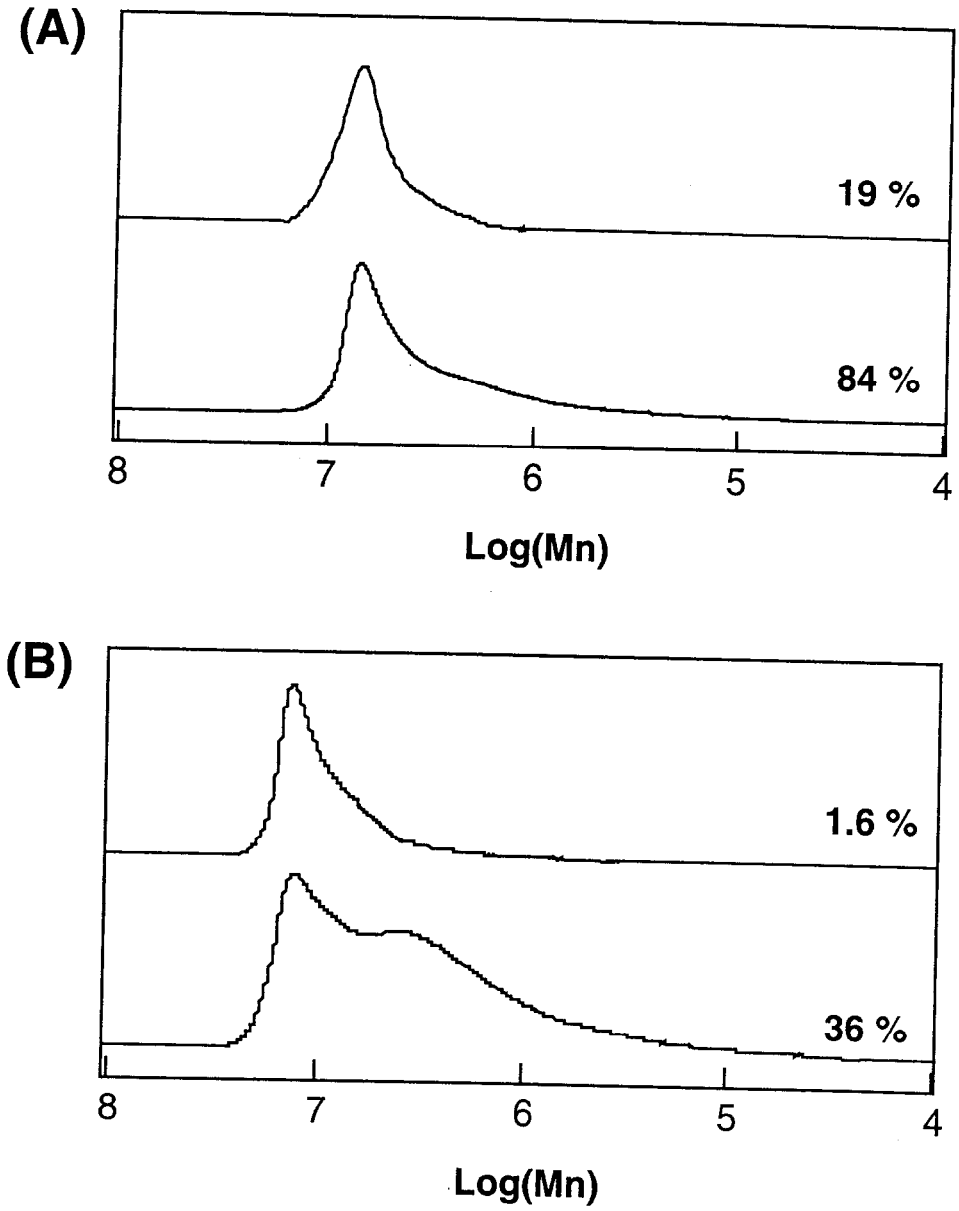

Figure 5-7. GPC charts of samples after photopolymerization of FLC monomers in glass cell with a gap of 2 μm. (A), after irradiation (1 mW/cm^2) of **MS11** at 60 °C; (B), after irradiation (0.1 mW/cm^2) of **MS2** at 40 °C. Numbers in the figure show conversion.

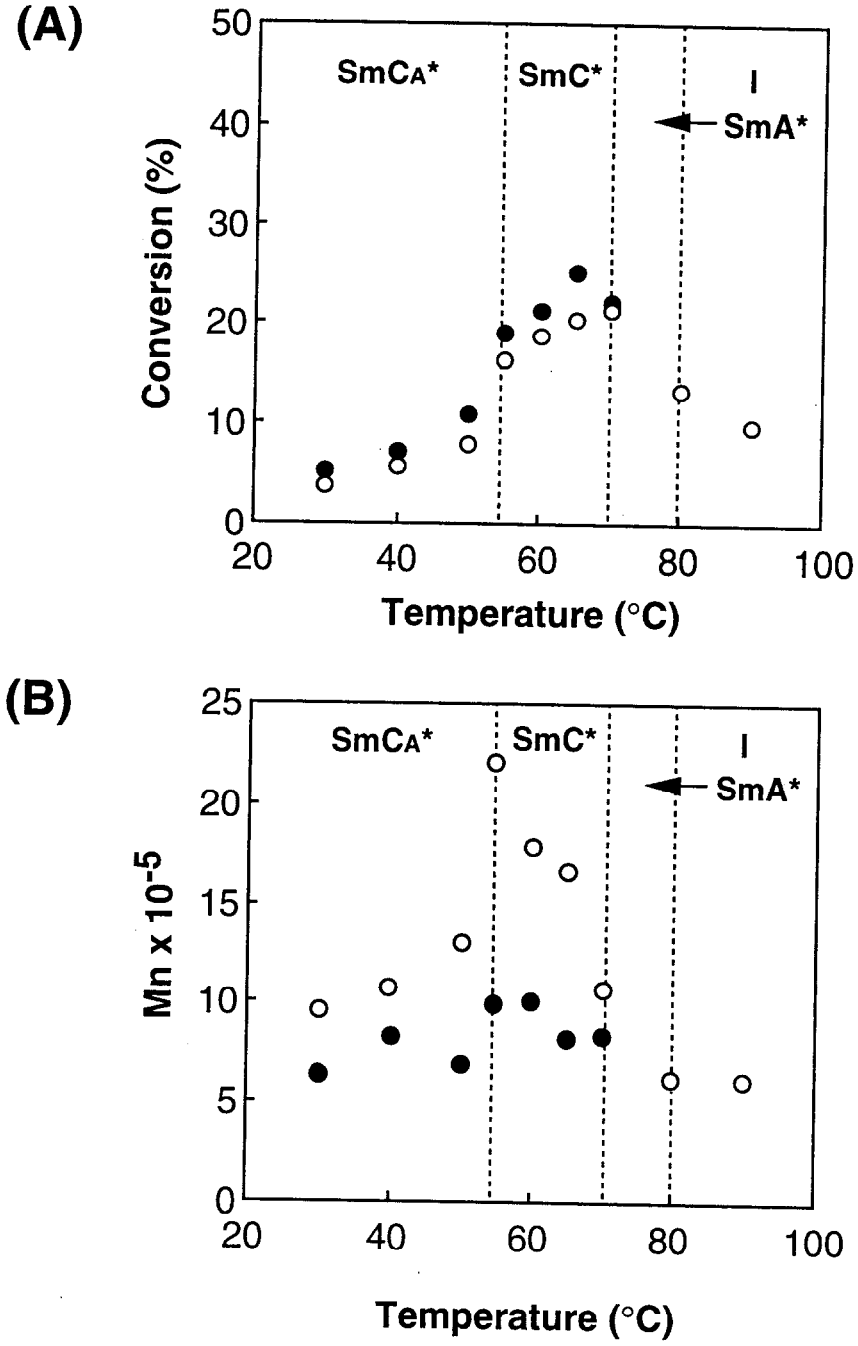

Figure 5-8. Polymerization behavior of **MS11** after 30-s photoirradiation (1 mW/cm^2) at various temperatures in a glass cell. (A), conversion; (B), number-average molecular weight; O, without an electric field; ●, with a dc electric field of 3 V/μm.

the early stage of polymerization (Chapter 4), while the polymerizability of **MS11** in the SmC_A* phase descreased. The conversions of **MS11** after 15-s irradiation were approximately 0 % irrespective of polymerization temperature, whereas those of acrylate were 10 % even after 5-s irradiation in the SmC* phase. In general, k_p increases with polymerization temperature, and k_p's for acrylates are approximately 5 (30 °C) and 2.5 times (50 °C) as large as those for methacrylates.[6] Consequently, it is expected that kinetic factor such as k_p is responsible for the difference in polymerizability between methacrylate and acrylate and this difference is larger at lower temperature. In addition, conversion decreased in the I phase. These results indicate that the k_p in organized systems is dependent on molecular alignment as well as mobility. On the other hand, Mn was largest at SmC_A*-SmC* phase transition temperature (Figure 5-8(B), O). This result differs from those of acrylate described in Chapter 4. Since resonance effect was higher for methacrylate radicals, lifetime of the methacrylate radicals may be longer than that of acrylates. Difference in reactivity and lifetime of propagating radicals seems to result in the observed difference in polymerization behavior between methacrylate and acrylate. In contrast, Mn of the resultant polymethacrylate was almost the same as that of polyacrylate. Kinetic chain length related to Mn is proportional to the ratio of k_p to k_t in steady state, and hence the similarity in Mn implies that the ratio of these two rate constants may be similar between methacrylate and acrylate.

Polymerization Behavior of MS2 Monomer

Polymerization of **MS2** having a short spacer was also conducted. **MS2** exhibited different polymerization behavior from **MS11**. At a light intensity of 0.1 mW/cm^2, the formation of polymer was confirmed in **MS2**, but not in **MS11** by GPC. It is obvious that functional groups are densely located because the number of polymerizable groups in volume is larger for **MS2** than for **MS11**. These suggest that density of polymerizable groups affects polymerizability. At 1 mW/cm^2, conversion

and Mn were independent of initial phase of monomer and applied electric field in the polymerization of **MS2**. This implies that phase transition to SmC_A* phase occurred during polymerization as demonstrated in Figure 5-5. To investigate the effect of phase structure of monomer on polymerization behavior, photopolymerization was conducted at a light intensity of 0.1 mW/cm^2. When the light intensity was low, phase transition did not occur during polymerization due to low conversion, and the effect of phase structure of monomer on the polymerization behavior could be investigated.

Figure 5-7(B) shows GPC charts of samples after photopolymerization of **MS2** in the SmC* phase at 40 °C. Even at low conversion (1.6 % conversion), a bimodal peak of polymer was observed. The Mn in the higher molecular weight part was approximately twice as much as that in the lower molecular weight part. The termination can take place in two ways: combination and disproportionation in which hydrogen transfer results in the formation of two molecules with one saturated and the other unsaturated end groups.[7] Each type of termination is known. For instance, polyacrylate radicals terminate predominantly by combination, whereas polymethacrylate radicals terminate by disproportionation as well as combination. However, for **MS11** a monomodal peak was observed in the early stage of polymerization. It can therefore be presumed that two active species exist in the polymerization mixture of **MS2** with different microphase structures without an electric field or with dc electric field even though no change in the macroscopic phase structure was observed. At higher conversion (36 % conversion) lower molecular weight fractions were observed in the GPC charts. This result indicates that transition to the G phase at higher conversion might significantly have retarded the polymerization.

Figure 5-9 shows conversion (A) and Mn (B) in the polymerization of **MS2** as a function of temperature. Conversion was high in the SmC* under electric field and the SmA* phases. As mentioned for **MS11**, polymerizability was mainly affected by k_p. Thus, conversion was low in the SmC* phase without electric field. In contrast, the SmC* phases with dc electric field have extremely high orientation and the

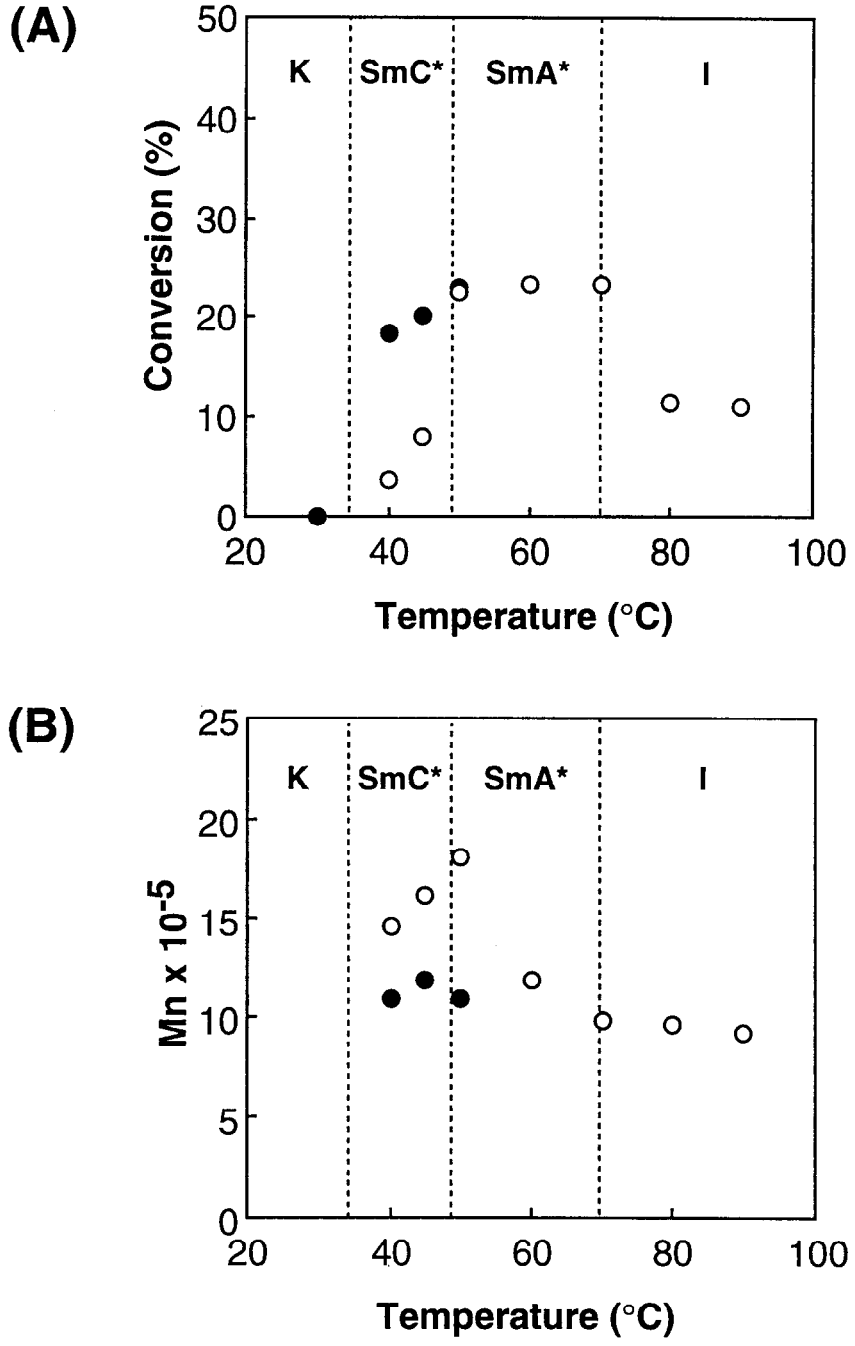

Figure 5-9. Polymerization behavior of **MS2** after 60-s photoirradiation (0.1 mW/cm^2) at various temperatures in a glass cell. (A), conversion; (B), number-average molecular weight; O, without an electric field; ●, with an electric field of 3 V/μm.

polymerizable groups may be closely located, which results in fast polymerization. Mn was largest at SmC*-SmA* phase transition temperature, which is different from the behavior of **MS11**. It might be interpreted in terms of microscopic diffusion and the distance between propagating radical and monomer.

Effect of Electric Field on Polymerization

It is expected that the polymerization rate would be enhanced significantly when the FLC monomers are highly aligned by application of the electric field. Such effects of the external electric field on the polymerization rate have been observed also for the chiral LC monomer showing SmA* phase and the polymerization rate seems to be dependent on the efficient collision between polymerizable groups.[8] On the other hand, it has been also reported that the change in the macroscopic alignment by external forces does not alter the polymerization kinetics.[9] The result obtained in this chapter exhibited that conversion increased and Mn of polymer produced decreased under dc electric field compared to those without electric field (Figures 5-8 and 5-9). As described in Chapter 4, for FLC acrylate monomer having a long alkyl spacer, the conversions obtained with dc electric field were much smaller than those obtained without the electric field. As described in Chapter 1, the reactivity of radicals is affected by the distance between propagating radical and monomer. For acrylates, since the distance in molecular alignment is disadvantageous for the polymerization, the phase structure in the FLC state is more disadvantageous. In contrast, methacrylates have α-methyl groups. The presence of the α-methyl groups might be useful to proceed efficiently for the reaction between propagating radical and monomer. In this case, the phase structure in FLC state is advantageous for polymerization.

To compare polymerization behavior between two monomers which have different length of the alkyl spacer, the author evaluated the relative conversion (the ratio of conversion under electric field to that without electric field) in the SmC* phase. It was found that the relative conversion of **MS2** was 3.1 and that of **MS11** was 1.2. As

described in the previous section, if spacer is long, the orientation of polymerizable groups of LC monomers is poor even though the core is highly oriented, whereas the orientation of mesogens affects that of functional groups for monomer possessing a short spacer. Thus, the change of macroscopic structure was more effective in the polymerization of **MS2** having a short spacer.

The monomer shows high orientation (ferroelectric surface-stabilized state) by applying dc electric field in the SmC* phase where the polymerizable groups adjoin. Then, it is expected that Mn increases by applying electric field. However, Mn decreased by applying dc electric field. Furthermore, it was observed that on application of the dc electric field the lower molecular weight fractions in the GPC chart shown in Figure 5-7(B) increased. The peak in the lower molecular weight fractions may be due to change in microphase structure. Application of dc electric field may decrease the diffusion of the system and polymerization under dc electric field might be strongly affected by change in microphase structure. It can therefore be reasonable that the lower molecular weight fractions increased by application of the dc electric field.

5-3-3. Birefringence of Sample after Photoirradiation in the I Phase

Figure 5-10 shows the textures in the cell observed on a polarizing microscope at room temperature. These are the textures observed after irradiation in the I phase of FLC monomers for 60 s. After photoirradiation of **MS11**, birefringence was induced (Figure 5-10(A)). This result indicates that the phase changed from the I phase to the SmC_A* phase. In the case of monomers possessing a long spacer, functional group and core are decoupled. The core is relatively free even if functional groups are attached. Therefore, reorientation occurs during polymerization. For **MS2**, no focal conic texture was confirmed (Figure 5-10(B)). The dark view has two possibilities: homeotropic SmA* phase or I phase. To determine the phase of sample after photoirradiation, the texture with conoscope was observed by optical polarizing microscopy. If the sample

Figure 5-10. Polarized optical micrographs of the texture observed in the 2-μm-gap cell after 60-s photoirradiation (1 mW/cm^2) of FLC monomers without an electric field in the I phase. (A), texture of sample after photopolymerization of **MS11** at 85 °C; (B), texture of sample after photopolymerization of **MS2** at 80 °C.

exhibits the homeotropic SmA* phase, texture with conoscope should be observed. However, no texture with conoscope was detected. These results suggest that sample after 60-s irradiation in the I phase showed an I phase. After 60-s photoirradiation of **MS2**, the phase should change from the I to the G phases via the SmA* phase during polymerization, since the conversion was higher than 70 %. However, even after 60-s irradiation the phase remained in the I phase macroscopically. For monomers with a short spacer, functional group and core are coupled. These may be due to the extreme decrease of the mobility of mesogens by the polymerization, which results in no reorientation to LC phase.

5-3-4. Alignment of Photopolymerized FLC

The molecular alignment of the FLCs was explored by optical polarizing microscopy after the photopolymerization of **MS11** was conducted in the 2-μm-gap cell at 60 °C in the SmC* phase. Before photoirradiation, the polarization flip was confirmed at first to occur by application of the alternating electric field (±3 V_{pp}/μm). The optical texture after photoirradiation was the same as that before photoirradiation, but the polymerized FLC showed no response to the electric field. This immobilization of molecular alignment could be attributed to low mobility of mesogens of the polymerized FLC owing to volume shrinkage as described in Chapter 4. It is reasonable that the decrease of the mobility of mesogens by the polymerization results in no change in the molecular alignment even in the presence of the external field.

Photopolymerization of monomer in the SmC* phase without electric field produced polydomain of LC phase. The application of the external electric field to the sample resulted in appearance of the immobilized SmC* phase in which all mesogens of the polymerized FLC were aligned into one direction, leading to the formation of a monodomain of LC phase. A similar result was obtained on photoirradiation of **MS2**. Such immobilization of the SmC* phase is quite favorable from viewpoint of optical applications. For instance, image storage was expected by applying an electric field

with reverse polarity, since the polarization flipped into the opposite direction only in unpolymerized part. Image storage has been obtained by changing the direction of the applied magnetic field[9] and network with a patternwise orientation has been prepared by locally applying electric fields.[10]

The diagram for the image storage is shown in Figure 5-11. (1) Dipoles and mesogens of FLC molecules in the SmC* phase are aligned into one direction by external electric field. (2) Using a photomask, the LC cell is irradiated, which leads to immobilization of mesogenic core by polymerization only at the irradiated part. (3) Direction of FLC monomer is changed by application of an electric field with reverse polarity. (4) The LC cell is again irradiated without photomask to immobilize the other part of the cell.

An LC cell containing a monomer and a photoinitiator was covered with a photomask and LC molecules were oriented in the SmC* phase, then photoirradiation was conducted with applying dc electric field for 60 s. The monomer was polymerized only in the irradiated part by this method. In this part, LC molecules showed no response to the electric field of 3 $V_{pp}/\mu m$. By applying an electric field with reverse polarity which was larger than the threshold value, the polarization flipped into the opposite direction in the unpolymerized part. After removing the photomask, photoirradiation was conducted for 60 s again.

The image storage was achieved by photopolymerization of **MS11** while it was unsuccessful in **MS2**. As shown in Table 1, **MS2** exhibited a narrow monotropic SmC* phase upon cooling and crystallization tended to occur quite rapidly upon removal of the photomask. However, by photoirradiation of **MS2** in the I phase (80 °C) for 60 s after removal of the photomask, the image was successfully stored. Figure 5-12 shows the texture of sample prepared by photoirradiation of **MS11** observed with polarizing microscope in the cell with 2 μm-cell gap. The author observed bright and dark views alternately every 45 ° by rotating the sample with respect to the plane of polarization. Furthermore, the stored image by photopolymerization in the ferroelectric

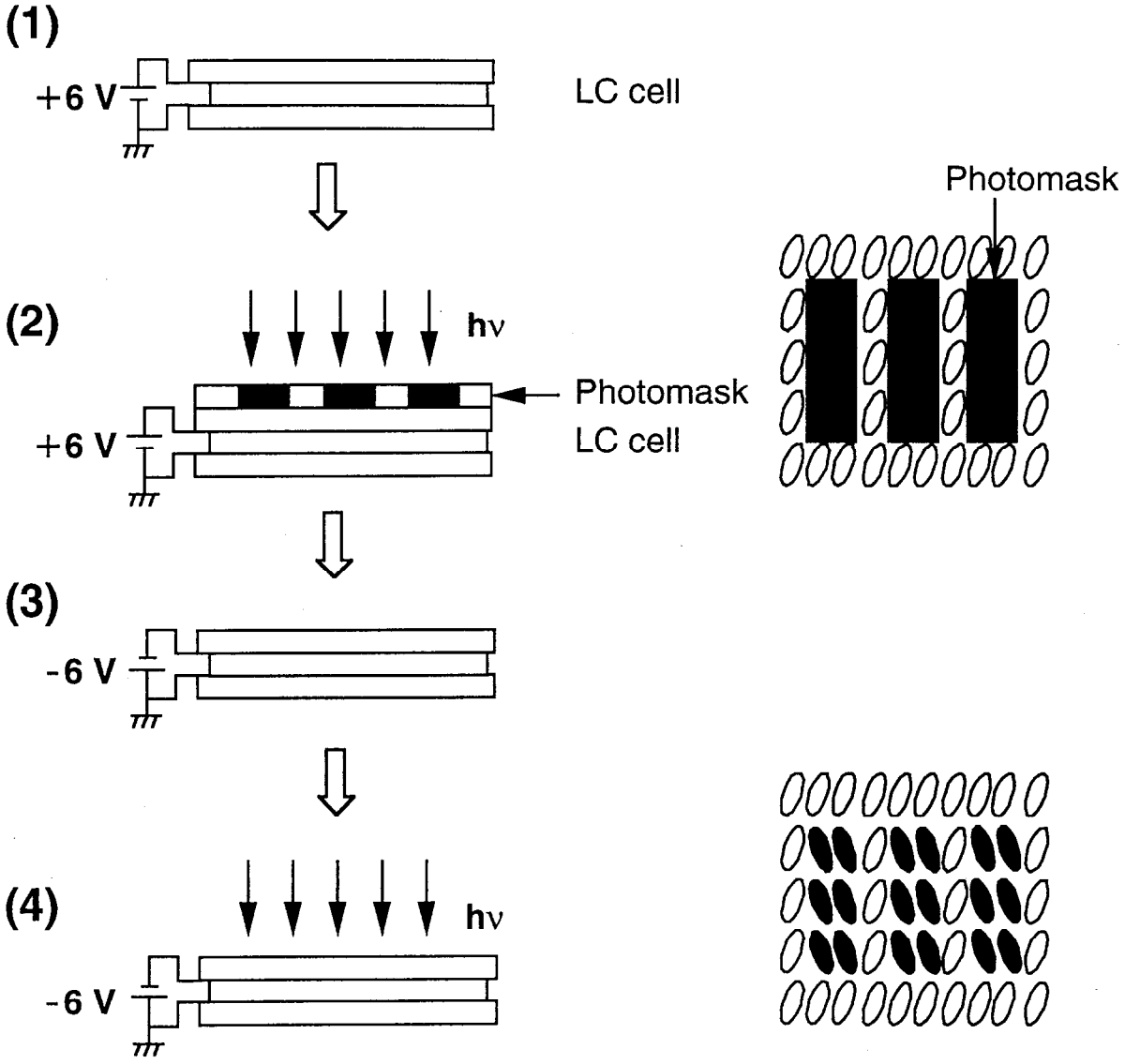

Figure 5-11. Diagram of image storage. (1), Dipoles of FLC molecules are aligned to produce polarization by external electric field. FLC molecules are also aligned into one direction. (2), With a photomask, the LC cell is irradiated, which leads to immobilization of mesogens by polymerization at the irradiated part. (3), Direction of FLC molecules is changed by application of an electric field with reverse polarity. (4), The LC cell is again irradiated without photomask to immobilize the other part of the cell.

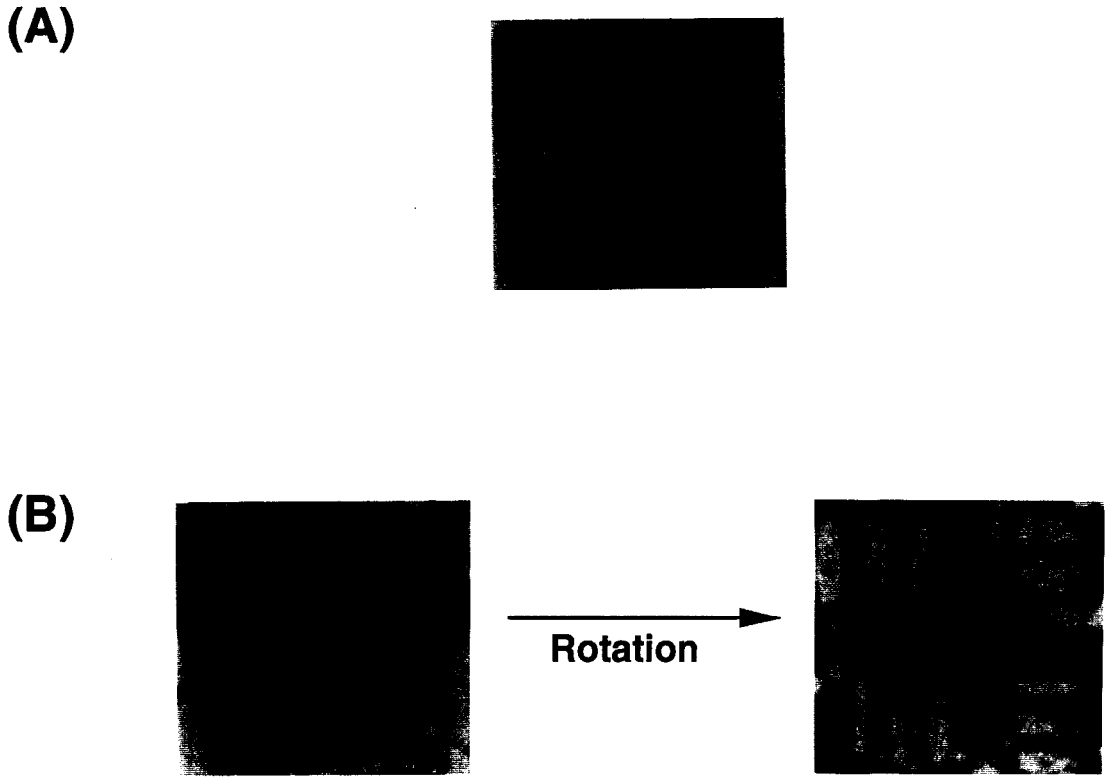

Figure 5-12. Image storage in polymerized **MS11**. Photoirradiation (1 mW/cm^2) was carried out at 60 °C. (A), test pattern used as photomask; (B), stored image after 18 months.

phase has been stable for 18 months at room temperature. These results suggest that the procedure is applicable to optical recording.

5-4. Conclusion

In-situ photopolymerization behavior was evaluated using two FLC monomers with a polymerizable group attached to the rigid core through a long alkyl spacer and a short alkyl spacer. Polymerizability of **MS11** was considerably different from that of **MS2**. The change of macroscopic structure by applying electric field was more effective in the polymerization of **MS2**. In addition, methacrylate exhibited different polymerization behavior from the corresponding acrylate. It might be related to the potential energy between propagating radical and monomer. Furthermore, the author conducted image storage by in-situ photopolymerization of FLC monomer. The image storage used bistable switching by applying electric field and immobilization of the ferroelectric phase by in-situ photopolymerization.

References

1 Finkelmann, H.; Ringsdorf, H.; Wendorff, J. H. *Makromol. Chem.* **1978**, *179*, 273.

2 Nishiyama, I.; Goodby, J. W. *J. Mater. Chem.* **1993**, *3*, 169.

3 Bartolino, R.; Doucet, J.; Durand, G. *Ann. Phys. (Paris)* **1978**, *3*, 389.

4 Hoyle, C. E.; Watanabe, T. *Macromolecules* **1994**, *27*, 3790.

5 Hoyle, C. E.; Kang, D. *Macromolecules* **1993**, *26*, 844.

6 Brandrup, J.; Immergut, E. H.; McDowell, W. *Polymer Handbook*; Wiley: New York, 1975; pp II45-II104.

7 Billmeyer, F. W. *Textbook of Polymer Science*; Wiley: New York, 1984; pp 49-81.

8 He, L.; Zhang, S.; Jin, S.; Qi, Z. *Polym. Bull.* **1995**, *34*, 7.

9 Hoyle, C. E.; Watanabe, T.; Whitehead, J. B. *Macromolecules* **1994**, *27*, 6581.

10 Hikmet, R. A. M.; Lub, J. *J. Appl. Phys.* **1995**, *77*, 6234.

Chapter 6

Effect of Frequency-Controlled Phase Structures on Photopolymerization Behavior of Ferroelectric Liquid-Crystalline Monomers

6-1. Introduction

In the SmC* phase, the LC molecules are aligned parallel to each other to form a layer with a tilt between the direction of the long axis of the LC molecule and the normal to the smectic layer.[1-3] The average direction of the molecular long axis is defined in each layer, and owing to the chiral group in the FLC molecules the structure is helicoidal with a precession of the director around the layer normal. When the FLC molecules are placed in a cell with a small gap, which is smaller than the helical pitch, the molecular long axis in every layer shows bistability in the same direction with the smectic layers oriented roughly perpendicular to the cell surface (Figure 6-1(A)). If an external electric field is applied across the cell, the polarization can be aligned upwards or downwards, depending on the polarity of the applied electric field. The polarization of all layers is also aligned in one direction (Figure 6-1(B)).[1] When the polarity of the electric field is reversed, the polarization flips. These two stable states are called surface-stabilized states and FLCs exhibit bistability.[2] On the other hand, ac electric fields have advantages over dc electric fields in aligning materials because less ion migration can take place.[4] In the FLC cell, the apparent optic axis is continuously tilted by applying an ac electric field, and then the field-induced tilt of the apparent optic axis offers the grey scales.[5] For low frequency, the direction of polarization can follow the alternating field (Figure 6-1(C)). In addition, the dielectric constant is fairly large

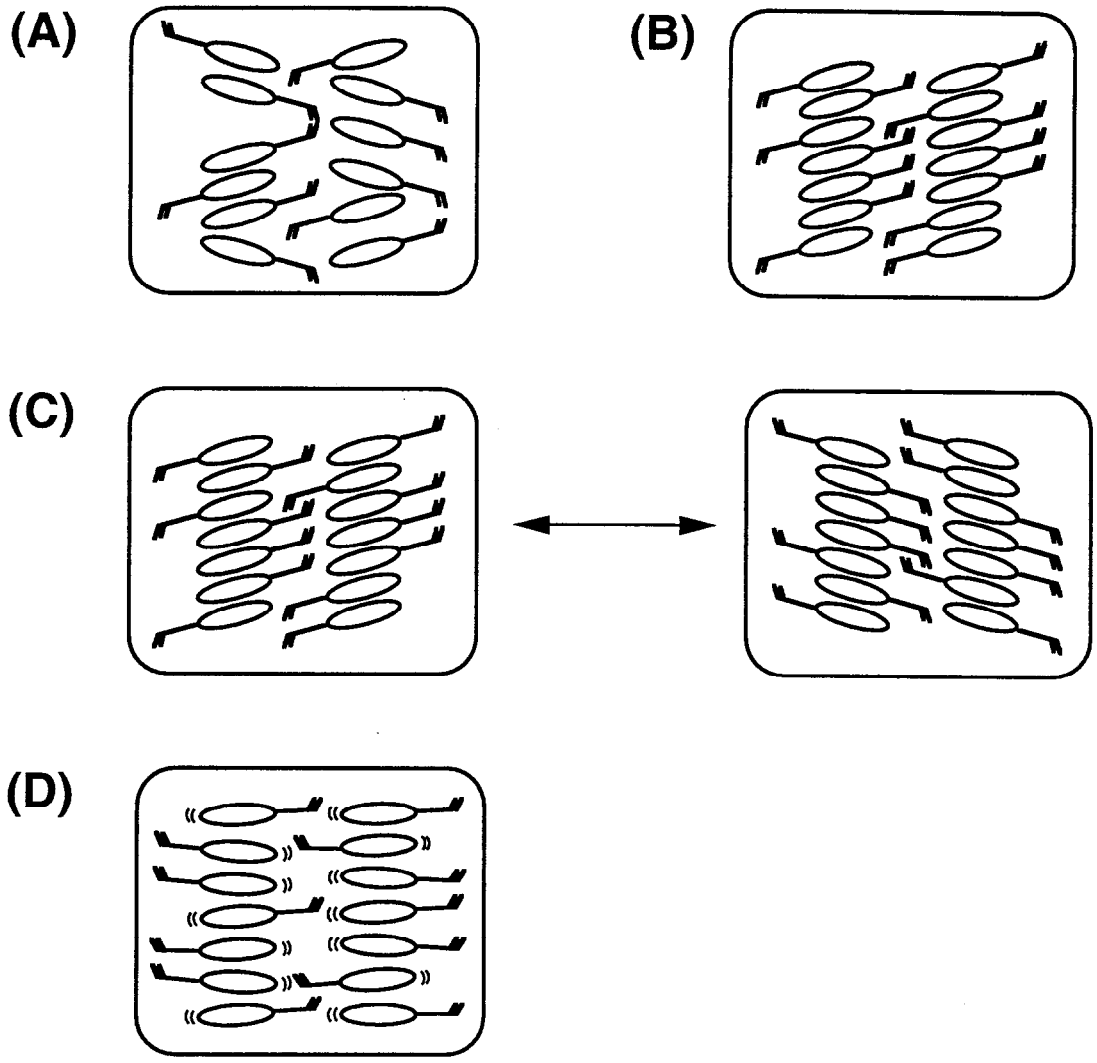

Figure 6-1. Plausible phase structures in the SmC* phase. (A), without electric field; (B), with dc electric field; (C), with ac electric field (low frequency); (D), with ac electric field (very high frequency).

under the low-frequency field. On the other hand, for high frequency the dipole moment can not follow the ac field (Figure 6-1(D)).[6] The dielectric constant under the high-frequency fields is similar to that of SmA* phase.[6,7]

In Chapter 5, in-situ photopolymerization behavior of FLC monomers possessing a long methylene spacer and a short methylene spacer was investigated. It has been clarified that the change of macroscopic structure by applying dc electric field is more effective in the polymerization of FLC monomer having a short spacer. In this chapter, chiral LC monomer was used with a polymerizable group attached to a rigid core through a short methylene spacer (carbon number of 2). To explore the effect of the condition of applied electric field on polymerization behavior of LC monomers, the author conducted photopolymerization of an FLC methacrylate monomer under various electric-field conditions.

6-2. Experimental Section

6-2-1. Materials

The FLC monomer used in this chapter was [R]-1-methylheptyl 4'-[4-(ω-methacryloyloxyethoxy)benzoyloxy]biphenyl-4-carboxylate (**MS2**). The synthetic route of the FLC monomer was described in Chapter 5.

6-2-2. In-Situ Photopolymerization Procedure

Photopolymerization was performed at 40 °C in a glass cell with a gap of 2 μm without an electric field, under a 3 V/μm dc electric field or ac electric field. The glass cell was composed of two ITO glass substrates with polyimide alignment layers rubbed in an antiparallel direction. Samples for photopolymerization were prepared by injecting the FLC monomer containing 1-hydroxycyclohexyl phenyl ketone as a photoinitiator (2 mol%) into the glass cell in the I phase at 85 °C using capillary action as mentioned in Chapter 5. In the photopolymerization under a dc electric field, the samples were cooled down slowly under an ac electric field (1 Hz, ±3 V_{pp}/μm) to

temperature at which they showed SmC* phase. In the photopolymerization under an ac electric field, the samples were cooled down slowly under an ac electric field (frequency in the polymerization, ±3 $V_{pp}/\mu m$) to temperature for photopolymerization. Then, the cell was irradiated at 366 nm with the ac electric field of 3 V/μm during polymerization.

6-2-3. Evaluation of Polymerized FLC

The Mn, Mw/Mn and conversion were determined by GPC as described in Chapter 4. The phase transition temperature and the phase structure were identified by DSC (10 °C/min) and optical polarizing microscopy. The degree of alignment of the polymerized FLC after photoirradiation with and without electric field in the 2-μm-gap cell was explored by means of optical polarizing microscopy. The molecular alignment was evaluated from the angular dependence of the transmittance of linearly polarized light through the sample cell.

6-3. Results and Discussion

6-3-1. Polymerizability by In-Situ Photopolymerization

Figure 6-2 shows time-conversion curves for photopolymerization at intensity of 0.1 mW/cm^2 in the SmC* phase (40 °C) in a glass cell with a gap of 2 μm. The conversion showed a tendency to increase with increasing irradiation time, irrespective of the electric-field conditions. As described in Chapter 5, the change in the phase structure could be negligible during the early stage of polymerization (< 20 % conversion). Therefore, in this chapter, the effect of phase structure on polymerization behavior was evaluated in the early stage of polymerization.

Polymerization behavior depended considerably on nature of the applied electric field. Polymerizability without electric field was different from that with dc electric field (Figure 6-2, O and ■). The explain of the result was described in Chapter 5. The conversion was extremely low in the polymerization without electric field and with

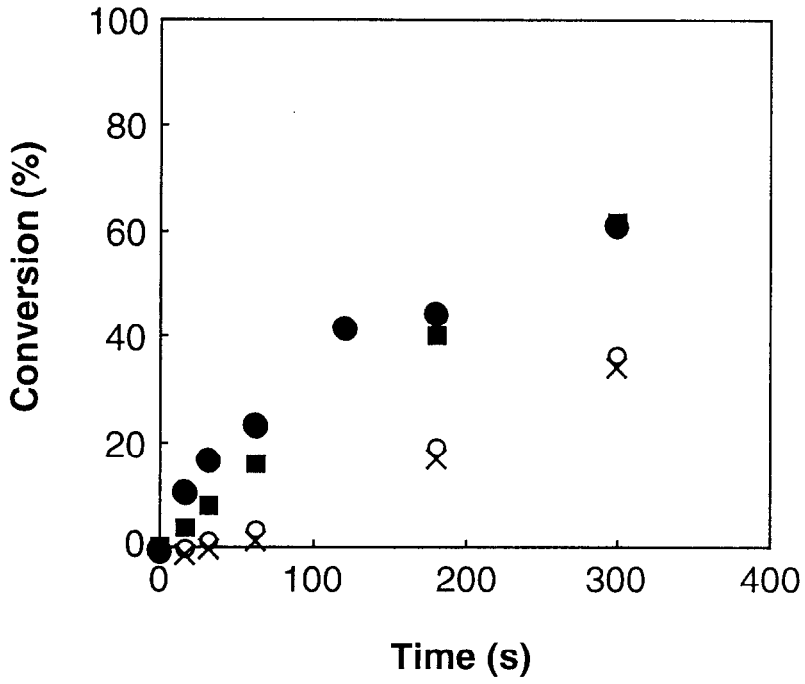

Figure 6-2. Time-conversion curves for photopolymerization of **MS2** (0.1 mW/cm^2) in the SmC* phase (40 °C) in a glass cell with a gap of 2 μm. ○, without electric field; ■, with dc electric field; ×, with ac (1 kHz) electric field; ●, with ac (100 kHz) electric field.

low-frequency electric field, whereas it was high in the polymerization with very-high-frequency electric field. The conversion could be rationalized by a compensation of the rate increase in propagation by the rate increase in termination with temperature.[8] Orientation and mobility mainly contribute to the rate increases in propagation and in termination, respectively. This explanation may also be applied to the present system. It is predicted that the system with very-high-frequency electric field has the orientation of LC phase structure and restricted mobility. Then, it is expected that k_p increases and k_t decreases, while leads to increase in polymerization rate. In addition, the conversion with dc electric field was higher than that without electric field and lower than that with very-high-frequency electric field. Phase structure under dc electric field has higher orientation and lower mobility than that with ac electric field. It is again expected that k_p increases and k_t decreases. However, because of the low mobility, k_p may be decreased. On the other hand, photopolymerization without electric field exhibited almost the same behavior as that with ac (50 Hz $\leq$ frequency $\leq$ 1 kHz) electric field (Figure 6-2, O and X). The direction of polarization can follow the alternating field with low frequency. Light scattering during reorientation[9] is the most plausible cause for the extremely low conversion under low-frequency electric field, since initiation efficiency is reduced if a point of the incident light is scattered. Consequently, the polymerizability of the FLC monomer in an early stage of polymerization is governed not only by molecular alignment but by mobility.

In addition, the author investigated difference of polymerization behavior between SmA* and SmC* phase under high-frequency electric field. As mentioned in the previous section, there is no difference in the dielectric constants between the former and the latter under the high-frequency electric field. Therefore, it is expected that the alignment in the SmC* phase resembles that in the SmA* phase, and the packing of polymerizable groups is better in the SmC* phase than in the SmA* phase. Figure 6-3 shows time-conversion curves for photopolymerization at 0.1 mW/cm^2 in these two phases. At low conversion (< 20 %), higher polymerizability was observed

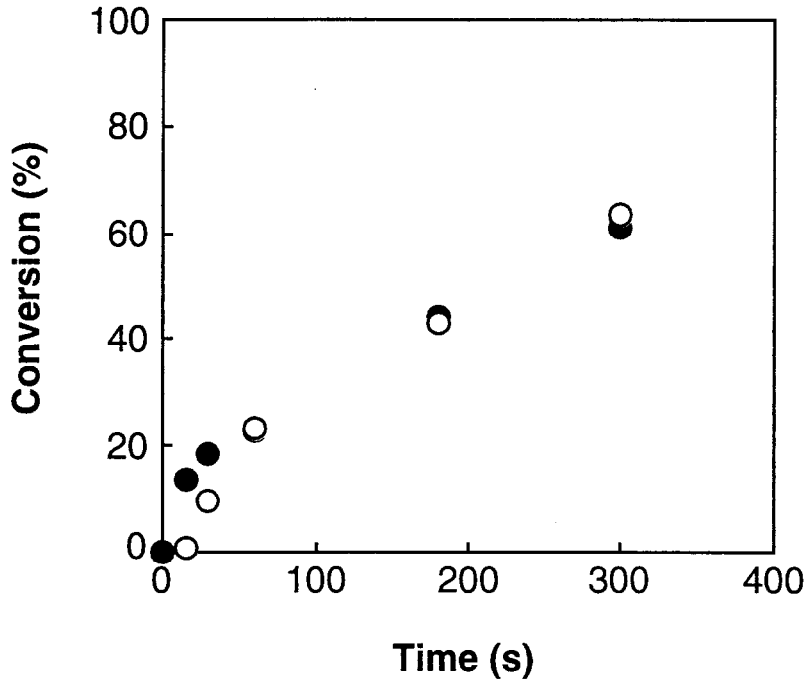

Figure 6-3. Time-conversion curves for photopolymerization of **MS2** (0.1 mW/cm^2) in a glass cell with a gap of 2 μm. ○, in the SmA* phase (60 °C) without electric field; ●, in the SmC* phase (40 °C) with ac (100 kHz) electric field.

in the polymerization in the SmC* phase under high-frequency electric field than that in the SmA* phase. Thus, polymerization behavior might be also affected by the packing of functional groups.

6-3-2. Molecular Weight of Polymer Obtained by In-Situ Photopolymerization

As described in Chapter 5, in the region with a low pol[illegible]than 20 %), the phase transition temperature changed only slightly. This result demonstrates that the phase structure hardly changes during the early stage of polymerization. On the other hand, the phase structure of the polymerization mixture change[illegible]gion with a higher polymer content. The author therefore evalu[illegible]charts of polymers from the early stage to the late stage of polymerization.

Figures 6-4, 6-5 and 6-6 show the GPC charts corresponding to polymers obtained in the polymerization without electric field, under dc electric field and under ac electric field at 40 °C in the SmC* phase, respectively. Even at low conversion (< 20 % conversion), bimodal peaks were observed for the polymers obtained by polymerization without the electric field or with dc electric field (Figures 6-4 and 6-5). In general, propagating radicals with 1,1-di-substituents undergo combination and disproportionation in termination process, while those with a single substituent undergo approximately 100 % combination.[10] Then, it may be expected that both combination and disproportionation occur in the polymerization of methacrylates. In fact, the Mn of polymer in higher-molecular-weight part ($M_{peak} \approx 750{,}000$) was approximately twice as much as that in lower-molecular-weight part ($M_{peak} \approx 370{,}000$). However, for **MS11** the peak was monomodal as mentioned in Chapter 5. It can therefore be presumed that polymerization of **MS2** without an electric field or with dc electric field does not accompany combination termination (higher molecular weight) and disproportionation termination (lower molecular weight) but during polymerization phase structure changes microscopically even though no macroscopic change in phase structure was observed. In contrast, the peak of the polymer produced with ac electric

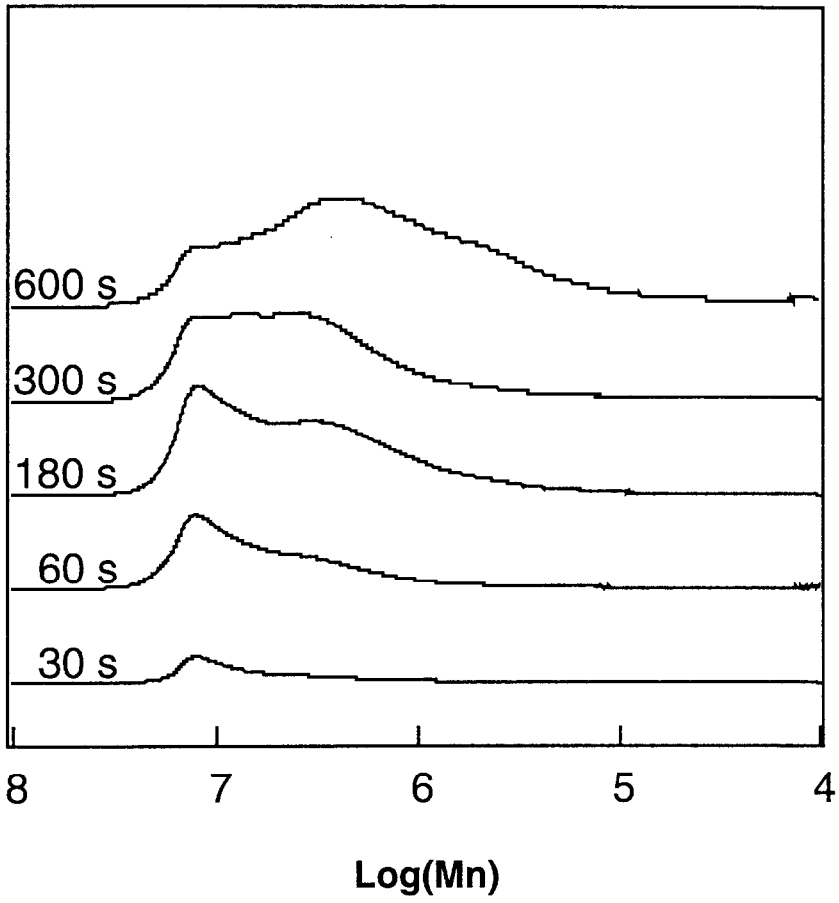

Figure 6-4. GPC charts of samples in the polymerization of **MS2** in the SmC* phase (40 °C) without electric field. Polymerization time: 30 s (1.6 % conversion), 60 s (3.5 % conversion), 180 s (19 % conversion), 300 s (36 % conversion), 600 s (55 % conversion).

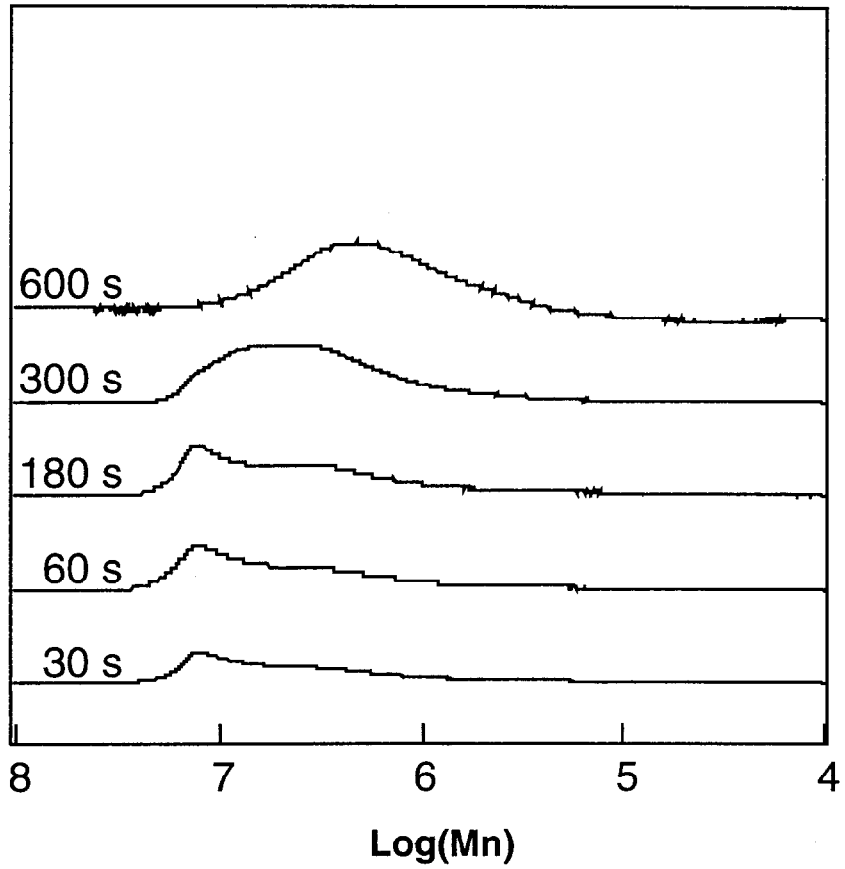

Figure 6-5. GPC charts of samples in the polymerization of **MS2** in the SmC* phase (40 °C) with dc electric field. Polymerization time: 30 s (7.8 % conversion), 60 s (18 % conversion), 180 s (40 % conversion), 300 s (61 % conversion), 600 s (74 % conversion).

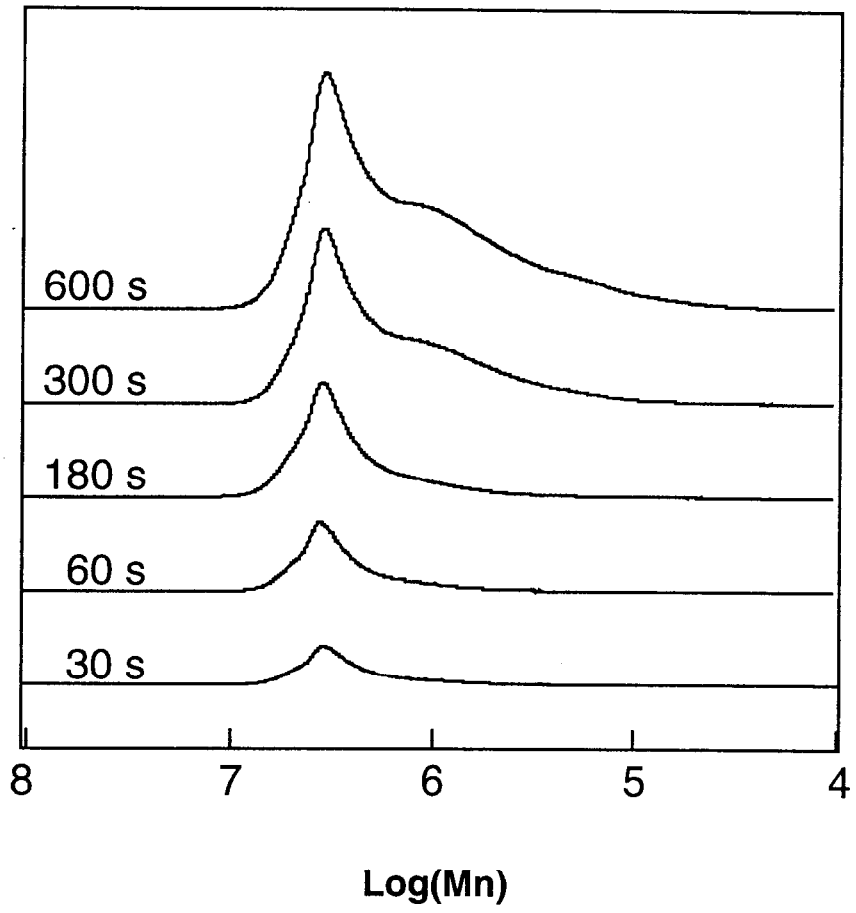

Figure 6-6. GPC charts of samples in the polymerization of **MS2** in the SmC* phase (40 °C) with ac (100 kHz) electric field. Polymerization time: 30 s (18 % conversion), 60 s (23 % conversion), 180 s (44 % conversion), 300 s (61 % conversion), 600 s (74 % conversion).

field was monomodal in the early stage of polymerization and was located between the two peaks of polymer obtained with dc electric field. It seems reasonable that chain transfer reaction and combination termination occur in the polymerization with ac electric field because of restricted but high mobility. In the late stage of polymerization, the peak corresponding to polymer with much lower molecular weight increased irrespective of field-condition. In addition, the ratio of peak area of the two peaks was smaller in the polymerization at higher temperature. These results suggest that the phase structure of polymerization mixture changed from SmC* to G phase in high polymer content (> 50 % conversion), and the numbers of polymer chains became small because of extremely small rate constant of propagation.

6-3-3. Alignment of Photopolymerized FLCs

The molecular alignment of the FLCs was explored by optical polarizing microscopy after photopolymerization was conducted in the 2-μm-gap cell for 60 s at 40 °C in the SmC* phase. The polymerized FLCs showed no response to the alternating electric field, although the polarization flip occurred by applying the alternating (1 Hz, ±3 V_{pp}/μm) electric field before photoirradiation. It may be due to the decrease of the mobility of mesogens by the linkage of polymer chains as discussed in Chapter 4. Figure 6-7 shows the optical textures of the samples after photopolymerization in the presence of a 3 V/μm dc voltage and ac voltage. The angular dependence of the transmittance of linearly polarized light through the FLC cell was significantly different between samples obtained with dc and ac electric field. As shown in Figure 6-7, the position of the sample cell between the crossed polarizers was adjusted at first so as to transmit thoroughly the linearly polarized light. When the sample cells were rotated with respect to the polarizers, only the FLC polymerized with dc electric field became dark. The contrast between the dark and the bright views was found to be highest at every 45 ° interval (Figure 6-8). The result is consistent with that obtained for acrylate mentioned in Chapter 4. These results indicate that application of

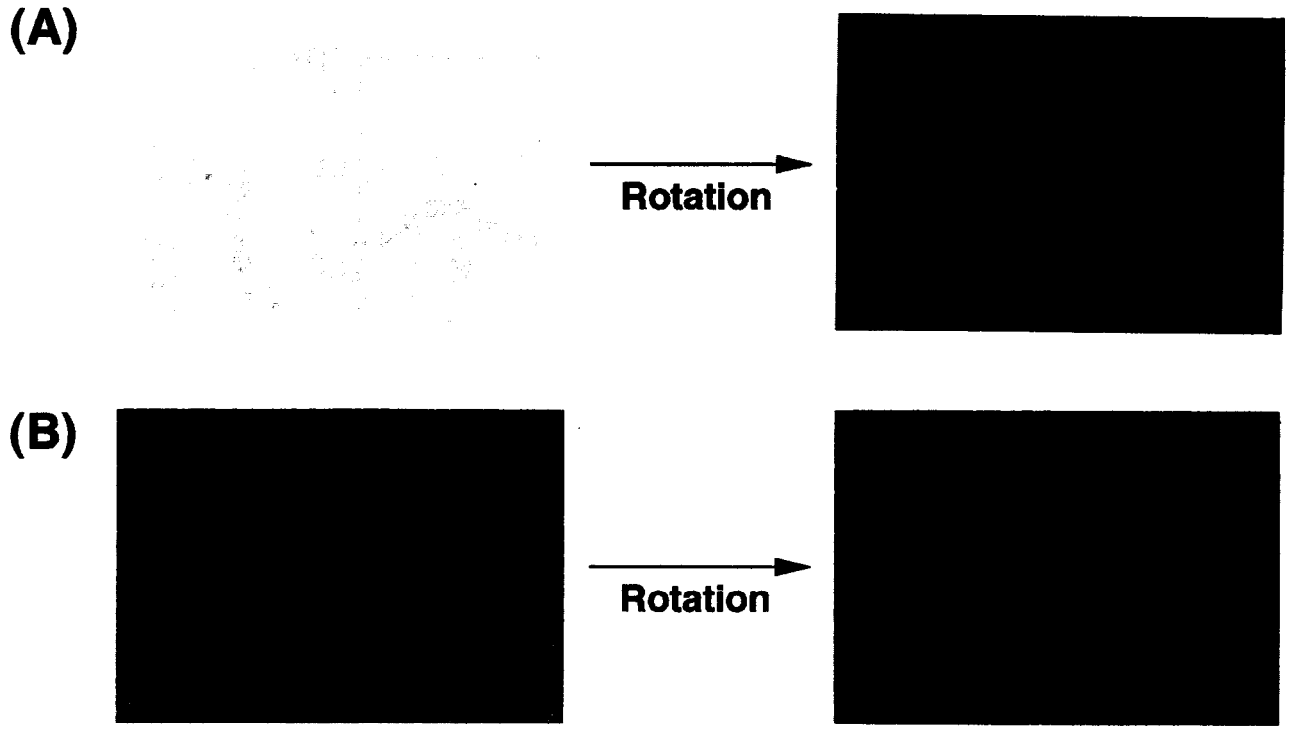

Figure 6-7. Angular dependence of the transmittance of linearly polarized light through 2-μm-gap LC cell. (A), texture obtained on application of dc electric field; (B), texture obtained on application of ac electric field.

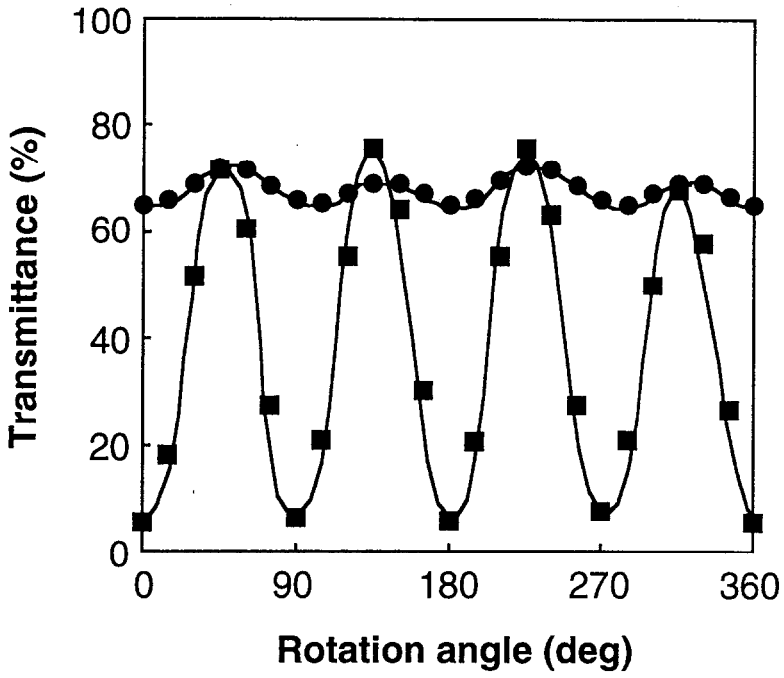

Figure 6-8. Transmittance of linearly polarized light through samples after photopolymerization as a function of rotation angle. ■, with dc electric field; ●, with ac (100 kHz) electric field.

the dc electric field to the sample results in appearance of the immobilized SmC* phase, in which all mesogens of the polymerized FLC are aligned into one direction to form a monodomain of the LC phase. In contrast, the FLC polymerized with ac electric field showed lower contrast between bright and dark views, irrespective of the field-frequency. This suggests that polymer obtained under the ac electric field forms polydomain of the LC phase. Mesogen and polymerizable group are coupled for monomers with a short methylene spacer. Therefore, polymerization might proceed regardless of the direction of the polymerizable group.

The transmittance of samples polymerized is shown in Figure 6-9. The transparency of the polymer film was different by the condition of applied electric field. The polymer film produced with dc electric field was transparent in visible region. However, the translucent film was obtained by photopolymerization without electric field and with ac electric field. These results may be due to the difference of light scattering between monodomain and polydomain. Upon application of an electric field during polymerization, films suitable for optical recording were obtained.

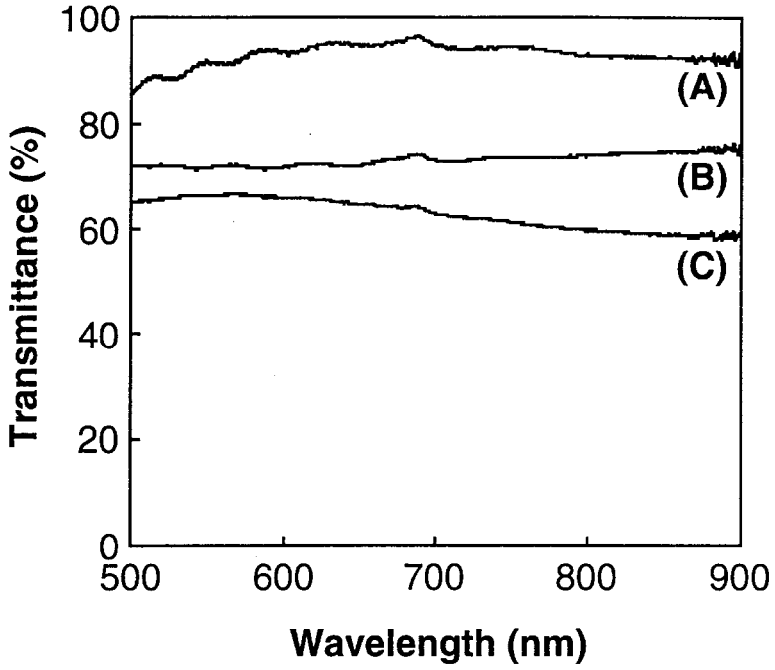

Figure 6-9. Transmittance of samples polymerized through 2-μm-gap LC cell. (A), with dc electric field; (B), with ac (1 Hz) electric field; (C), with ac (1 kHz) electric field.

6-4. Conclusion

The author evaluated the effect of the condition of applied electric field on photopolymerization behavior. Polymerization in the early stage of polymerization was accelerated by applying dc electric field compared to that without an electric field. In addition, polymerizability was fairly dependent on the field-frequency of ac electric field. It was observed that polymerization was suppressed by application of field-frequency less than 1 kHz in the early stage of polymerization, whereas polymerization was accelerated by application of 100 kHz field-frequency. The molecular weight of polymers produced was strongly governed by microphase structure. Furthermore, the alignment of the samples after photopolymerization was investigated by optical polarizing microscopy. It was found that high orientation of polymer could be obtained by photoirradiation in the SmC* phase with dc electric field. On the other hand, FLCs polymerized with ac electric field formed an immobilized polydomain, irrespective of the frequency of the applied electric field.

References

1 Fukuda, A.; Takezoe, H. *Structures and Properties of Ferroeletric Liquid Crystals* (Corona, Tokyo, 1990)

2 Clark, N. A.; Lagerwall, S. T. *Appl. Phys. Lett.* **1980**, *36*, 899.

3 (a), Decobert, G.; Dubois, J. C.; Esselin, S.; Noël, C. *Liq. Cryst.* **1986**, *1*, 307. (b) Ouchi, Y.; Takezoe, H.; Fukuda, A.; Kondo, K.; Kitamura, T.; Yokokura, H.; Mukoh, A. *Jpn. J. Appl. Phys.* **1988**, *27*, L733. (c) Skarp, K.; Handschy, M. A. *Mol. Cryst. Liq. Cryst.* **1988**, *165*, 439. (d) Ikeda, T.; Sasaki, T.; Ichimura, K. *Nature* **1993**, *361*, 428. (e) Sasaki, T.; Ikeda, T.; Ichimura, K. *J. Am. Chem. Soc.* **1994**, *116*, 625. (f) Trollsås, M.; Sahlén, F.; Gedde, U. W.; Hult, A.; Hermann, D.; Rudquist P.; Komitov, L.; Lagerwall, S. T.; Stebler, B.; Lindström, J.; Rydlund, O. *Macromolecules* **1996**, *29*, 2590.

4 Shiota, A.; Ober, C. K. *Macromolecules* **1997**, *30*, 4278.

5 Mori, T.; Toyoda, Y.; Mikami, N.; Masumi, T.; Nunoshita, M. *Appl. Phys. Lett.* **1994**, *64*, 1065.

6 (a) Minami, N.; Higuchi, R.; Sakurai, T.; Ozaki, N.; Yoshino, K. *Jap. J. Appl. Phys.* **1986**, *25*, L833. (b) Suenaga, H.; Maeda, S.; Iijima, T.; Kobayashi, S. *Mol. Cryst. Liq. Cryst.* **1987**, *144*, 191. (c) Eber, N.; Bata, L.; Scherowsky, G.; Schliwa, A. *Ferroelectrics* **1991**, *122*, 139.

7 Bahr, Ch.; Heppke, G. *Liq. Cryst.* **1987**, *2*, 825.

8 Doornkamp, A. T.; Alberda van Erkenstein, G. O. R.; Tan, Y. Y. *Polymer* **1992**, *33*, 2863.

9 Mitsuishi, M.; Ito, S.; Yamamoto, M.; Fischer, T.; Knoll, W. *Mol. Cryst. Liq. Cryst.* **1997**, *308*, 1.

10 Bamford, C. H.; Dyson, R. W.; Eastmond, G. C. *Polymer* **1969**, *10*, 885.

Chapter 7

Properties of Polymers Produced by Polymerization of Ferroelectric Liquid-Crystalline Monomers

7-1. Introduction

Highly functionalized and high-performance PLCs have attracted much more attention as materials for recording and electrooptic devices. In preparation of functionalized synthetic polymers, it is important to control molecular weight, molecular weight distribution, polymer sequence, stereoregularity and high-ordered structures.[1] By controlling these factors, liquid crystallinity, solubility, flexibility, glass transition temperature, and many other properties are also controlled.[2,3] In particular, many studies have been performed on the control of stereoregularity of synthetic polymers by radical,[4] cationic,[5] anionic,[6] and coordination[7] polymerization techniques. Stereoregularity arises mainly from non-bonded interactions (steric hindrance) between a growing chain and an entering monomer (chain-end control)[4-6,7d,7h] and between a catalyst and an entering monomer (enantiomorphic-site control).[7a-7c,7e-7g,7i] In both cases, chiral species in the vicinity of the growing chain-end including the catalyst act as an active site to control the stereoregularity of the polymers produced.[8] Alternatively, it may be possible that the stereoregularity can be controlled by molecular alignment in liquid-crystalline systems. LCs spontaneously form organized molecular systems and their alignment can be controlled readily by the application of an external field.[9] So it is expected that polymerization in a highly aligned state such as an LC phase can produce polymers with special properties. Such control by

molecular alignment in whole polymerization processes could be promising as a novel approach to control of the stereoregularity.

It has been reported that structural characteristic, especially stereoregularity, is given by the orientation of the matrix. Polymerization has been conducted in the various conditions in polymer matrix, LC, inclusion crystal, under external forces such as magnetic and electric field.[10] Radical polymerization of various alkyl methacrylates in LC solvent has been studied.[11] It was found that the polymerization of the methacrylates of butyl and longer alkyl chain deviated from Bernoullian statistics and gave polymers more isotacticity than those of methyl and ethyl methacrylates. Solid-state polymerization of a binary mixture of non-LC monomer and LC compound has been carried out using electron beam.[12] However, the tacticity of polymer produced in solid-state polymerization was almost the same as that of polymer obtained in solution. The stereoregular polymer has been obtained by means of polymerization of LC monomer in K and Sm phases under a magnetic field.[13]

From the results in Chapters 4, 5, and 6, it is expected that polymerization in ferroelectric phase can produce polymers with specific properties. To explore the effect of molecular packing in an LC phase on property of polymer produced, the author conducted polymerization (solution polymerization and photopolymerization) of FLC methacrylate monomers with a polymerizable group attached to a rigid core through a short methylene spacer (carbon number of 2) and a long methylene spacer (carbon number of 11).

7-2. Experimental

7-2-1. Materials

The two FLC monomers, [R]-1-methylheptyl 4'-[4-(ω-methacryloyloxy-undecyloxy)benzoyloxy]biphenyl-4-carboxylate (**MS11**), [R]-1-methylheptyl 4'-[4-(ω-methacryloyloxyethoxy)benzoyloxy]biphenyl-4-carboxylate (**MS2**), used in this chapter are the same as those used in Chapter 5. The thermal properties of the LCs

were determined by DSC, optical polarizing microscopy, and X-ray diffractometry (MAC Science MXP, equipped with a thermal controller, model 5301).

7-2-2. Preparation of Polymers by Solution Polymerization

The FLC polymers were prepared by the method described in Chapter 4. Polymerization was conducted in DMF with AIBN as an initiator.

7-2-3. In-Situ Photopolymerization Procedure

Photopolymerization (**MS11**, 60 °C for 30 s; **MS2**, 40 °C for 60 s) was performed for in a glass cell with a gap of 2 μm under dc electric field of 3 V/μm as described in Chapter 4.

7-2-4. Evaluation of Polymerized FLCs

The Mn and Mw/Mn were determined by GPC as described in Chapter 4. The X-ray measurements for molecular alignment in various phases were performed using CuKα1 radiation from a 1.6 kW anode X-ray generator at the temperature at which the samples show each phase. The ^{13}C NMR spectra were measured in chloroform-*d* at 60 °C with a JEOL GX-500 NMR spectrometer operated at 125.65 MHz. Broad band decoupling was used to remove the ^{13}C-^{1}H coupling. The center peak of chloroform-*d* was used as an internal reference (77.0 ppm).

7-3. Results and Discussion

7-3-1. Phase Transition Temperature of Polymers

Table 7-1 shows the Mn, Mw/Mn and phase transition temperature of each polymer obtained by solution polymerization and photopolymerization, respectively. It was observed that there was marked difference in Tg of polymers produced by solution polymerization and photopolymerization. This may be due to large difference in Mn.

Table 7-1. Mn, Mw/Mn and phase transition temperature of polymers

Polymer	Mn[a]	Mw/Mn[a]	Phase transition temperature (°C)[b]
MS11[c]	6.4 x 10^4	3.5	G 37 SmC_A* 150 SmA* 161 I
MS11[d]	1.0 x 10^6	2.0	G 50 SmC_A* 157 SmA* 166 I
MS2[c]	6.3 x 10^4	4.1	G 138 SmA* 220 Decomposition
MS2[d]	1.1 x 10^6	3.5	G 180 SmA* 220 Decomposition

[a] Determined by GPC using polystyrenes standard.

[b] G, glass; SmC_A*, antiferroelectric chiral smectic C; SmA*, chiral smectic A; I, isotropic.

[c] Obtained by solution polymerization at 60 °C.

[d] Obtained by in-situ photopolymerization in the ferroelectric phase.

7-3-2. X-Ray Diffraction Patterns of Monomers and Polymers Obtained by Photopolymerization

The X-ray diffraction patterns observed for the FLC samples before and after photopolymerization in the ferroelectric phase are shown in Figures 7-1 and 7-2. The smectic layer spacings calculated from the diffraction angle were 36.8 and 31.8 Å for **MS11** and **MS2** in the SmC* phase, respectively. On the other hand, in the SmA* phase the smectic layer spacings were 38.7 (**MS11**) and 31.8 Å (**MS2**). The calculated molecular length in their most extended configuration was 41.3 and 31.3 Å for **MS11** and **MS2**, respectively (Figure 7-3). The layer thickness in the SmA* phase determined by the X-ray measurement corresponds roughly to a molecular length of **MS2** monomer. For **MS11** monomer, a slight difference by ca. 2.6 Å may come from the conformationally disordered structure of molecules at high temperature. This result is agreement with that of Tashiro et al.[14]

Similar values of the smectic layer spacing (36.2-37.1 Å) to that of **MS11** monomer in the SmC* phase (36.8 Å) were obtained for polymer produced by photoirradiation of **MS11**. However, a different result was obtained for polymer produced by photopolymerization of **MS2**. A similarity in the spectra between **MS2** and polymerized **MS2** suggests that the side chain of polymerized **MS2** may be

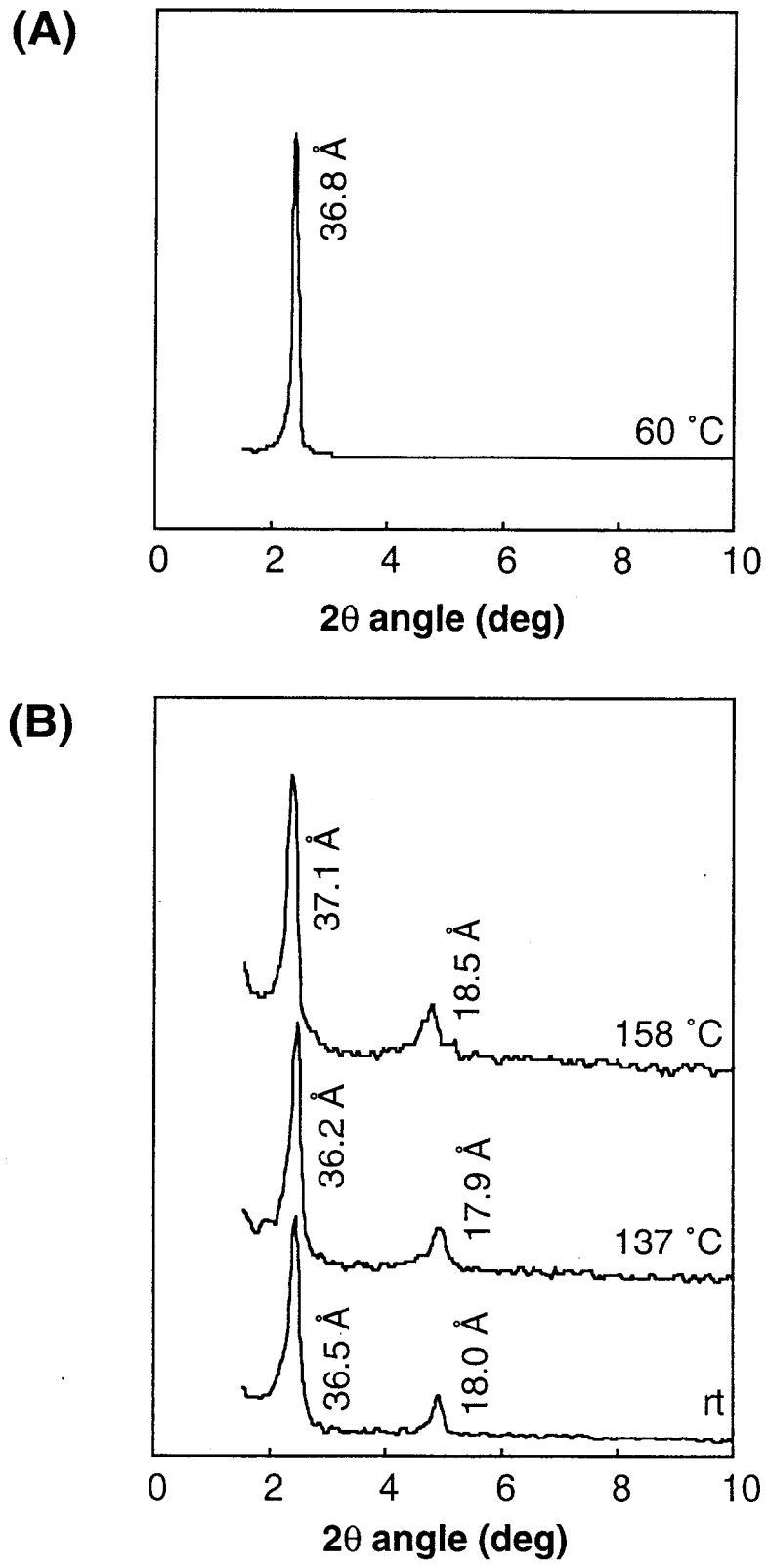

Figure 7-1. X-ray diffraction patterns measured at various temperatures. (A), **MS11** monomer; (B), polymer produced by photopolymerization of **MS11**. The sample was thoroughly washed with methanol to remove unreacted monomers and initiator.

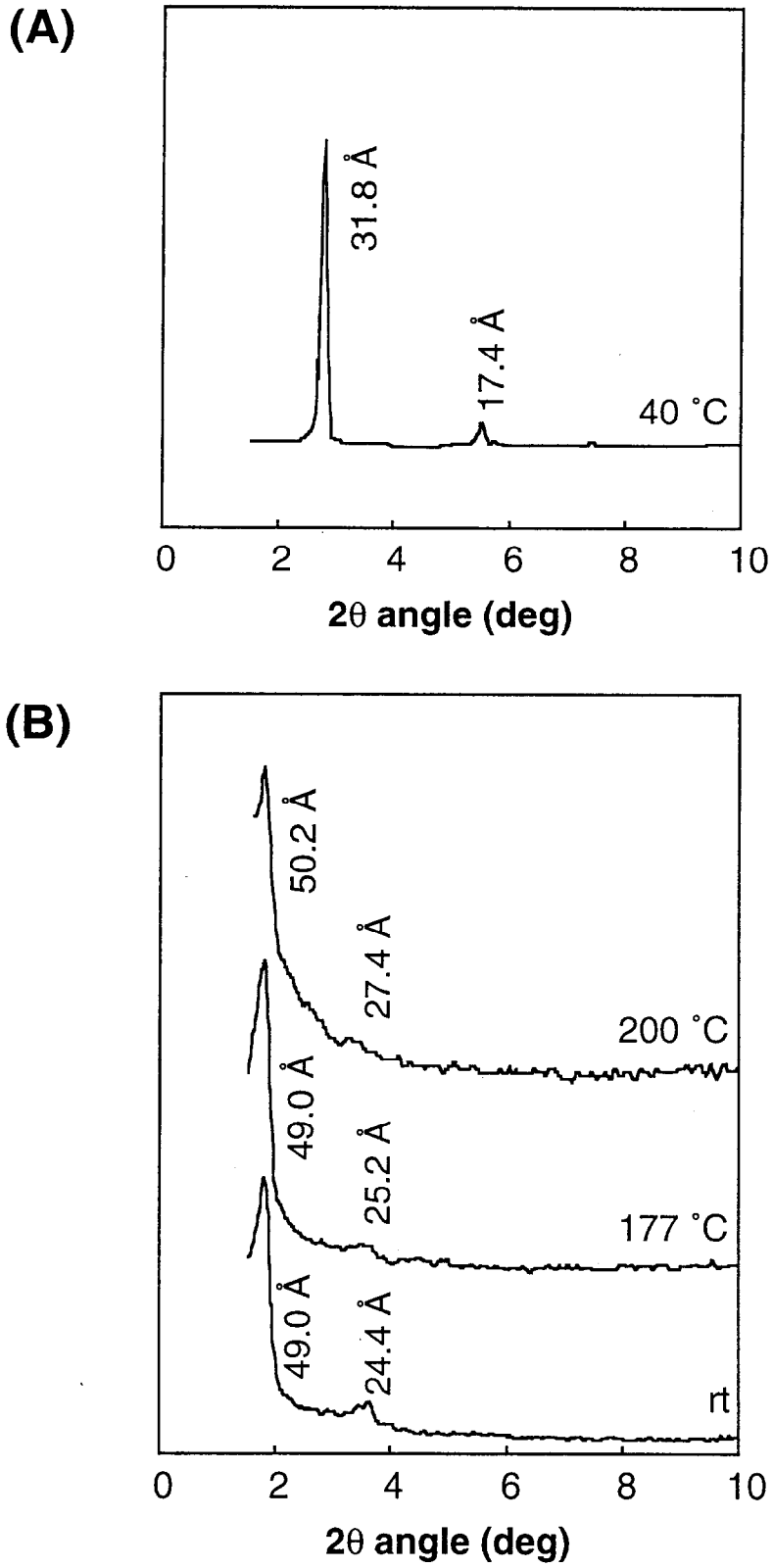

Figure 7-2. X-ray diffraction patterns measured at various temperatures. (A), **MS2** monomer; (B), polymer produced by photopolymerization of **MS2**. The sample was thoroughly washed with methanol to remove unreacted monomers and initiator.

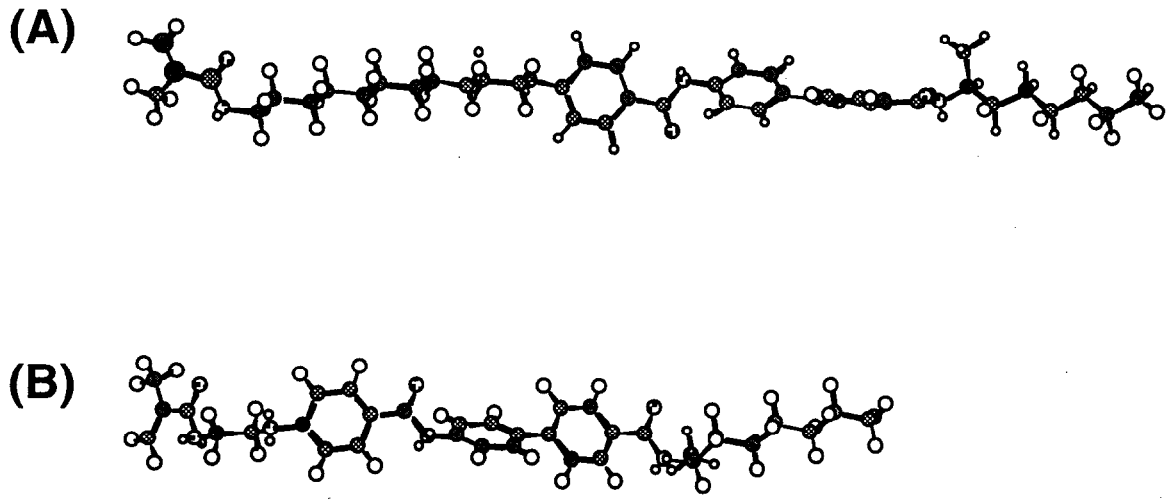

Figure 7-3. Calculated minimized energy conformation of FLC monomers. (A), **MS11** monomer; (B), **MS2** monomer.

assumed basically to have a length close to 31.8 Å. However, the polymerized **MS2** showed an interlayer spacing from 49.0 to 50.2 Å. If the layer normal is vertical in the layer sheets as expected from the conventional structure of the general Sm phase, the side-chain length should be (49.0 or 50.2)/2 = 24.5 or 25.1 Å. The value is too short and contradicts the above-mentioned length of 31.8 Å. Rather the author assumes that the layers are constructed by an interdigitation of two side-chain groups by ca. 6.7 Å. Consequently, the orientation of polymerized **MS11** retained that of **MS11** monomer, whereas the orientation of **MS2** monomer was changed by polymerization.

7-3-3. Tacticity of Polymers Produced

Assignment of ^{13}C NMR absorptions of poly(methyl methacrylate) has been carried out by several investigators. Inoue et al. assigned α-methyl and quaternary carbon absorptions by triads, methylene carbon absorptions by tetrads, and carbonyl carbon absorptions by pentads.[15] Peat and Reynolds also reported the same assignments for α-methyl, quaternary and carbonyl carbon absorptions.[16] Figures 7-4 and 7-5 show ^{13}C NMR spectra of the quaternary carbon signals (around δ 45 ppm) and the carbonyl carbon signals (around δ 177 ppm) of polymers produced by solution polymerization and photopolymerization of **MS2**, respectively. The tacticity of polymers produced is summarized in Table 7-2. The syndiotacticity of poly(**MS2**) was higher than that of poly(**MS11**). Radical polymerization proceeds as repulsive forces between substituent groups is reduced. If substituent groups are bulky, syndiotacticity increases. For **MS2** monomer with a short spacer between a polymerizable group and a core, the position of addition may be directly affected by repulsive forces between cores. In contrast, since **MS11** monomer has a long spacer, the position of addition may not be so much affected by repulsive forces between the cores. On the other hand, there is little difference in tacticity of polymers by solution polymerization and photopolymerization.

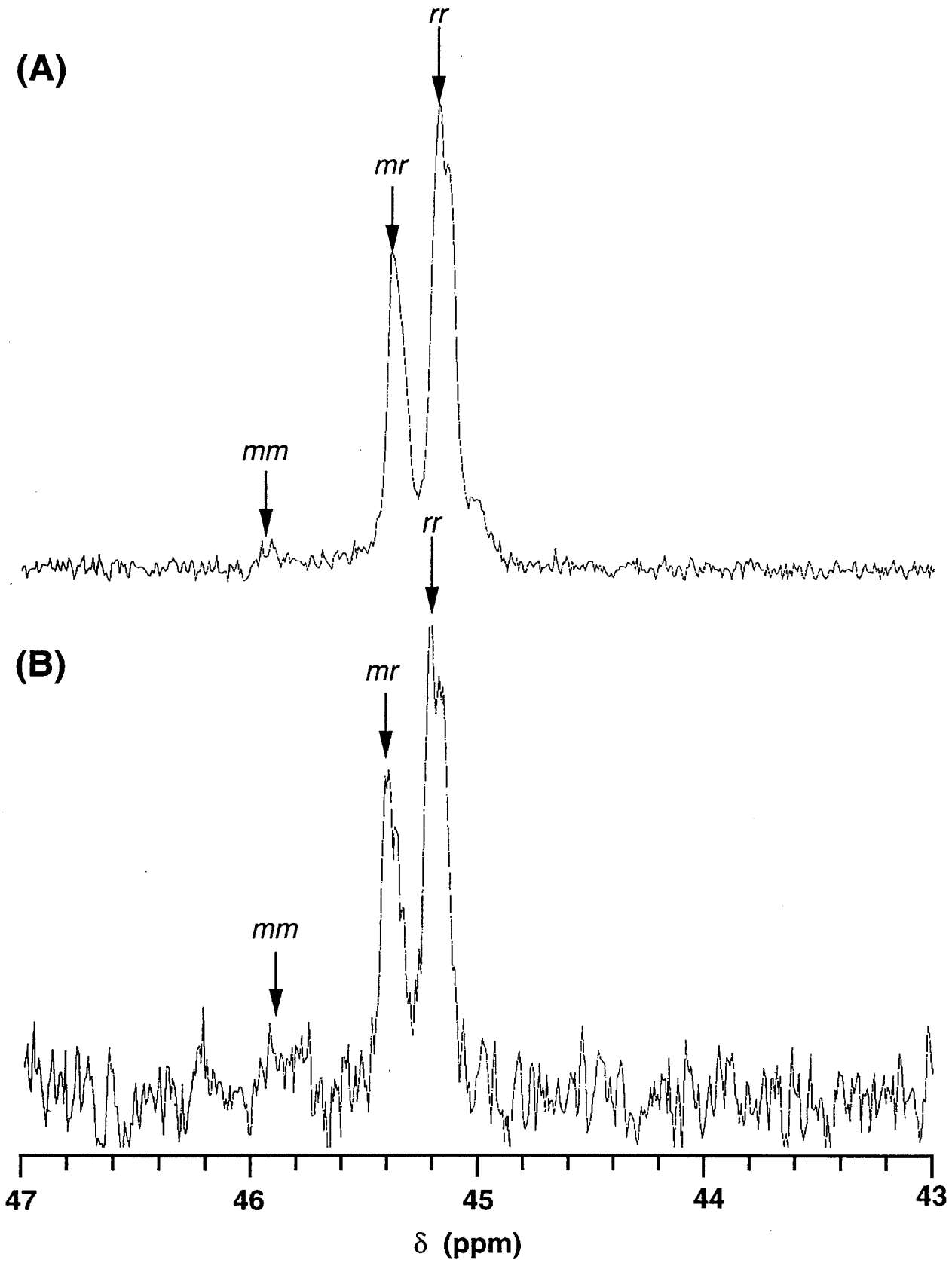

Figure 7-4. ^{13}C NMR spectra of quaternary carbon of polymerized **MS2** in $CDCl_3$ at 60 °C. The sample was thoroughly washed with methanol to remove unreacted monomers and initiator. (A), solution polymerization; (B), photopolymerization.

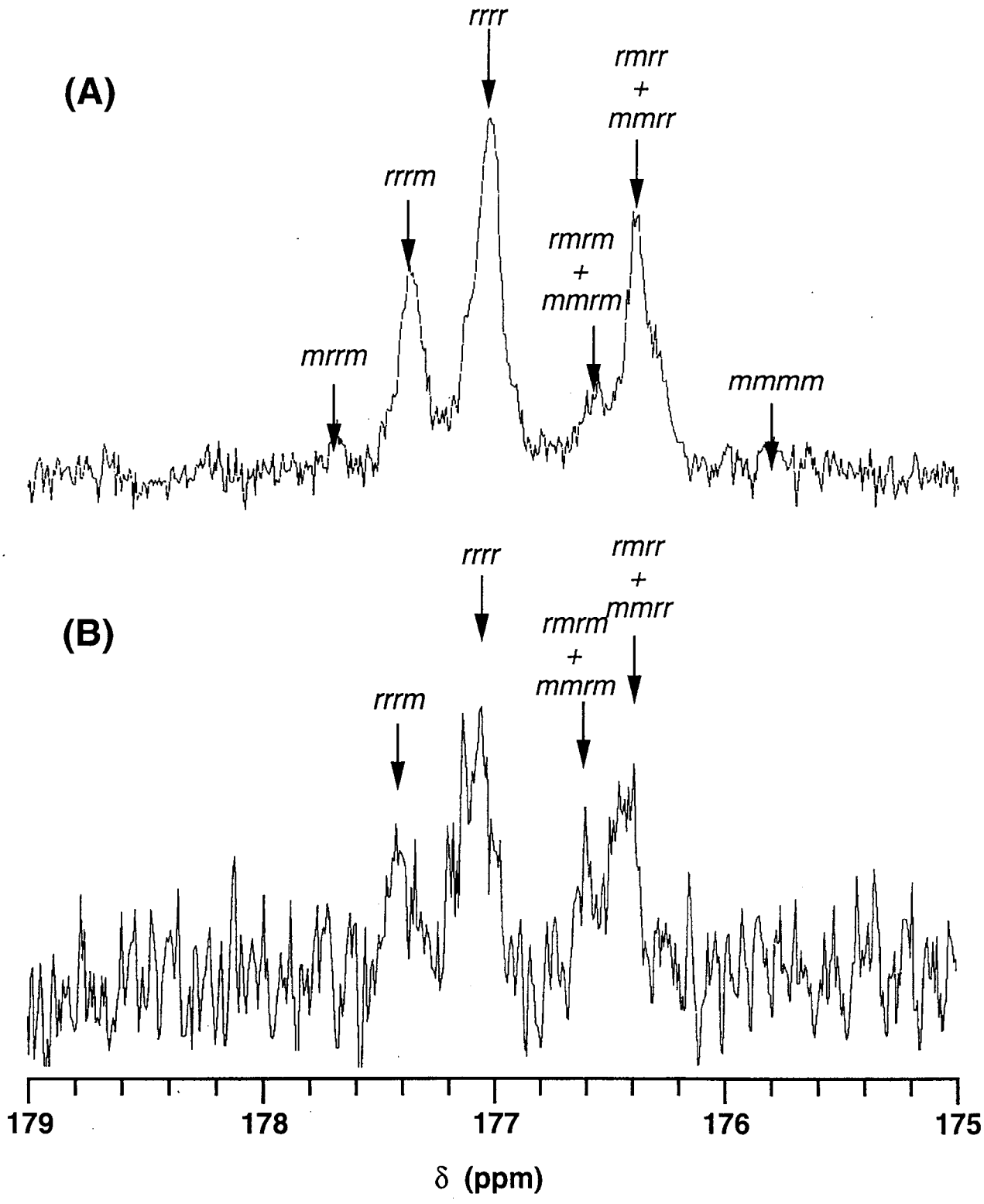

Figure 7-5. ^{13}C NMR spectra of carbonyl carbon of polymerized **MS2** in $CDCl_3$ at 60 °C. The sample was thoroughly washed with methanol to remove unreacted monomers and initiator. (A), solution polymerization; (B), photopolymerization.

In the polymerization by chain-end control, if the probability of an incoming monomer having the same configuration as the chiral chain-end carbon is represented as P, probabilities for production of three triad sequences can be represented by Bernoullian statistics as follows.[17] Then, equation (7-1) can be applied to check whether stereospecific polymerization proceeds by chain-end control or not. The values of $4[mm][rr]/[mr]^2$ were calculated and shown in Table 7-2. The triad tests indicated that poly(**MS11**) was produced by chain-end control while poly(**MS2**) was not.

$$mm = P^2$$

$$mr = 2P(1-P)$$

$$rr = (1-P)^2$$

P: probability for production of "m" dyad

$$4[mm][rr]/[mr]^2 = 1 \qquad (7\text{-}1)$$

Table 7-2. Microstructures of polymers

Polymer	Triad fraction (%)[a]			Triad test[b]
	mm	mr	rr	$\frac{4[mm][rr]}{[mr]^2}$
MS11[c]	5.6	37.5	56.9	0.91
MS11[d]	7.3	35.6	57.1	1.3
MS2[c]	2.7	34.8	62.5	0.56
MS2[d]	-[e]	37.3	62.7	-[f]

[a] Calculated from quaternary carbon signal in ^{13}C NMR spectra.

[b] $4[mm][rr]/[mr]^2 = 1$ for chain-end control.

[c] Obtained by solution polymerization at 60 °C.

[d] Obtained by in-situ photopolymerization in the ferroelectric phase.

[e] Not detected.

[f] Not calculated.

The monomer enters the smectic polymer phase and then has two possibilities of choosing a growing chain end. However, since the substituent group is bulky, syndiotactic-rich polymer was presumably obtained. Bovey and Tiers have estimated the difference in activation enthalpies for isotactic and syndiotactic propagation, $\Delta(\Delta H_p)$,[18]

$$\Delta(\Delta H_p) = \Delta H_i - \Delta H_s$$

The value obtained was $\Delta(\Delta H_p) \approx 1$ kcal/mol. It is possible to predict polymer structures from a consideration of the preferred conformation of the propagating radical which results from hindered rotation around the terminal carbon-carbon bond, and the modes of approach of the monomers.[19]

7-4. Conclusion

Stereoregularity of the polymerized FLCs was evaluated by ^{13}C NMR spectroscopy. Tacticity of polymers obtained was affected by spacer length attached to the polymerizable group. Unfortunately, the stereoregularity could not be controlled by the molecular alignment in the LC phase. Since in the free radical polymerization the structure of the propagating species is not subject to the effects of solvents or counterions which have a large influence on ionic polymerization, the configurations of the asymmetric carbon atoms will be determined by steric and electronic interactions of the substituents on the monomer.

References

1 (a) Keii, T.; Soga, K., ed. *Catalytic Olefin Polymerization*; Kodansha: Tokyo, 1989. (b) The Chemical Society of Japan, ed. *Seimitsu Jyuugou (Controlled Polymerization)*; Gakkai Shuppan Center: Tokyo, 1993.

2 (a) Hahn, B.; Wendorff, J. H.; Portugall, M.; Ringsdorf, H. *Colloid Polym. Sci.* **1981**, *259*, 875. (b) Frosini, V.; Levita, G.; Lupinacci, D.; Magagnini, P. L. *Mol. Cryst. Liq. Cryst.* **1981**, *66*, 21.

3 Nakano, T.; Hasegawa, T.; Okamoto, Y. *Macromolecules* **1993**, *26*, 5494.

4 (a) Suenaga, J.; Sutherlin, D. M.; Stille, J. K. *Macromolecules* **1984**, *17*, 2913. (b) Okamoto, Y.; Nakano, T.; Fukuoka, T.; Hatada, K. *Polym. Bull.* **1991**, *26*, 259. (c) Yoshioka, M.; Matsumoto, A.; Otsu, T. *Polym. J.* **1991**, *23*, 1191. (d) Yoshioka, M.; Matsumoto, A.; Otsu, T. *Polym. J.* **1991**, *23*, 1249. (e) Porter, N. A.; Allen, T. R.; Breyer, R. A. *J. Am. Chem. Soc.* **1992**, *114*, 7676. (f) Kakuchi, T.; Kawai, H.; Katoh, S.; Haba, O.; Yokota, K. *Macromolecules* **1992**, *25*, 5545. (g) Nakano, T.; Mori, M.; Okamoto, Y. *Macromolecules* **1993**, *26*, 867.

5 (a) Ohsumi, Y.; Higashimura, T.; Okamura, S. *J. Polym. Sci., Part A-1* **1966**, *4*, 923. (b) Ohsumi, Y.; Higashimura, T.; Okamura, S. *J. Polym. Sci., Part A-1* **1967**, *5*, 849. (c) Higashimura, T.; Ohsumi, Y.; Okamura, S.; Chujo, R.; Kuroda, T. *Makromol. Chem.* **1969**, *126*, 87. (d) Higashimura, T.; Ohsumi, Y.; Okamura, S.; Chujo, R.; Kuroda, T. *Makromol. Chem.* **1969**, *126*, 99. (e) Matsuzaki, K.; Ito, H.; Kawamura, T.; Uryu, T. *J. Polym. Sci., Polym. Chem. Ed.* **1973**, *11*, 971. (f) Toman, L.; Pokorný, S.; Špěváček, J. *J. Polym. Sci., Part A: Polym. Chem.* **1989**, *27*, 2217. (g) Aoshima, S.; Ito, Y.; Kobayashi, E. *Polym. J.* **1993**, *25*, 1161. (h) Hellermark, C.; Gedde, U. W.; Hult, A. *Polymer* **1996**, *37*, 3191.

6 (a) Okamoto, Y.; Suzuki, K.; Ohta, K.; Hatada, K.; Yuki, H. *J. Am. Chem. Soc.* **1979**, *101*, 4763. (b) Okamoto, Y.; Yashima, E.; Hatada, K. *J. Polym. Sci. Part*

C: Polym. Lett. **1987**, *25*, 297. (c) Borgne, A. L.; Spassky, N.; Jun, C. L.; Momtaz, A. *Makromol. Chem.* **1988**, *189*, 637. (d) Wulff, G.; Wu, Y. *Makromol. Chem.* **1990**, *191*, 2993. (e) Okamoto, Y.; Nakano, T.; Ono, E.; Hatada, K. *Chem. Lett.* **1991**, 525. (f) Nakano, T.; Okamoto, Y.; Hatada, K. *J. Am. Chem. Soc.* **1992**, *114*, 1318.

7 (a) Sinn, H.; Kaminsky, W.; Vollmer, H. J.; Woldt, R. *Angew. Chem., Int. Ed. Engl.* **1980**, *19*, 390. (b) Hagiwara, T.; Ishimori, M.; Tsuruta, T. *Makromol. Chem.* **1981**, *182*, 501. (c) Kaminsky, W.; Miri, M.; Sinn, H.; Woldt, R. *Makromol. Chem. Rapid Commun.* **1983**, *4*, 417. (d) Ewen, J. A. *J. Am. Chem. Soc.* **1984**, *106*, 6355. (e) Kaminsky, W.; Kulper, K.; Brintzinger, H. H.; Wild, F. R. W. P. *Angew. Chem., Int. Ed. Engl.* **1985**, *24*, 507. (f) Ewen, J. A.; Jones, R. L.; Razavi, A. *J. Am. Chem. Soc.* **1988**, *110*, 6255. (g) Cavallo, L.; Guerra, G.; Oliva, L.; Vacatello, M.; Corradini, P. *Polym. Commun.* **1989**, *30*, 16. (h) Venditto, V.; Guerra, G.; Corradini, P.; Fusco, R. *Polymer* **1990**, *31*, 530. (i) Yasuda, H.; Yamamoto, H.; Yokota, K.; Miyake, S.; Nakamura, A. *J. Am. Chem. Soc.* **1992**, *114*, 4908.

8 Kaminsky, W.; Arndt, M. *Catalyst Design for Tailor-Made Polyolefins*, Soga, K.; Terano, M., ed.; Kodansha: Tokyo, 1994, pp 179-192.

9 Kelker, H.; Hatz, R. *Handbook of Liquid Crystals*; Verlag Chemie: Weinheim, 1980, chapter 4.

10 (a) Buter, R.; Tan, Y. Y.; Challa, G. *J. Polym. Sci., Polym. Chem. Ed.* **1973**, *11*, 1003. (b) Turro, N. J.; Pierola, I. F.; Chung, C.-J. *J. Polym. Sci., Polym. Chem. Ed.* **1983**, *21*, 1085. (c) Matsuzaki, K.; Kanai, T.; Ichijo, C.; Yuzawa, M. *Makromol. Chem.* **1984**, *185*, 2291. (d) Deshpande, D. D.; Aravindakshan, P. *J. Macromol. Sci., Chem.* **1984**, *A21*, 509.

11 Tanaka, Y.; Yamaguchi, F.; Shiraki, M.; Okada, A. *J. Polym. Sci., Polym. Chem. Ed.* **1978**, *16*, 1027.

12 Shindo, T.; Uryu, T. *J. Polym. Sci., Part A* **1992**, *30*, 363.

13 Amerik, Y. B.; Krentsel, B. A. *J. Polym. Sci., Part C* **1967**, *16*, 1383.

14 Tashiro, K.; Hou, J.; Kobayashi, M. *Macromolecules* **1994**, *27*, 3912.

15 Inoue, Y.; Nishioka, A.; Chujo, R. *Polym. J.* **1971**, *4*, 535.

16 Peat, I. R.; Reynolds, W. F. *Tetrahedron Lett.* **1972**, 1359.

17 Shelden, R. A.; Fueno, T.; Tsunetsugu, T.; Furukawa, J. *J. Polym. Sci., Polym. Lett.* **1962**, *3*, 23.

18 Bovey, F. A. *J. Polym. Sci.* **1960**, *47*, 481.

19 Fischer, H. *Kolloid Z.* **1965**, *206*, 131.

Chapter 8

Summary

This thesis consists of general introduction and six experimental chapters, each of which is summarized as follows.

Chapter 2. Polymerization of Liquid-Crystalline Monomers Having Schiff-Base Structure

Vinyl monomers having Schiff-base structure were synthesized and the thermal and photopolymerization behavior of the monomers was explored in different phases of the monomers. It was found that the conversion of monomers increased with temperature in the N phase, while it decreased in the I phase. This result suggests that the polymerization behavior may be affected by molecular alignment. Arrhenius plots for the initial rates of photopolymerization fell on a straight line, while those of thermal polymerization changed the slope at the N-I phase transition temperature. The birefringence partially remained in the polymer produced in the N phase, although the polymer produced in solution polymerization showed no LC phase. In addition, the orientation of the crosslinked polymer obtained by the photopolymerization was better than that of the polymer produced by the thermal polymerization.

Chapter 3. Thermal and Photopolymerization of Liquid-Crystalline Monomers with Biphenyl Moiety

Thermal polymerization and photopolymerization of vinyl monomers having biphenyl structure were conducted at various temperatures. It was found that the initial rate of polymerization and conversion increased with temperature despite phases of the monomer. The Mn of the polymer produced in the thermal polymerization in the Sm

phase was higher than that in the I phase, whereas that of the polymer obtained by photopolymerization in the Sm phase was lower than that in the I phase. These results suggest that the polymerization behavior is affected by the initiation method in the polymerization of LC monomers.

Chapter 4. In-Situ Photopolymerization Behavior of a Chiral Liquid-Crystalline Acrylate Monomer Showing a Ferroelectric Phase

In-situ photopolymerization behavior of a FLC monomer possessing a chiral moiety is discussed on the basis of molecular alignment in the LC phase. In an early stage of polymerization, polymerizability was highest in the SmC* phase in the absence of an external electric field. The polymerization behavior was found to depend mainly on the molecular alignment in the initial stage of polymerization. In contrast, in the late stage of polymerization, the polymerization behavior of the FLC monomers was governed by their diffusion rather than their alignment. This may be due to the change in the phase structure during polymerization. It was also found that the application of electric field to the FLC monomer resulted in appearance of the immobilized SmC* phase in which all mesogens of the resulting FLC polymer were aligned in one direction leading to the formation of a monodomain of LC phase.

Chapter 5. In-Situ Photopolymerization Behavior of Chiral Liquid-Crystalline Methacrylate Monomers and Image Storage Using Ferroelectric Properties

Polymerizability of methacrylate differed from that of the corresponding acrylate. Conversion of methacrylate under dc electric field was lower than that without electric field, whereas conversion of the corresponding acrylate under dc electric field was higher than that without electric field. This may be due to the distance of radical and monomer to lower the potential energy. In addition, the relative conversion (the ratio of conversion under electric field to that without electric field) in the SmC* phase was considerably different by FLC monomers. This result suggests

that the change in macroscopic structure is more effective in the polymerization of FLC monomers in which the polymerizable groups are more densely packed. Furthermore, the image storage was performed by in-situ photopolymerization with dc electric field.

Chapter 6. Effect of Frequency-Controlled Phase Structure on Photopolymerization Behavior of Ferroelectric Liquid-Crystalline Monomers

Polymerization behavior in the early stage of polymerization was considerably different by the condition of applied electric field. Under high-frequency electric field (100 kHz), the conversion was highest and the molecular weight distribution was much narrower than those obtained under dc electric field and without the electric field. In addition, the peak of polymer produced with the ac electric field was monomodal, whereas the peak of polymer obtained with dc electric field and without the electric field was bimodal even in the low polymer content. These results may be interpreted in terms of the difference in mobility of microphase structure by condition of applied electric field.

Chapter 7. Properties of Polymer Produced by In-situ Photopolymerization of Ferroelectric Liquid-Crystalline Monomers

Stereoregularity of the polymerized FLCs was evaluated by ^{13}C NMR spectroscopy. Tacticity of polymers obtained was affected by spacer length attached to the functional group. Unfortunately, the stereoregularity could not be controlled by the molecular alignment in the LC phase.

List of Publications

Chapter 2 Polymerization of Liquid-Crystalline Monomers Having Schiff-Base Structure.

Sayuri Ogiri, Masanori Ikeda, Akihiko Kanazawa, Takeshi Shiono, and Tomiki Ikeda.

Polymer **1999**, *40*, 2145.

Chapter 3 Polymerization of Liquid-Crystalline Monomers with Biphenyl Moiety.

Sayuri Ogiri, Masanori Ikeda, Akihiko Kanazawa, Takeshi Shiono, Tomiki Ikeda, and Haruyoshi Takatsu.

Mol. Cryst. Liq. Cryst. **1998**, *319*, 159.

Chapter 4 In Situ Photopolymerization Behavior of a Chiral Liquid-Crystalline Monomer Showing a Ferroelectric Phase.

Sayuri Ogiri, Akihiko Kanazawa, Takeshi Shiono, Tomiki Ikeda, Isa Nishiyama, and John W. Goodby.

Macromolecules **1998**, *31*, 1728.

Chapter 5 In-Situ Photopolymerization Behavior of Chiral Liquid-Crystalline Monomers and Image Storage Using Ferroelectric Properties.

Sayuri Ogiri, Hiroyuki Nakamura, Akihiko Kanazawa, Takeshi Shiono, Tomiki Ikeda, and Isa Nishiyama.

Macromolecules, submitted.

Photopolymerization Behavior of Ferroelectric Liquid-Crystalline Monomers.

Sayuri Ogiri, Hiroyuki Nakamura, Akihiko Kanazawa, Takeshi Shiono, and Tomiki Ikeda.

J. Photopolym. Sci. Tech. **1998**, *11*, 193.

Chapter 6 Effect of Applied Electric Field on Photopolymerization Behavior of Ferroelectric Liquid-Crystalline Monomers.

Sayuri Ogiri, Makoto Nakano, Hiroyuki Nakamura, Akihiko Kanazawa, Takeshi Shiono, and Tomiki Ikeda.

Macromolecules, to be submitted.

Chapter 7 Photopolymerization Behavior of Ferroelectric Liquid-Crystalline Monomers and Properties of Polymer Produced.

Sayuri Ogiri, Makoto Nakano, Hiroyuki Nakamura, Akihiko Kanazawa, Takeshi Shiono, Tomiki Ikeda, and Yu Nagase.

Macromolecules, to be submitted.

Other publications not described in this thesis

I. Original papers

Micellization of Fluorocarbon Surfactants in Mixtures of Water and Polar Solvent.

Kunio Esumi and Sayuri Ogiri.

Colloids Surf. A **1995**, *94*, 107.

II. Review articles

1) 液晶モノマーの重合：重合性と分子配向性
大桐 小百合，金澤 昭彦，池田 富樹
日本接着学会誌 **1997**, *33*, 150.

2) ラジカル重合～高分子の精密合成と新材料～
第４編　ラジカル重合における材料設計
第２章　新規ポリマー
第１２節　液晶ポリマー
大桐 小百合，池田 富樹
発刊予定日 1999. 5. 30.

III. Publication at international conference

1) Polymerization of Liquid-Crystalline Monomers: Photoinitiated Polymerization Behavior of Chiral Liquid-Crystalline Vinyl Monomers and Properties of Polymer Produced.

Sayuri Ogiri, Akihiko Kanazawa, Takeshi Shiono, Tomiki Ikeda, and Isa Nishiyama.

The International Conference on Radiation Curing, RadTech Asia'97 (Yokohama, Japan) **1997**, 120.

2) Photopolymerization Behavior of Ferroelectric Liquid-Crystalline Monomers.

Sayuri Ogiri, Hiroyuki Nakamura, Akihiko Kanazawa, Takeshi Shiono, and Tomiki Ikeda.

The International Symposium on Materials & Processes for Giga-bit Lithography 1998 (Chiba, Japan) **1998**, 193.

Acknowledgments

I would like to express my sincere gratitude to Professor Tomiki Ikeda for his constant guidance and helpful discussion throughout the duration of this work. I obtained much knowledge and inspiration from him. This study could never have been continued without his guidance.

I wish to express my grateful appreciation to Associate Professor Takeshi Shiono for helpful advice and discussion.

I grateful acknowledge to Professor Tamejiro Hiyama for his helpful comment and encouragement.

I am deeply indebted to Dr. Akihiko Kanazawa for his considerable supports and encouragement.

I gratefully thank Dr. Isa Nishiyama of Japan Energy Ltd. (at present, Toho-Titanium Co., Ltd.) for valuable comments.

I would like to thank Dr. Yu Nagase of Sagami Chemical Research Center for X-ray measurement.

Grateful acknowledgement is made to all members of Ikeda-Shiono laboratory for their kind assistance and cooperation.

Finally, I would like to express my acknowledgement to my parents and my friends for their heartfelt encouragement and support.

December 28, 1998

Sayuri Ogiri